

Financial Methods in Competitive Electricity Markets

by

Shijie Deng

B.S. (Peking University) 1991

M.S. (University of Minnesota, Minneapolis) 1993

A dissertation submitted in partial satisfaction of the

requirements for the degree of

Doctor of Philosophy

in

Engineering-Industrial Engineering
and Operations Research

in the

GRADUATE DIVISION

of the

UNIVERSITY OF CALIFORNIA, BERKELEY

Committee in charge:

Professor Shmuel Oren, Chair

Professor Darrell Duffie

Professor George Shanthikumar

Professor Pravin Varaiya

Fall 1999

The dissertation of Shijie Deng is approved:

Chair

Date

Date

Date

Date

University of California, Berkeley

Fall 1999

Financial Methods in Competitive Electricity Markets

©1999

by

Shijie Deng

Financial Methods in Competitive Electricity Markets

by

Shijie Deng

Doctor of Philosophy in Industrial Engineering and Operations Research

University of California at Berkeley

Professor Shmuel S. Oren, Chair

Abstract

The restructuring of electric power industry has become a global trend. As reforms to the electricity supply industry spread rapidly across countries and states, many political and economical issues arise as a result of people debating over which approach to adopt in restructuring the vertically integrated electricity industry. This dissertation addresses issues of transmission pricing, electricity spot price modeling, as well as risk management and asset valuation in a competitive electricity industry.

A major concern in the restructuring of the electricity industries is the design of a transmission pricing scheme that will ensure open-access to the transmission networks. I propose a priority-pricing scheme for zonal access to the electric power grid that is uniform across all buses in each zone. The Independent System Operator (ISO) charges bulk power traders a per unit *ex ante* transmission access fee based on the expected option value of the generated power with respect to the random zonal spot prices. The zonal access fee depends on the injection zone and a self-selected strike price determining the scheduling priority of the transaction. Inter zonal transactions are charged (or cred-

ited) with an additional *ex post* congestion fee that equals the zonal spot price difference. The unit access fee entitles a bulk power trader to either physical injection of one unit of energy or a compensation payment that equals to the difference between the realized zonal spot price and the selected strike price. The ISO manages congestion so as to minimize net compensation payments and thus, curtailment probabilities corresponding to a particular strike price may vary by bus. I calculate the rational expectation equilibria for several numerical examples and demonstrate that the efficiency losses of the proposed second best scheme relative to the efficient dispatch solutions are modest.

The rest of the dissertation deals with the issues of modeling electricity spot prices, pricing electricity financial instruments and the corresponding risk management applications. The aforementioned global trend of restructuring opens the electricity wholesale markets worldwide. Modeling the spot prices of electricity is important for the market participants who need to understand the risk factors in pricing electricity financial instruments such as electricity forwards, options and cross-commodity derivatives. It is also essential for the analysis of financial risk management, asset valuation, and project financing.

In the setting of diffusion processes with multiple types of jumps, I examine three mean-reversion models for modeling the electricity spot prices. I impose some structure on the coefficients of the diffusion processes, which allows me to easily compute the prices of contingent claims (or, financial instruments) on electricity by Fourier methods. The jump-diffusion models which I propose have the features of mean-reversion, stochastic volatility, and regime switching. I derive the pricing formulas for various electricity derivatives and examine how the prices vary with different modeling assumptions.

I demonstrate a couple of risk management applications of the electricity financial instruments. I also construct a real options approach to value electric power generation and transmission assets both with and without accounting for the operating characteristics of the assets such as start-up cost, ramp-up time and variable heat rate. The implications of the mean-reversion jump-diffusion models on financial risk management and real asset valuation in competitive electricity markets are illustrated. With a discrete trinomial lattice modeling the underlying commodity prices, I estimate the effects of operational characteristics on the asset valuation by means of numerical examples that incorporate these aspects using stochastic dynamic programming.

Shmuel S. Oren, Chair

Date

Dedication

To my parents, Ruixian and Wanli Deng, and to people who I love.

Contents

1	Overview	1
1.1	Transmission Pricing	5
1.2	Modeling Electricity Spot Prices	10
1.3	Risk Management and Asset Valuation	16
1.4	Contributions of this Work	19
2	Priority Network Access Pricing	23
2.1	Introduction	23
2.2	A priority insurance mechanism	27
2.2.1	Single spot market	31
2.2.2	Multiple spot markets: zonal pricing	34
2.2.3	The choice of premium function $X(c)$	37
2.3	Numerical examples	38
2.3.1	Single spot market: three-node network	39
2.3.2	Multiple spot markets: 4-node and 6-node networks	46
2.4	Conclusion	53
3	Stochastic Models for Electricity Prices	55
3.1	Introduction	56
3.2	Mean-Reverting Jump-Diffusion Price Models	60
3.2.1	Model 1: A mean-reverting deterministic volatility process with two types of jumps	61
3.2.2	Model 2: A regime-switching mean-reverting process with two types of jumps	65
3.2.3	Model 3: A mean-reverting stochastic volatility process with two types of jumps	68
3.3	Electricity Derivative Pricing	70
3.3.1	Illustrative Models	72
3.3.2	Electricity Derivatives	77
3.3.3	Parameter Estimation	86
3.4	Conclusion	89
4	Risk Management and Asset Valuation	90
4.1	Risk Management with Electricity Derivatives	91
4.2	Real-Options Valuation of Capacity without Physical Constraints	95
4.3	Capacity Valuation with Operational Characteristics	103

4.3.1	Construction of the Discrete Price Processes	105
4.3.2	Valuation of Electricity Generation Assets with Operational Characteristics	111
4.3.3	Numerical Examples and Comparative Statics	116
4.3.4	Conclusion	122
5	Summary and Future Research	125
5.1	Transmission Pricing	125
5.2	Electricity Spot Price Modeling	126
5.3	Risk Management and Asset Valuation	127
A	Proofs in Chapter 2	130
A.1	Proof of Proposition 1	130
B	Technical Conditions in Chapter 3	132
B.1	Conditions for $\varphi \cdot e^{-rt}$ to be a martingale in Section 3.2	132

List of Figures

1.1	Electricity Historical Spot Prices	14
1.2	Generation Stack for Electricity in a Region	15
2.1	An electricity network with several spot markets	28
2.2	Timeline of the priority insurance scheme	30
2.3	A three-node network	39
2.4	Objective of economic dispatch	41
2.5	Insurance premium function	42
2.6	Insured cost distribution curves	43
2.7	Objective of the ISO's minimization problem	44
2.8	Rational expectation of network access price interval	45
2.9	The comparison between 1st best and 2nd best solutions	46
2.10	An example of four-node network	47
2.11	An example of six-node network	52
3.1	Implied Volatility of Call (Sept.) Options at Cinergy	56
3.2	Electricity Historical Spot Prices	57
3.3	Simulated Spot Prices under the Three Models	72
3.4	Forward Curves under Different Models (Contango)	80
3.5	Forward Curves under Different Models (Backwardation)	80
3.6	Call Options Price under Different Models	82
3.7	Volatility-Smile under Different Models	83
3.8	Spark Spread Call Price under Different Models	86
4.1	Payoff of a Spark Spread Call Option	92
4.2	Hedging Transmission Risks	95
4.3	Capacity Value with/without Jumps (Model 1a)	100
4.4	Sensitivity of Capacity Value to Electricity Spot Volatility (Model 1a) . .	101
4.5	Sensitivity of Capacity Value to the Correlation Coefficient (Model 1a) . .	101
4.6	Value of Capacity: Spark Spread approach vs. DCF approach	102
4.7	Construction of a Trinomial Lattice	106
4.8	Valuation of A Power Plant with/without Physical Characteristics Under GBM Price Models	119
4.9	Valuation of A Power Plant with/without the Start-up Cost under GBM Price Models	120
4.10	Valuation of A Power Plant with/without Physical Characteristics Under Mean-Reversion Price Models	122

4.11 Valuation of A Power Plant with/without the Start-up Cost Under Mean-Reversion Price Models	123
--	-----

List of Tables

2.1	Supply functions	52
3.1	Parameters for the Illustrative Models	87
4.1	Parameters (Model 1a) for Capacity Valuation	99
4.2	Parameters for GBM Price Models	117
4.3	Value of a NG fired Power Plant under GBM Price Models	118
4.4	Parameters for Mean-Reversion Price Models	121
4.5	Value of a NG fired Power Plant under Mean-Reversion Price Models	121

Acknowledgments

This dissertation would not be possible without the support and collaboration of many persons around me. First, I would like to thank Shmuel Oren, my principal thesis adviser, for his continuous support and mentorship through my time at Berkeley. I have substantially benefited from him not only in the academic aspects but also in many other aspects. I feel so lucky that I had him as my advisor from the beginning of my graduate school career at Berkeley.

I have been very fortunate to have Darrell Duffie serve on my dissertation committee. I am indebted to him for many fruitful discussions during those “short meetings” and for his valuable suggestions on my work. I am also very grateful to George Shanthikumar and Pravin Varaiya for their patience, support and encouragement.

I would also like to thank a wealth of other people, who have been helpful in this endeavor. These include my friends and colleagues at Stanford, IBM Research, Edison Source, Pacificorp and EPRI, as well as past and present IEOR graduate students at Berkeley.

And last but not least, my family members, especially my parents, always provided me with the kind of love and support that I needed the most during times of trouble and anxiety. My wonderful younger brother, Shiming, has been a great source of help during this whole process. Finally, I thank my wife and our son for pushing me through this endless “tunnel” sooner than I expected.

Chapter 1

Overview

The electricity supply industry in many countries has traditionally been a vertically integrated industry consisting of generation, transmission and distribution sectors. In recent years, the evolution of various technological factors that are conducive to competition has caused tremendous changes in this industry. To name a few, the development of low-cost small-scale power generating technologies such as the combined cycle generating technology made it possible to build small and medium size power plants; the advances in telecommunication enables the electric power system operator to closely monitor the load and supply information. All of these factors have been conducive to reforms transforming the vertically integrated electric power industry into a competitive marketplace.

Researchers have long been pointing out the economic inefficiencies in the operating performance of the existing generating facilities, the productivity of operating labor, and the long-run investments in generating capacity under the traditional regulatory regime. Enormous economic welfare losses can be related to these inefficiencies. Gilbert and

Henly (1991) have estimated the welfare loss due to electricity pricing deviating from marginal costs, i.e. operating inefficiency, for Northern California. They find that annual losses amount to about 7% of costs for the conditions that they examine. Were these results scaled up to the U.S. industry as a whole, then welfare losses would be about \$12 billion annually. In seeking improvements in efficiency, many countries including the United Kingdom, Australia, Chile, Argentina, New Zealand, Norway and the United States have been, or are currently undertaking efforts to restructure their electricity supply industries.

Evidence drawn from the experience in the United Kingdom suggests that the efficiency gain from privatizing and deregulating the electricity sector can be large. The British government announced the radical electricity market reforms as an effort to privatize its electricity supply industry in England and Wales in February 1988. In March 1990, the state-owned Central Electricity Generating Board (CEGB), responsible for generation and transmission, was divided into three competing generating companies (PowerGen, National Power, and Nuclear Electric) and the National Grid Company (NGC), responsible for transmission. A wholesale market, the Electricity Pool (UK Pool), was created to allow loads and generators to buy and sell electricity, while recognizing the constraints involved in operating an electrical system. It was found that privatizing the generators and introducing competition in generation resulted in dramatic improvements in labor productivity by reducing the workforce in half within three years, and in tighter control over investment costs.

In the United States, the deregulation was preceded by two very influential regulatory acts - the Public Utilities Regulatory Policy Act of 1978 (PURPA) and the Energy

Policy Act (EPAAct) of 1992. Seen broadly, PURPA opened the door to competitively supplied power but with considerable restrictions. Among other things, PURPA required utilities to purchase power from independent generation service providers for an amount equal to the utilities' avoided cost¹. With its major intentions being promoting environmentally friendly generation facilities and achieving some economic efficiency², PURPA brought into existence the independent power producers (IPPs) and made it clear that successfully owning and operating small-scaled independent power plants is economically viable. While PURPA stimulated the wave of introduction of new generation technologies and demonstrated the economic feasibility of IPPs, the EPAAct paved the way for IPPs, or more generally the independent generation service providers, to compete with the vertically integrated utilities in power generation. The EPAAct demonstrated that it is possible to coordinate transmission and distribution services across the vertically integrated utilities and IPPs without sacrificing reliability of service. It greatly extended the powers of the Federal Energy Regulatory Commission (FERC) to mandate transmission access, in particular, to order open access to regional transmission networks. In the implementation of the EPAAct, the utilities were required to provide wholesale power wheeling service between IPPs and other utilities at the same terms with which it provided itself.

The passage of the two regulatory acts and the proven ability to coordinate across utilities's transmission networks have been pivotal in the progressive introduction of competition in the electricity industry. However, it is believed that the large gap between

¹The intended meaning of avoided cost is that, due to the use of external supply, the utilities would save a certain amount of money, representing fuel and other variable costs, as well as capital costs if the external power source resulted in deferment or cancellation of new generation capacity investments.

²There have been questions and complaints about whether PURPA achieves the desired results.

the wholesale electricity prices and the implicit price of generation services embedded in the retail electricity prices were the driving forces behind the decisions by the several states in the Northeast and California to proceed with their deregulations. In 1996, FERC issued the Orders 888 and 889 which required incumbent utility companies to make transmission capacity and information pertaining to transmission capacity available to all parties on equal terms. This action by FERC greatly accelerated the ongoing deregulation processes in the above states.

As for the electricity market structure and market rules, regulators in different states have their own preferences. In the Pennsylvania-New Jersey-Maryland (PJM) interconnection, a market structure is organized around an independent “PoolCo” that would serve as the market maker and also regulate transmission access according to the nodal spot pricing principles of Schweppe *et al.* (1988) and Hogan (1992). In California, two entities are created to separately handle the responsibilities of market-making and network operations - a Power Exchange (PX) that would perform the market-making functions, and an Independent System Operator (ISO) that would be primarily responsible for the operation of the grid and, if necessary, the rationing of access to congested paths.

With electricity deregulation gradually becoming the dominating trend around the world, many political and economic issues arise as a result of people debating over which approach to adopt in restructuring the vertically integrated electricity industry. Among these issues, we are particularly interested in the ones that concern transmission pricing, electricity spot price modeling, and risk management and asset valuation in competitive electricity markets. The purpose of this dissertation is to develop and apply

methodologies from financial economics to address these three issues. I will provide the reader with a brief overview and illustrate the pertinent problems for each issue.

The remainder of the chapter is organized as follows. In Section 1.1, I introduce the role of a transmission pricing scheme in the electricity restructuring and the problems in designing an appropriate one. In Section 1.2, I explain the needs and complexities in modeling electricity spot prices. The demands for risk management tools and motivations for a new methodology for project financing and asset valuation in the competitive electricity markets are illustrated in Section 1.3. Finally, I summarize the contributions made by this dissertation to the literature of electricity deregulation and competitive electricity markets in Section 1.4.

1.1 Transmission Pricing

No matter how the markets for electricity are organized, one of the common goals of the restructuring is to create an efficient and competitive decentralized market for generation. The roles of transmission network access rules and associated access prices are crucial in achieving this goal.

First of all, the transmission access rules and transmission prices should support efficient competition at the generation level. Historically, the owner or a group of owners who own both the generation and transmission capacity is usually the transmission network operator, or the so called system operator (SO), who is responsible for the physical control of the network, balancing loads and supplies in real time, dispatching generators based on network constraints, and scheduling operations with interconnected

control areas. One can conceivably foresee the potential competitive problems created by the common ownership of transmission and generation facilities that seek to compete with independent generation service providers. Basically, owners of the monopoly transmission network have the incentive and ability to discriminate in favor of generators in which they have a financial interest and against those in which they do not. A natural approach for solving this problem is to separate the ownership of generation and the grid operations by creating an Independent System Operator (ISO) who is responsible for transmission only but has no financial interests in generation capacity. For the ISO, it is very important to design a transmission pricing scheme which ensures open-access and the nondiscriminatory usage of the transmission network by all network users in order to support an efficient competitive generation sector.

Besides the consideration of supporting efficient competition in generation, promoting the daily operational efficiency is another key concern in designing a transmission pricing scheme. In an interconnected transmission network, electricity flows according to the Kirchoff's laws instead of the artificially designated contract paths. The actions by the transmission network users in one region could adversely affect the network users in a remote region. This is known as the "loop flow" problem. While open access to the transmission network is essential to a competitive generation sector, it imposes great challenges on coordinating bilateral or multilateral trades and efficient dispatching by an ISO. In particular, the ISO needs a set of transmission access rules to perform congestion management in order to maintain system security when congestion occurs. The associated transmission prices should serve the purpose of rationing scarce transmission capacity in an economically efficient manner. There is no doubt that the short-term

operational efficiency of the bulk power system relies on the appropriateness of a transmission pricing scheme and the corresponding congestion management protocol.

Transmission prices are also expected to provide economic signals for new investments in transmission and compensate the owners of existing transmission assets. Since transmission investments often serve as substitutes to generation investments, it is intuitive to use the transmission prices to guide such investment decisions in the transmission system. As for compensating owners of transmission assets, a properly designed transmission pricing scheme should provide the owners with appropriate returns on their investments in order to attract new investments. Without fair compensation to the current owners, potential investors will see this as the effective expropriation of existing assets and thus be discouraged from investing in transmission in the future.

It has been suggested that six principles should be followed when designing a transmission pricing scheme (Energy Modeling Forum 15 Meeting, 1996, e.g. Green (1997)). The transmission prices should:

1. promote the efficient day-to-day operation of the bulk power system;
2. signal locational advantages for investment in generation and demand;
3. signal the need for investment in the transmission system;
4. compensate the owners of existing transmission assets;
5. be simple and transparent; and
6. be politically implementable.

Transmission pricing schemes in different jurisdictions have different emphases in terms of the above principles. In the UK, the transmission company NGC imposes two kinds of transmission charges for recovering its own costs. One is for network connection to the Regional Electricity Companies and generators; the other charge is for use of transmission system by generators and suppliers. The transmission use of system charges send signals about the appropriate location for new generation and demand albeit not strong enough. However, the present transmission charges in UK almost do nothing in promoting the efficient day-to-day operation of the bulk power system. In New Zealand, as a comparison, there is a single state-owned utility, Trans Power, responsible for transmission and grid operation, including purchase of ancillary services. The transmission pricing framework adopted there mainly consists of the nodal spot pricing approach (Schweppe, *et al.* (1988) and Hogan (1992)) for promoting short term efficiency and a “fixed charge” approach for recovering sunk investment costs. The nodal spot pricing approach determines the dispatch of generation and load using an explicit system model which includes transmission losses and constraints. A system coordinator runs the system model to produce an operating schedule and spot prices based on generators’ bid-in marginal generation costs. Generators and loads face the same nodal spot price at each node. Such a system should lead to fully efficient day-to-day operation unless generators possess market power to manipulate their bids. Transmission prices, or nodal price differentials, are also used by Trans Power to make investment decisions for transmission. System expansions are justified if the difference in nodal spot prices with and without a scheme equals the cost of the scheme.

Some recently adopted transmission pricing systems are based upon spot prices sim-

ilar to the New Zealand system because of the promising aspect of short-run efficiency. However, as noted earlier, the short-run efficiency of the nodal spot pricing approach relies on generators and loads revealing their true marginal costs or willingness-to-pay. Therefore, the day-to-day efficient operation of a power system depends on the incentive effects by the generators and loads, which are not addressed by the nodal spot pricing approach. From the implementation point of view, one other difficulty of the nodal spot pricing approach is that it impedes trading and price discovery due to low liquidity at the nodal markets, lack of transparency in how prices are determined, and the fact that exact prices are only known *ex post*. In practice, some jurisdictions divide their transmission networks into zones and assign transmission prices to zones rather than nodes as a means of simplification and increasing liquidity. For example, California is divided into two major congestion zones for the purpose of transmission pricing, northern California and southern California, which are connected by a major often-congested transmission link (Path 15).

In designing yet another transmission pricing scheme which implements open access, I shall mainly focus on the aforementioned principles 1, 2, 5 and 6. I propose an incentive-compatible network access pricing scheme in an electric power system which can be divided into zones according to one or several hub markets such as the California system. I will contrast it with some existing alternative schemes and examine the trade-offs between economic efficiency and simplicity of implementation in Chapter 2.

1.2 Modeling Electricity Spot Prices

The unique physical attributes of electricity, and the heavy regulation of its supply and sale, have in the past prevented it from being traded in open markets. This scenario has been changed completely since 1990. Electricity markets emerge as a consequence of the restructuring of electric power industries around the world. I shall briefly describe the electricity market forms in several Organization for Economic Cooperation and Development (OECD) member countries according to the chronological order of the opening of their electricity markets.

Among the OECD countries, the United Kingdom was the first country to restructure its electricity supply industry and introduce a spot market for electricity in England and Wales. Since April 1, 1990, almost all the electricity generated and consumed in England and Wales must be bought and sold through the day-ahead spot market (E&W Pool). The E&W Pool exists as a set of procedures and rules that enable the most economic generating sets to be operated to meet national demand at any one time. It sets a market price for electricity for each half-hour of each day.

Following the lead of UK, several other OECD countries have implemented similar restructuring plans and formed wholesale markets for electricity. Norway started its rapid two-year transition from a highly centralized electricity supply industry to a market-based system in 1991. A Norwegian futures market for electricity began to operate in the fall of 1992. Beginning January 1, 1996, an international power exchange (Nord Pool), which integrates the Norwegian and Sweden electrical systems, opened in Oslo, Norway. Denmark, Finland and Russia each have one participant in this international

Nordic power market. Nord Pool is composed of two markets - one market is the Daily Power Market or Spot Market where electricity is traded on a day-ahead basis for 24 hourly periods; and the other market for within-day electricity is called the Regulation Power Market in Norway and the Balancing Market in Sweden. In addition, weekly financial futures contracts with maturity time ranging from one week to three years are traded in the futures market.

In Australia, the first established wholesale electricity market is the Victoria Power Exchange (Victoria Pool) which commenced operation on July 1, 1994. Another state-level wholesale market for electricity recently started its operation in New South Wales on May 10, 1996. In the Victoria Pool, the electricity prices are set on a half-hourly basis using bids submitted on a day-ahead basis by generators and demand-side bidders. However, the Victoria Pool prices are *ex post* prices, which are based on the actual demand served in each half-hour, rather than *ex ante* prices as is the case in E&W Pool, which are based on estimated demands prepared on a day-ahead basis. Due to this *ex post* nature, there is no need for a balancing or real-time market in the Victoria Pool.

On October 1, 1996, a wholesale electricity market in New Zealand began operation. Generators submit bid functions specifying the amount of capacity they are willing to supply as a function of the price for all half-hours during the following day. The offers and bids may be freely changed up to four hours before the intended dispatch time. Similar to the Victoria Pool, electricity prices are determined *ex post* by using the generator supply bids as of the beginning of each half-hour trading period to meet the actual metered load.

Although the United States has been slow to undertake the radical restructuring pro-

cess in general, several states have already established their own electricity markets for generation similar to those in the OECD countries and many other states are planning to follow suit. In California, an electricity wholesale market known as the Power Exchange started its operation on March 31, 1998. Electricity is also traded in the hour-ahead and real-time markets managed by the California ISO. In PJM, there is only one market for electricity and market participants settle trades according to *ex post* nodal prices published by the PJM ISO. Running in parallel with the spot markets, there is a futures market for electricity at the New York Mercantile Exchange (NYMEX). Monthly futures contracts on electricity at four major delivery points in US, two in the east and two in the west, are traded with maturity time ranging from one month to eighteen months.

As I just described, most of the electricity markets take the form of forward markets, either day-ahead or hour-ahead, complemented by real-time markets. This is mainly due to a key feature of electricity which is the near non-storability and the complexity of operating an interconnected electric power network. The term “spot price” hereafter refers to not only the real-time spot prices but also a broad range of market prices such as the day-ahead and hour-ahead forward prices.

With more and more countries and states joining force in restructuring their electricity supply industries, electricity markets in these jurisdictions have been growing rapidly. In US, for instance, the volume of trade for electricity reported by US power marketers has surged from 27 million MWh (Megawatt-hour) in 1995 to 1,195 million MWh in 1997 (Source: Edison Electric Institute). The trend of deregulation inevitably exposes the portfolios of generating assets and various supply contracts held by various market participants to market price risk. It has so far changed and will continue to

change not only the ways in which the traditional electric power utility companies and the IPPs operate and manage their physical assets such as power plants, but also the ways in which they value and select potential investment projects. The needs of trading electricity, performing risk management and asset valuation, and financing new investments require in-depth understanding of the price behaviors and sophisticated modeling of electricity spot prices.

Among all the energy commodities, electricity poses the biggest challenge for researchers and practitioners to model its price behaviors. A distinguishing characteristic of electricity is that it cannot be stored or inventoried economically once produced³. Moreover, the aggregate electricity supply and demand has to be balanced continuously so as to prevent the electric power networks from collapsing. Since the supply and demand shocks cannot be smoothed by inventories, electricity spot prices are volatile. In the summer of 1998, the electricity prices fluctuated between \$0/MWh and \$7000/MWh in the Midwest of US. It is not uncommon to see a 150% implied volatility in traded electricity options. Electricity has become *de facto* the most volatile commodity since its first appearance as a traded commodity. Besides the tremendous price volatility, several key physical characteristics of the supply and demand for electricity have important implications on the behaviors of electricity spot prices. I shall point out these prominent price behaviors before getting into the modeling issues.

First thing to notice is that electricity spot prices show strong mean-reversion. This is a common feature in prices of many other traded commodities. The reason is that when

³In hydro electric power systems, it can be stored as water in reservoirs; and in thermal power systems, it can be stored in the form of fuel inventories but the rate at which it can then be converted to electricity is constrained by generation capacity and other physical constraints.

the price of electricity is high, its supply tends to increase thus putting a downwards pressure on the price; when the spot price is low, the supply of electricity tends to decrease thus providing an upwards lift to the price.

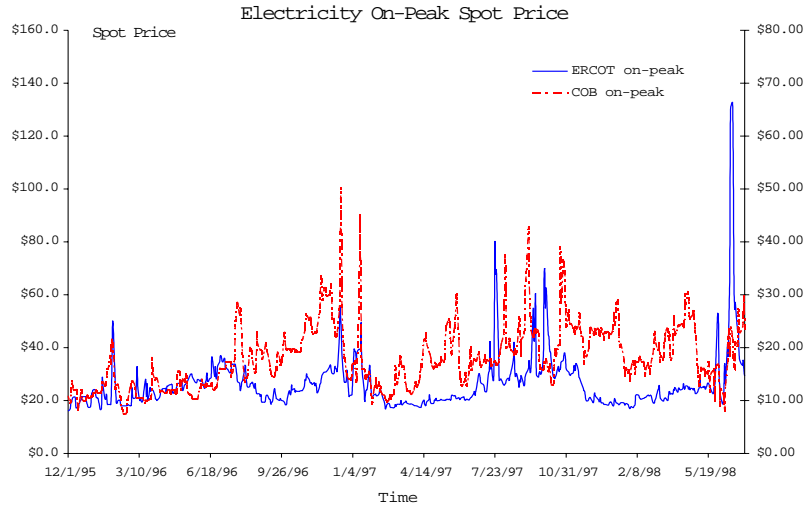


Figure 1.1: Electricity Historical Spot Prices

Another salient feature in electricity spot prices is the presence of price jumps and spikes. Figure (1.1) plots the historical on-peak electricity spot prices in Texas (ERCOT) and at the California and Oregon border (COB). Such jumpy behavior in electricity spot prices is mainly attributed to the fact that a typical regional aggregate supply curve for electricity almost always has a kink at certain capacity level and the curve has a steep upward slope beyond that capacity level. Figure (1.2) shows a snap shot of the marginal cost curve of the electricity supply resource stack in western U.S. A forced outage of a major power plant or a sudden surge in demand will either shift the supply curve to the left or lift up the demand curve (dashed curve in Figure (1.2)) therefore causing a price jump. Jumps and spikes resulting from limited amount of installed supply capacity coupled with low demand elasticity exacerbate the price volatility of electricity.

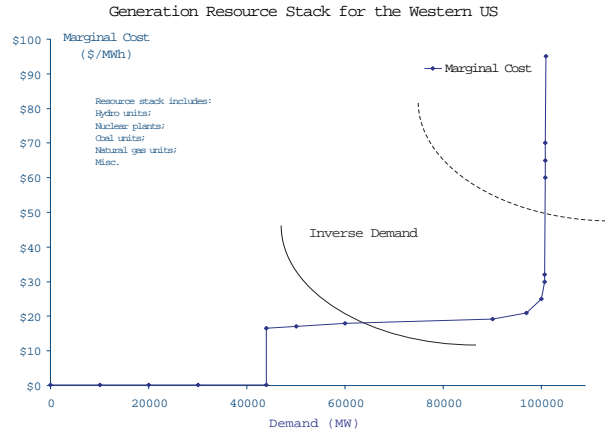


Figure 1.2: Generation Stack for Electricity in a Region

Electricity prices also demonstrate stochastic volatility and regime-switching in some markets. Since the temperature is one of the dominating factors which influence the aggregate load level, the randomness in temperature implies that the volatility of spot prices can be a random factor. In markets where the majority of installed electricity supply capacity is hydropower such as in the Nord Pool and the Victoria Pool, electricity spot prices exhibit regime-switching, namely, the prices alternate between “high” and “low” regimes corresponding to the respective precipitation levels.

To accurately model electricity spot prices, one must fully understand and take into consideration the above physical characteristics of electricity. Resorting to jump-diffusion processes, I examine three stochastic price models which capture the mean-reversion, regime-switching, jumps and spikes and several other prominent price behaviors of electricity. I will provide the specification for these models and illustrate how to compute prices of various electricity derivatives under each model using Fourier transform methods in Chapter 3.

1.3 Risk Management and Asset Valuation

Electricity spot prices are bound to be volatile as a consequence of the unique physical attributes of electricity. Uncontrolled exposure to market price risks could lead to devastating consequences. During the summer of 1998, wholesale power prices in the Midwest of US surged to a stunning amount of \$7,000/MWh from the normal price range of \$30-\$60/MWh causing the defaults of two power marketers in the east coast which negatively impacted the electricity markets in the US. More and more market participants are recognizing the importance and necessity of risk management, at least after observing the market anomalies in the US.

The motives for risk hedging by corporations should in principle come from maximizing firm value. Hedging achieves value enhancement by reducing the likelihood of encountering financial distress thus avoiding financial distress costs, or by reducing the variance of taxable incomes thus lowering the present value of future tax liabilities. From my personal experience, it appears that the regulatory rulings can also motivate firms to implement hedging. In California, the regulators granted the incumbent investor-owned utilities (IOUs) a fixed time-frame to recover their stranded generation costs through the Competition Transition Charge. In fear of adverse market conditions causing insufficient recovery of the stranded costs, one major utility company hired investment bankers to structure and carry out a substantial hedging strategy for the stranded-cost recovery.

As the competitive and volatile electricity markets prevail, utility companies and IPPs seek to hedge their productions while power marketers feel the urgent needs in quantifying, monitoring and controlling their trading risks in the wholesale and retail

power markets. Overall, an increasing number of market participants start to search for appropriate risk management tools and methodology in order to establish their risk management programs in one way or another.

Besides the surging demands for hedging daily operations and trading activities, there are also increasing demands for planning and hedging investments in generating capacity. Planning and hedging generation investments boil down to valuing generation assets. At the present time, a significant portion of the demands for generation asset valuation is spurred by the mandated divestiture of existing generation assets owned by major utility companies in various jurisdictions. For example, in California, most of the fossil-fuel plants held by the three IOUs which account for about 60% of the total installed capacity in California have been or will be divested to other parties.

Another primary source of demands for asset valuation rises from the interests in investing in new generation capacity. It is envisioned that most of the efficiency gains in restructuring the electricity supply industries are to be associated with long-run investments in generating capacity. Under the state-ownership or required rate-of-return regulatory regime, utility companies were allowed to earn a regulated rate of return above their cost of capital. Once regulators approved the construction costs of a power generating plant, the costs would be passed onto consumers through regulated electricity prices over the life of the investment, independent of the fluctuation in market value of the investment over time due to changing energy prices, improving technology, and evolving supply and demand conditions. Most of the investment risks in generating capacity were allocated to consumers rather than producers. Firms therefore had little incentives to avoid excessive cost of investment and they focused rather on improving

and maintaining quality of service than on developing and adopting new generation technology.

Now the situations have been dramatically changed by the reforms in the electric power sectors around the world. For instance, before the 1990 restructuring of the electricity supply industry in the UK, the consensus is that under the Central Electricity Generating Board, power stations costed between 50% and 100% more than in other developed countries, and took as much as twice as long to commission. However, after the 1990 structural reforms, the advanced combined cycle gas turbine (CCGT) generating units with capacity costs of £350 ⇔ 500 per kilowatt (kW) gradually displace the inefficient coal plants. CCGT plants also act as substitutes for nuclear units which could have capacity costs as high as £2,446 per kW of actual capacity (based on the 1988 prices of the Advanced Gas-cooled Reactor). As for new entrants to the UK electricity market, an extra 11.2 Gigawatt (GW) of CCGT plants have been constructed or put into construction by 1996 which is considered a substantial entry comparing to the total capacity of about 60 GW.

The traditional approach for valuing an investment project such as the construction of a power plant is to take the projected cash flow based on the forecasted regulator-approved electricity prices and the costs, and then discount the expected future profits by the cost of capital of the investing firm. This so-called discounted cash flow (DCF) approach becomes inappropriate in a deregulated electricity industry because a) electricity prices would no longer be set by the regulators but by a market; b) the operational flexibility of a power plant, which is not captured in the DCF valuation approach, needs to be reflected in the plant valuation since the owner of the power plant would have

strong incentive to capitalize on such flexibility under the market-based regime. In the competitive electricity markets, a new methodology for asset valuation and project financing is required in place of the DCF methodology.

In Chapter 4, I will demonstrate a couple of hedging applications of electricity derivatives in electricity generation and transmission. Abstracting operational characteristics, I illustrate that the future cash flow of a power plant can be closely approximated by payoffs of a set of properly designed financial instruments. Based on this observation, I construct a real options approach to obtain a market-based valuation of a power generating asset. I then improve the valuation approach by incorporating into it the operating characteristics of a power plant such as the start-up cost, output-dependent heat-rate, and ramp-up time. The implications of operational characteristics on real asset valuation are illustrated through numerical examples.

1.4 Contributions of this Work

In this thesis, the goal is to develop and apply financial economic methodologies to address issues in transmission pricing, electricity spot price modelling and market-based asset valuation. I attempt here to provide solutions both to the problems faced by the regulators when designing an electricity market and to the problems concerned by the market players when participating an electricity market.

In Chapter 2, I tackle the problem of transmission access pricing design, which is one of the focal points for the regulators. I propose a priority-pricing scheme in the form of insurance for zonal access to an electric power grid that is uniform across all nodes

in each zone. The Independent System Operator (ISO) charges transmission network users a per unit *ex ante* transmission access fee based on the expected option value of the generated power with respect to the random zonal spot prices. The zonal access fee depends on the injection zone and a self-selected strike price determining the scheduling priority of the transaction. Inter-zonal transactions are charged (or credited) with an additional *ex post* congestion fee that equals the zonal spot price difference. The unit access fee entitles a transmission network user to either physical injection of one unit of energy or a compensation payment that equals to the difference between the realized zonal spot price and the selected strike price. The ISO manages congestion so as to minimize net compensation payments and thus, curtailment probabilities corresponding to a particular strike price may vary by node. I calculate the rational expectation equilibria for a three-, four- and six- node system and demonstrate that the efficiency losses of the proposed second best scheme relative to the efficient dispatch solutions are modest.

Chapter 3 and Chapter 4 take on the problems concerned by the electricity market participants. In the two chapters, I extend the existing literature on electricity spot price modeling by examining several stochastic models that capture the realistic aspects of electricity prices. For the proposed electricity price models, I provide a framework for pricing electricity derivatives, designing risk management strategies, and evaluating generation or transmission investments in competitive electricity markets.

Under the setting of diffusion processes with multiple jumps, I investigate the modeling of electricity spot prices and the pricing of various electricity derivatives in Chapter 3. My proposed price models reflect the realistic features in the electricity spot prices

such as seasonality, mean-reversion, regime-switching, stochastic volatility, as well as jumps and spikes. By imposing proper restrictions on the jump-diffusion processes (i.e. affine jump-diffusion processes) and applying Fourier transform methods as developed in Duffie, Pan and Singleton (1998), I obtain the pricing formulas for various electricity financial instruments. These derivative pricing formulas provide valuable tools to facilitate the trading of electricity financial instruments. I also illustrate the implications by different spot price models on electricity derivative pricing. I confirm the intuition that the jumps and spikes account for the tremendous implied volatility observed in the traded far-out-of-the-money electricity call options. One particular interesting finding is that the jumps and spikes do affect the electricity forward prices due to the nonstorability nature of electricity, whereas if the underlying is storable then this fact would not be true. On the technical side, I incorporate the regime-switching structure into the affine jump-diffusion models for modeling the systematic alternation of electricity prices between the “high state” and the “low state”.

Based on the no-arbitrage principle, I propose a methodology for capacity valuation and project selection in a competitive electricity market in Chapter 4. I start with illustrating how to hedge the operation and production risks by making use of tailored electricity financial instruments or derivatives. In particular, if the value of a physical asset, such as a power plant, is fully derived from the market value of its outputs, then the market risks of owning the asset can be completely hedged by a portfolio of financial instruments on the output commodity (or commodities) which replicates the payoffs of this asset. Furthermore, I claim that, in the absence of transaction costs, the value of the physical asset is given by the value of the replicating portfolio. Such an approach to

asset valuation is termed as the “real options approach”. Applying the pricing formulas developed in Chapter 3, I illustrate how modeling assumptions regarding spot prices such as those proposed in Chapter 3 affect asset valuation outcomes.

Recognizing the fact that there are often transaction costs incurred when exercising the embedded options of a real asset due to the physical characteristics of the asset, I further incorporate the operating characteristics into the real options approach to asset valuation in the context of valuing electric power plants. I employ discrete-time price models for the underlying commodity prices and formulate the valuation of a real asset with operating characteristics such as start-up cost, ramp-up time, and variable heat rate as a stochastic dynamic program. By means of numerical examples, I illustrate that the significance of operating characteristics to power plant valuation varies with modeling assumptions regarding the electricity and the generating fuel price processes. Given price models for electricity and the fuel, the impacts of operational characteristics of a power plant on its valuation is inversely related to its operating efficiency, i.e. the more (less) efficient is a power plant in converting the fuel to electricity, the less (more) affected is its valuation by the operational characteristics.

Finally in Chapter 5, I provide the reader with a summary of this dissertation. I make some observations about the ongoing debates and developments regarding the issues discussed here. I conclude by pointing out several aspects that are left out of my discussions which deserve further investigation for future research.

Chapter 2

Priority Network Access Pricing

Transmission pricing and congestion management protocols are basic ingredients of any restructuring scheme aimed at promoting open access and competition in electricity markets. In this chapter, I propose a transmission network access pricing scheme with the corresponding congestion management protocol which is organized as a priority insurance scheme offered by the ISO to the transmission network users. I contrast this scheme with a few current proposals for charging transmission services in the US.

2.1 Introduction

The Federal Energy Regulatory Commission (FERC) of US has recognized the crucial role of open access to transmission networks in Orders 888 and 889, which provide general principles for the pricing and utilization of scarce transmission capacity. Order 888 required owners of the transmission facilities to provide non-discriminatory transmission services to third-party users under comparable terms and conditions that they would

serve themselves. Order 889 demanded that information regarding the availability and prices of transmission services must be made available to all users of the transmission systems in a timely and non-discriminatory manner.

One of the basic trade-offs involved in implementing FERC's open access ruling is choosing between economic efficiency and the simplicity of pricing and congestion management protocols. While it is generally agreed upon that transmission pricing should provide economic signals that will induce efficient use of the transmission grid, it is not clear how precise such signals must be in order to capture most of the economic benefits from efficient congestion management. It is important to design a mechanism for regulating network access that is simple to implement, facilitates energy trading and will promote efficient network utilization.

Two extreme approaches on the spectrum of promoting short-run operational efficiency are the Contract Network/Nodal Pricing approach (Hogan [21]) on one hand and the so called "postage stamp" approach on the other hand. In the nodal pricing approach, congestion management is performed through a central optimal dispatch, while transmission charges are determined *ex post* and set to the nodal spot price differences (i.e. the market opportunity cost associated with using a particular transmission line). Under the assumption of perfect information (regarding generation cost) and abstraction of intertemporal aspects of the production costs and constraints this approach is "first-best" i.e. it produces the economic dispatch solution. It has been argued, however, that the claimed efficiency of the nodal pricing approach is based on unrealistic assumptions, the implementation of the idealized nodal pricing paradigm is overly complex and it relies on a highly centralized market structure that inhibits competition and

customer choice. Furthermore, the *ex post* determination of the transmission prices is a severe obstacle to efficient bilateral energy trading. (see Wu, Varaiya, Spiller and Oren [38]). The postage stamp approach, on the other hand, imposes a uniform charge on each unit of electricity shipped regardless of anything else (zonal differentiation has also been proposed). The simplicity of the postage stamp approach is compelling and it makes it easy for energy traders to incorporate transmission costs into their trading decisions. Unfortunately even with zonal differentiation this approach does not provide correct economic signals for transmission network usage or for congestion management. Neither does it provide locational economic signals for generation investments.

An alternative to the nodal pricing, which in equilibrium can also achieve the first-best outcome, is proposed by Chao and Peck [6]. It is based on parallel markets for link based transmission capacity rights and energy trading under a set of trading rules imposed by the ISO. The trading rules specify the transmission capacity rights required to support bilateral energy trades between any two buses and are adjusted continuously to reflect changing system conditions. The decentralization in this approach and its reliance on market forces rather than on a central planning paradigm is attractive. However, its implementation would require a highly sophisticated level of electricity markets and information technology. Wilson [35] has demonstrated yet another way to achieve the first-best solution by implementing a priority insurance scheme where the insurance premium varies for each pair of nodes. Neither of the above alternatives to nodal pricing offers a compelling improvement in terms of simplicity which is the primary objective of this paper.

I propose a priority insurance framework for assigning access privileges to the electric-

ity transmission network where the premium or access fee is only differentiated according to the self-selected level of coverage but does not vary across buses (interchangeable with nodes) within a set defined as a congestion zone. Instead, the probability of curtailment associated with each coverage level varies across buses and is endogenously derived from the congestion management protocol employed by the ISO, seeking to minimize net compensation to curtailed transactions. The reduced degrees of freedom in the premium design constrain the resulting equilibrium to produce a second best solution. However, the general direction of the market signals facilitates efficient use of scarce network resources by inducing transactions that have higher opportunity values or that impact more congestion prone segments of the grid to seek higher levels of insurance in order to obtain higher scheduling priorities at their respective buses. Furthermore, the opportunity to under-insure at injection nodes that do not impact congestion allows higher profit margins at such nodes thus providing the correct locational signals for generation investment.

The rest of the chapter is organized as follows. I present the formulation for both cases of a single spot market and multiple zonal spot markets in Section 2.2; in Section 2.3, I demonstrate how this scheme is implemented through numerical examples and evaluate the efficiency losses; in the last section, I conclude with some observations and remarks.

2.2 A priority insurance mechanism

I consider a market design patterned after the California restructuring plan where the network is partitioned into a few congestion zones and consumers in each zone face a uniform zonal spot price for electricity. The transmission system is operated by an Independent System Operator (ISO) that collects transmission service fees and is charged with efficient congestion management. However, the proposed transmission pricing scheme and congestion management protocol are new. I formally define a zone as a subset of nodes sharing a common spot market (See Figure 2.1) All zones are mutually exclusive and collectively exhaustive. In my model, I assume that the transmission network has a fixed transmission capacity configuration and there is no uncertainty as to the availability of the transmission capacity. In each zone i , there exists a single zonal spot price $S_i \equiv S(\omega_i)$ contingent upon a random variable, ω_i , which is given exogenously. The fluctuation of S_i reflects the randomness in the supply and demand conditions. An unexpected hot summer day would cause a surge in demand for electricity, which naturally results in a high value of S_i and increasing usage of the transmission network, possibly causing congestion. In such cases, the ISO needs to have an effective and efficient mechanism to allocate the limited transmission capacity to network users. The proposed scheme offers bulk power traders wishing to engage in physical bilateral transactions a priority differentiated transmission network access tariff specific to the zone in which power is injected. In addition, a bilateral transaction across different zones is subject to an *ex post* congestion charge (or credit) that is equal to the spot price difference between the corresponding zones. It is assumed that curtailed transactions are settled

Electricity Network with Zonal Markets

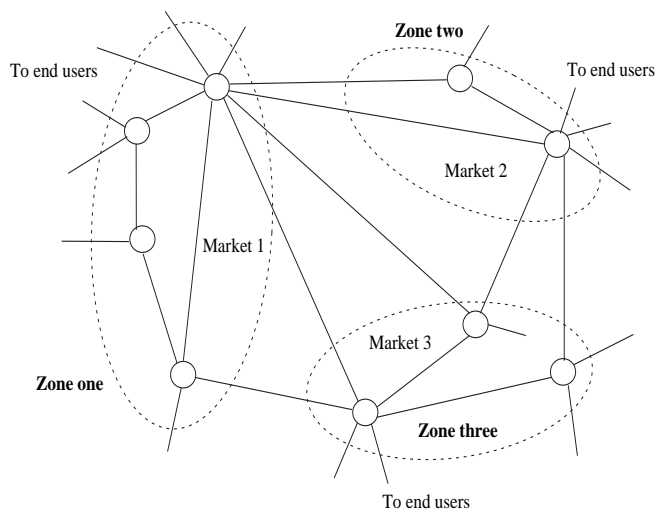


Figure 2.1: An electricity network with several spot markets

either financially or through the purchase of replacement power and that the settlement price equals the spot price at the buyer's zone.

Under the above framework, physical access to a transmission network by a generator producing power at marginal cost $\$c$ per MWh can be valued as a financial “Call” option¹ with strike price c in the zonal spot market corresponding to the injection node. Such an option is exercised only when the zonal spot price S_i in the injection zone i exceeds the strike price and it yields the difference $S_i \Leftrightarrow c$. Hence, the actuarial value of the option is $E_{S_i}[Max(0, S_i \Leftrightarrow c)]$ with expectation taken over the random zonal spot price. Motivated by this observation this transmission pricing scheme proposes to impose a per MWh *ex ante* transmission access charge in the form of an option insurance premium. The premium $X_i(c)$ in zone i equals the option value corresponding to the zonal spot price forecast and a self-selected strike price c determining the curtailment compensation.

¹A financial call option on an asset is a financial contract which provides its holder with the right, but not the obligation, to purchase the underlying asset at a prespecified contract price (or “strike” price) at certain contract maturity time.

This payment would entitle a generator (or trader) to either physical access to the grid or a compensation payment that equals the difference between the realized zonal spot price and the self-selected strike price. The ISO would then relieve congestion so as to minimize total compensation payments to curtailed transactions net of the *ex post* inter-zonal congestion payments.

If each transmission user were to select a strike price that reveals his/her true marginal generation cost, then the above scheme would result in economic dispatch or least cost displacement². Furthermore, network users would be indifferent between physical access and financial compensation. They would accrue zero profit whereas all the gains from producing at a cost below the spot price would go to the ISO (and ultimately to the transmission assets/rights owners). The simplicity of this approach comes from the fact that I use a single transmission access tariff that depends only on the strike price irrespective on the injection node within a zone. However, because of that simplification, users have an incentive to underinsure their transactions by selecting strike prices that are higher than their true marginal costs. In doing so they would estimate the probability of being curtailed and choose a strike price that will maximize their expected profits. Self-selected strike prices will depend on the true marginal cost and the probability of being curtailed at a particular injection node. In general, low marginal cost and high probability of curtailment will induce the selection of a lower strike price, i.e. higher insurance level and higher service priority. Thus, the economic signal for congestion management is in the right direction although not exact.

The proposed mechanism can be described as a three-stage process (Figure 2.2).

²See Proposition 2.2.1.

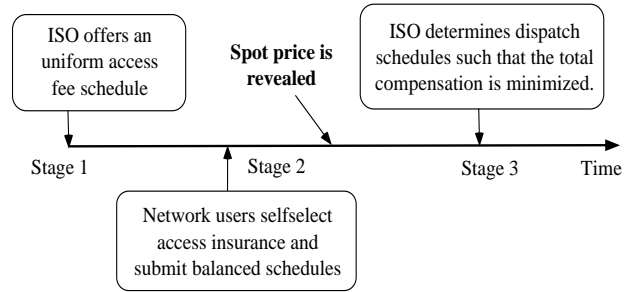


Figure 2.2: Timeline of the priority insurance scheme

Stage one The ISO posts a single insurance schedule $\{c, X_i(c)\}$ in each zone i , where $X_i(c)$ is the premium paid for insurance level c , allowing network users to insure network access rights for their transaction units (multiple units can be insured at different levels)

It is assumed to be common knowledge that, when the spot price, S_i , is revealed, the ISO will manage the network congestion based on the criterion of minimizing total compensation payments net of inter-zonal congestion rent receipts. The implication of this assumption is that network users will form rational expectations about the locational service quality associated with a particular level of insurance at each node. The locational service quality is characterized in terms of a set of spot price contingencies under which transmission access at a specific bus is granted to a transaction unit insured at level c .

Stage two Before the random zonal spot prices are revealed, network users self-select an insurance level on each contracted unit in their schedules so as to maximize their expected profits. They do not need to specify the specific transaction nodes when purchasing their insurance. However, in a multi-zonal case the injection zones need to be revealed at this stage.

The spot price revelation in this time line may be interpreted as an accurate short-term spot price forecast employed by the network users to form their preferred schedule. This would be a more realistic interpretation when the reference settlement prices are the real time spot prices for imbalances.

Stage three At the third and final stage, network users submit their preferred schedules specifying an injection node and a selected insurance level for each transaction unit to the ISO. The ISO then grants transmission access or curtails submitted schedules so as to minimize total compensation payments net of *ex post* congestion revenues for inter-zonal transactions. The curtailed transactions are paid the differences between their revealed opportunity costs and the zonal spot price corresponding to the injection node.

I next layout the formulation in both the single spot market case and the multiple zonal spot markets case. In the following formulations and the remainder of this chapter I use a lossless DC-flow model to approximate the transmission constraints. The formulation can be generalized, however, to account for losses and reactive power and voltage constraints.

2.2.1 Single spot market

When there exists only one spot market in a network, the ISO simply imposes one insurance premium schedule $X(c)$ (**stage one**), which is a decreasing function of the strike price c , for the entire network.

2.1.1 A network user's self-selection problem (stage two) Given the ISO's insurance premium function $X(c)$, a network user at node i subscribes to insurance level c for a transaction unit injecting at node i with true generation (or, opportunity) cost v . By purchasing the insurance, the user expects the transaction unit with insured cost c to obtain network access when the spot price S falls in the region $\Omega_i(c)$ (e.g. $\Omega_i(c) = [v, S_i(c)]$ where $S_i(c) = k_{i1} \Leftrightarrow k_{i2}c$ for some constants k_{i1} and k_{i2}) and be curtailed when the spot price S falls in $\bar{\Omega}_i(c)$, the complement region of $\Omega_i(c)$. With the rational expectation $\Omega_i(c)$, the network user chooses the optimal c so as to maximize expected profit. Namely, the network user at node i would solve the following problem to get the optimal insurance level for a type i transaction unit with true opportunity cost v

$$(NU1) \quad c_i^*(v) = \arg \max_c \int_{\Omega_i(c)} (s \Leftrightarrow v) dG(s) + \int_{\bar{\Omega}_i(c)} (s \Leftrightarrow c)^+ dG(s) \Leftrightarrow X(c) \quad (2.1)$$

where $(s \Leftrightarrow c)^+ \equiv \max(s \Leftrightarrow c, 0)$, and $G(\cdot)$ is the cumulative distribution function of the random variable S .

2.1.2 The ISO problem (stage three) After the random spot price is revealed (or accurately predicted), all network users submit their usage requests as well as their insured cost (insurance level) c for each request. By aggregating the requested transactions according to their injection node and insurance levels the ISO ends up with insured cost distribution curves (or, curtailment supply curves) $\tilde{D}_i(c)$ at each node i . I implicitly assume in this formulation an unlimited supply of displacement power (part of which can be curtailed demand) at the zonal spot price. When the network is congested, the ISO relieves the congestion by curtailing transactions such that the total insurance com-

pensation payment is minimized. That is, for a revealed spot price S , the ISO solves the following minimization problem subject to transmission constraints:

$$\begin{aligned}
& (ISO1) \\
& \min_{\{q_i\}} \quad \sum_{i \in N} \int_{q_i}^{\widetilde{D}_i(s)} [s \Leftrightarrow \widetilde{v}_i(q)] dq \\
& s.t. \quad \sum_{i=1}^n q_i = 0 \\
& \quad \quad q_i = \sum_{j \neq i} q_{ij} \\
& \quad \quad |q_{ij}(q_1, q_2, \dots, q_{n-1})| \leq C_{ij}, 1 \leq i < j \leq n
\end{aligned} \tag{2.2}$$

where $\widetilde{v}_i(\cdot)$ is the inverse function of $\widetilde{D}_i(\cdot)$; q_i is the net amount of power injected or ejected at node i ; $q_{ij}(q_1, q_2, \dots, q_{n-1})$ is the power flow function on line (i, j) ; and C_{ij} is the available capacity of line (i, j) . Therefore, the ISO has a compensation-minimizing dispatch schedule $(q_1^*(s), q_2^*(s), \dots, q_n^*(s))$. And for every realized spot price $S = s$, there exists a corresponding $c_i(s)$ being the marginal insurance level granted transmission access (i.e., allowed to inject power) at node i .

Definition 2.2.1 *The above priority insurance mechanism is coherent in an electricity network if there exists an insurance premium function $X(c)$ and rational expectations of a set of dispatch contingencies $\{\Omega_i(c) : i = 1, 2, \dots, n\}$ for all transactions injecting at node i such that a) $\{\widetilde{D}_i(c)$ for all $i\}$ are the distribution curves of the insured costs of all transaction units resulting from the network users' self-selection problem (NU1); b) $(q_1^*(s), q_2^*(s), \dots, q_n^*(s))$ is a solution to (ISO1) given $\{\widetilde{D}_i(c)$ for all $i\}$ for every revealed spot price s ; c) $q_i^*(s) = \widetilde{D}_i(c_i(s))$ for all i, s .*

I will later show in a more general setup of multiple spot markets that if every network user reveals the truth by purchasing insurance which is equal to the true cost

then this priority insurance scheme results in the economic dispatch (first-best) solutions. However, network users in general have incentives to underinsure their access rights with the aforementioned choice of the insurance premium function. My objective is to identify the coherent priority insurance schemes, to characterize the scheme with the smallest possible deadweight efficiency loss due to imperfect contracting, and to estimate those losses.

2.2.2 Multiple spot markets: zonal pricing

When there exist multiple zonal spot markets and the network is partitioned into several zones, the formulation is some what different. In this case, the ISO offers one insurance premium schedule $X_m(c)$ in each zone m . The ISO charges no *ex post* fee for transactions within one zone but imposes an **additional** *ex post* congestion fee (or counterflow credit) of $S_m \Leftrightarrow S_n$ per unit for transactions going from zone n to zone m , where S_m denotes the random spot price in zone m .

2.2.1 The network user self-selection problem Like in the single spot market case, a network user choosing to purchase insurance level c for one unit injected at node i of zone m , expects physical access when the zonal spot prices S_1, S_2, \dots, S_k fall in the spot price contingency set $\Omega_i(c)$. Thus a network user chooses the optimal c such that the expected profit is maximized. The optimal c for a transaction unit injected at node i belonging to zone $m(i)$ with true cost v is determined by solving the following problem:

$$\begin{aligned}
 (NU2) \quad c_i^*(v) = & \arg \max_c \int_{\Omega_i(c)} (s_{m(i)} \Leftrightarrow v) dG(s_1, \dots, s_k) \\
 & + \int_{\Omega_i(c)} (s_{m(i)} \Leftrightarrow c)^+ dG(s_1, \dots, s_k) \Leftrightarrow X_{m(i)}(c)
 \end{aligned} \tag{2.3}$$

where $\Omega_i(c)$ is the region of spot price contingencies in which the insurance level c would guarantee physical access to the network for a transaction unit injected at node i ; $\bar{\Omega}_i(c)$ is the complement of $\Omega_i(c)$; and $G(\cdot)$ is the joint cumulative distribution function of the random variables $\{S_1, S_2, \dots, S_k\}$.

In practice, we may offer a set of discrete insurance levels $\{c_1, c_2, \dots, c_k\}$ and the corresponding set of premia $\{x_1, x_2, \dots, x_k\}$. If the number of insurance levels is small we may wish to use different sets of insurance levels in different zones. I will illustrate the merits of such an approach through a couple of examples.

2.2.2 The ISO problem By aggregating all submitted insurance levels c , the ISO ends up with curtailment supply curves $\tilde{D}_i(c)$ at each node i . When the network is congested, the ISO relieves the congestion by curtailing transactions so as to minimize the total compensation payments. Namely, the ISO solves the following minimization problem subject to transmission constraints:

$$\begin{aligned}
(ISO2) \quad & \min_{\{q_i\}} \sum_{i \in N_S} \int_{q_i}^{\tilde{D}_i(S_{m(i)})} [S_{m(i)} \Leftrightarrow \tilde{v}_i(q)] dq \Leftrightarrow \frac{1}{k} \sum_{1 \leq m < n \leq k} (S_m \Leftrightarrow S_n) \left(\sum_{j \in Z_m} q_j \Leftrightarrow \sum_{j' \in Z_n} q_{j'} \right) \\
& s.t. \quad \sum_{i=1}^n q_i = 0 \\
& \quad q_i = \sum_{j \neq i} q_{ij}, \quad i = 1, 2, \dots, n. \\
& \quad |q_{ij}(q_1, \dots, q_{n-1})| \leq C_{ij}, \quad 1 \leq i < j \leq n,
\end{aligned} \tag{2.4}$$

where N_S denotes the set of supply nodes; Z_m denotes the node set of zone m ; $m(i)$ denotes the zone to which node i belongs; and q_i is the net amount of power injected or ejected at node i . Hence, the ISO has a compensation-minimizing dispatch schedule

$(q_1^*(s), q_2^*(s), \dots, q_n^*(s))$ for every realized zonal spot price vector (s_1, s_2, \dots, s_m) . There exists again a corresponding $c_i(s_1, s_2, \dots, s_m)$ at node i , which is the insurance level purchased by the marginal transaction unit granted network access at node i for a revealed zonal spot price vector (s_1, s_2, \dots, s_m) . If all network users reveal the truth by purchasing insurance level $c^*(v) = v$ (true cost), then the ISO's compensation-minimizing schedule is indeed the social welfare (gain from trade) maximizing schedule which is defined as follows.

Definition 2.2.2 *For a set of zonal spot prices (S_1, S_2, \dots, S_k) , a dispatch schedule (q_1, q_2, \dots, q_n) is a social welfare maximizing (or, economic dispatch/first-best) schedule if it is a solution to the (ED) problem.*

$$\begin{aligned}
& (ED) \\
& \max_{\{q_i\}} \sum_{i \in N_D} q_i \cdot S_{m(i)} \Leftrightarrow \sum_{i \in N_S} \int_0^{q_i} D_i^{-1}(q) dq \\
& \text{s.t.} \quad \sum_{i=1}^n q_i = 0 \\
& \quad q_i = \sum_{j \neq i} q_{ij}, \quad i = 1, 2, \dots, n. \\
& \quad |q_{ij}(q_1, q_2, \dots, q_{n-1})| \leq C_{ij}, \quad 1 \leq i < j \leq n,
\end{aligned} \tag{2.5}$$

where N_D and N_S denote the demand node set and the supply node set, respectively; $D_i^{-1}(q)$ is the true inverse supply cost curve at supply node i .

I summarize the above as a proposition and provide the proof in the appendix.

Proposition 2.2.1 *Suppose all network users purchase insurance with strike price revealing their true costs, i.e. $c_i^*(v) = v$. Then I have $\widetilde{D}_i(c^*(v)) = D_i(v)$ where $D_i(v)$ is the true cost curve at node i , and the solutions $(q_1^*(s), q_2^*(s), \dots, q_n^*(s))$ of the ISO problems (ISO1 & ISO2) are also the corresponding social welfare maximizing solutions.*

Proof. See Appendix A. ■

The concept of a coherent insurance scheme in the multiple spot markets case is similarly defined as in **Definition 2.2.1** with $(NU2)$ replacing $(NU1)$ and $(ISO1)$ replacing $(ISO2)$.

2.2.3 The choice of premium function $X(c)$

It is important to note that a proper choice of the insurance premium function $X(c)$ by the ISO is key in this scheme. The choices of premium functions provide the self-selection incentives and lead to different insurance purchase distributions with different social welfare implications. In this section I focus on a special case where the ISO chooses $X(c)$ as the expected benefit accrued to a transaction unit, with true cost v being the insured cost c , from physical access to the grid. In the following proposition I show that under this premium function no transaction unit would have any incentive to overinsure its access to the network, i.e., the optimal solution $c^*(v)$ to the self-selection problem is always no less than the true cost v . One of the implications of this result is that there is no adverse selection of revealed injection node at **stage three** where users submit their preferred schedules. If a user were to overinsure, there might be an incentive to reveal a false injection node in order to obtain compensation when the user would have curtailed supply voluntarily due to low spot price realization. But with underinsurance, compensation is never paid when a user's true cost exceeds the spot price and hence there is no incentive for misrepresenting the injection node.

Proposition 2.2.2 *If the ISO chooses*

$$X_m(c) = E_{S_m}(\text{Max}(S_m \Leftrightarrow c, 0)) \quad (2.6)$$

as the insurance premium function in each zone m where $E_{S_m}[\cdot]$ is the expected value operator, then $c^*(v) \geq v$ where $c^*(v)$ is the optimal solution to the self-selection problem (NU1&2) of a transaction unit with true cost v .

Proof. Consider a transaction unit with true cost v . If the unit is overinsured, i.e. $c < v$, then the following is true,

$$\begin{aligned} 0 &= E_{S_m}(\text{Max}(S_m - c, 0)) - X_m(c) \\ &\quad \text{(By the definition of } X_m(c)) \\ &= \int_{\Omega_i(c)} \max(s_{m(i)} - c, 0) dG(s_1, s_2, \dots, s_k) \\ &\quad + \int_{\bar{\Omega}_i(c)} \max(s_{m(i)} - c, 0) dG(s_1, \dots, s_k) - X_{m(i)}(c) \\ &\geq \int_{\Omega_i(c)} \max(s_{m(i)} - v, 0) dG(s_1, s_2, \dots, s_k) \\ &\quad + \int_{\bar{\Omega}_i(c)} \max(s_{m(i)} - c, 0) dG(s_1, \dots, s_k) - X_{m(i)}(c) \end{aligned}$$

The right-hand side expression of the above inequality is the objective function of the self-selection problem (NU2). Since this objective function achieves value zero if the transaction unit is insured at its true cost level v i.e. $c = v$, it follows that $c^*(v) \geq v$. ■

2.3 Numerical examples

In this section, I take a classical three-node network (Figure 2.3) with one spot market to show how a coherent priority insurance scheme is obtained. I then compute the

efficiency loss of the particular scheme with respect to the economic dispatch solution. As previously mentioned, I use a DC-flow approximation and assume no transmission losses in all my examples. In the specific three-node network, each transaction is uniquely characterized by its injection node since I only consider one net demand node. As for examples of the multiple spot markets case, I present a four-node network and a six-node network with two spot markets (two zones) and explore the efficiency properties when network users' choices are restricted to one and two discrete levels of insurance in each zone.

2.3.1 Single spot market: three-node network

Consider a three node network with transmission line capacity

$$(C_{12}, C_{13}, C_{23}) = (136MW, 300MW, 254MW)$$

and equal admittance of 1. Node 3 is the location of the spot market with uniformly

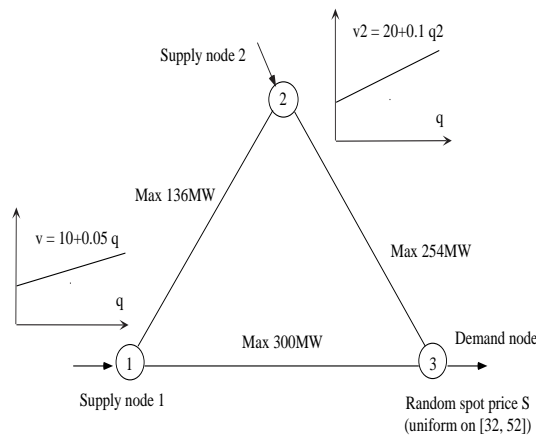


Figure 2.3: A three-node network

distributed random spot price $S \sim U(32, 52)$. The cumulative distribution function of S is:

$$G(s) = \begin{cases} 0 & , \quad s \leq 32 \\ \frac{s \Leftrightarrow 32}{20} & , \quad 32 < s \leq 52 \\ 1 & , \quad s > 52 \end{cases} \quad (2.7)$$

I first compute the economic dispatch (first-best) solution for each realization of the spot price S and the expected social welfare (gain from trade) of the first-best solutions. A social planner's objective of maximizing social welfare is equivalent to minimizing the shaded areas representing the displacement costs, as depicted in Figure 2.4. Therefore, a social welfare maximizing ISO solves the following problem to obtain the economic dispatch for a realized $S(\omega) = s$:

$$\begin{aligned} SW(s) &\equiv \min_{(q_1, q_2, q_3)} \sum_{i=1}^2 \int_{q_i}^{D_i(s)} [s \Leftrightarrow v_i(q)] dq \\ s.t. \quad &\sum_{i=1}^3 q_i = 0 \\ &\begin{pmatrix} \Leftrightarrow 136 \\ \Leftrightarrow 254 \\ \Leftrightarrow 300 \end{pmatrix} \leq \begin{pmatrix} \frac{1}{3} & \Leftrightarrow \frac{1}{3} \\ \frac{1}{3} & \frac{2}{3} \\ \Leftrightarrow \frac{2}{3} & \Leftrightarrow \frac{1}{3} \end{pmatrix} \begin{pmatrix} q_1 \\ q_2 \end{pmatrix} \leq \begin{pmatrix} 136 \\ 254 \\ 300 \end{pmatrix}. \end{aligned} \quad (2.8)$$

where q_i is the quantity of power injected or ejected at node i ($i = 1, 2, 3$). For any realization of the spot price $S = s$, the solution of (2.8) is given by

$$\begin{cases} \hat{q}_1 = \frac{20}{9}(210 \Leftrightarrow s) \\ \hat{q}_2 = \frac{20}{9}(2s \Leftrightarrow 15) \\ \hat{q}_3 = \Leftrightarrow \frac{20}{9}(s + 195) \end{cases} \quad , \quad 32 \leq s \leq 52 \quad (2.9)$$

And the expected social welfare is $E[SW] = 10697$.

Objective of Economic Dispatch with
True Cost Curves

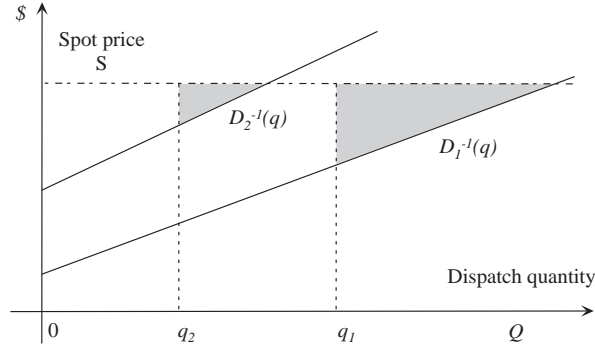


Figure 2.4: Objective of economic dispatch

I now turn to the computation of a coherent priority insurance scheme where the ISO posts the insurance premium function $X(c)$ given in (2.10). The economic interpretation of $X(c)$ is that it equals the expected benefit accrued to a transaction unit with true unit cost c receiving physical access to the network and hence avoiding a settlement cost at the spot market price. This premium can also be interpreted as the actuarial value of a financial “call option” with strike price c with respect to the underlying spot market.

$$\begin{aligned}
 X(c) &= E_S[\max(S \Leftrightarrow c, 0)] \\
 &= \begin{cases} 42 \Leftrightarrow c & , \quad 0 \leq c \leq 32 \\ \frac{1}{40}(52 \Leftrightarrow c)^2 & , \quad 32 < c \leq 52 \\ 0 & , \quad c > 52 \end{cases} \quad (2.10)
 \end{aligned}$$

I conjecture that a network user who selects insurance level (or, insured cost) c for a transaction injected at node 1 expects the transaction unit to get access for $S \in [\max(32, v), S_1(c)]$ where $S_1(c) = k_1 \Leftrightarrow k_2 c$ and k_i ($i = 1, 2$) is a parameter to be calculated. The degrees of freedom in computing the rational expectation equilibrium allow us to parameterize the contingency set, in which access is provided, in terms of a two parameter

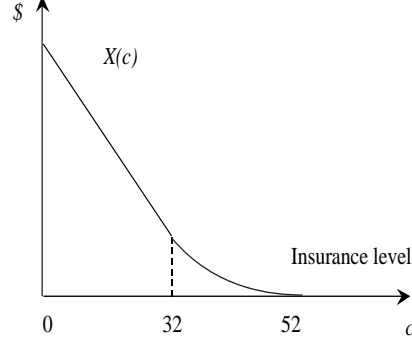


Figure 2.5: Insurance premium function

linear function defining $S_1(c)$. Then the optimal c chosen for a transaction unit with true cost v injected at node 1 is given by the solution of the following problem

$$\begin{aligned}
c_1^*(v) &= \arg \max_c \int_{\max(v,32)}^{S_1(c)} (s \Leftrightarrow v) dG(s) + \int_{S_1(c)}^{52} (s \Leftrightarrow c)^+ dG(s) \Leftrightarrow X(c) \\
&= \begin{cases} \underline{c}_1 & , \quad v \leq v'_1 \\ \frac{(k_1-32)+k_2 v}{2k_2} & , \quad v'_1 < v \leq v''_1 \\ \bar{c}_1 & , \quad v > v''_1 \end{cases} \quad (2.11)
\end{aligned}$$

Similarly, I conjecture that the spot price interval in which a unit transaction with insurance level c injecting at node 2 gets access takes the form of $[S_2(c), 52]$ where $S_2(c) = k_3 + k_4 c$ and k_i ($i = 3, 4$) is a parameter to be calculated. Then the optimal insurance level for a transaction unit with true cost v injected at node 2 is determined by the self-selection problem:

$$\begin{aligned}
c_2^*(v) &= \arg \max_c \int_{\max(c,32)}^{S_2(c)} (s \Leftrightarrow c) dG(s) + \int_{S_2(c)}^{52} (s \Leftrightarrow v) dG(s) \Leftrightarrow X(c) \\
&= \begin{cases} \underline{c}_2 & , \quad v \leq v'_2 \\ \frac{(52-k_3)+k_4 v}{2k_4} & , \quad v'_2 < v \leq v''_2 \\ \bar{c}_2 & , \quad v > v''_2 \end{cases} \quad (2.12)
\end{aligned}$$

For each S , I obtain the marginal insurance levels c_1 and c_2 at node 1 and 2, respectively, such that $S = k_1 \Leftrightarrow k_2 c_1(S) = k_3 + k_4 c_2(S)$. The shapes of the resulting inverse insurance distribution curves $\tilde{D}_i^{-1}(q)$ ($i = 1, 2$) are illustrated in Figure (6). When the

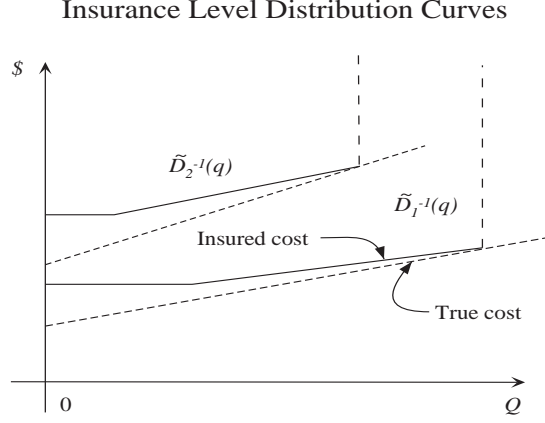


Figure 2.6: Insured cost distribution curves

random spot price is revealed, network users submit their usage requests along with their insurance levels. Therefore, the above insurance distribution (or, curtailment supply) curves $\tilde{D}_i(c)(i = 1, 2)$ are revealed to the ISO. In case of network congestion, the ISO determines dispatch schedules based on the criterion of minimizing total curtailment compensation payments, i.e. the ISO solves (2.13).

$$\begin{aligned}
 IP(s) &\equiv \min_{(q_1, q_2, q_3)} \sum_{i=1}^2 \int_{q_i}^{\tilde{D}_i(s)} [s \Leftrightarrow \tilde{D}_i^{-1}(q)] dq \\
 s.t. & \sum_{i=1}^3 q_i = 0 \\
 & \begin{pmatrix} \Leftrightarrow 136 \\ \Leftrightarrow 254 \\ \Leftrightarrow 300 \end{pmatrix} \leq \begin{pmatrix} \frac{1}{3} & \Leftrightarrow \frac{1}{3} \\ \frac{1}{3} & \frac{2}{3} \\ \Leftrightarrow \frac{2}{3} & \Leftrightarrow \frac{1}{3} \end{pmatrix} \begin{pmatrix} q_1 \\ q_2 \end{pmatrix} \leq \begin{pmatrix} 136 \\ 254 \\ 300 \end{pmatrix}.
 \end{aligned} \tag{2.13}$$

The solution of (2.13) is

$$\begin{cases} q_1^* = \frac{20}{k_2}(30 + k_1 \Leftrightarrow 10k_2 \Leftrightarrow 2s) \\ q_2^* = \frac{10}{k_4}(2s \Leftrightarrow k_3 \Leftrightarrow 20k_4 \Leftrightarrow 29) , & 32 \leq s \leq 52 \\ q_3^* = \Leftrightarrow q_1^* \Leftrightarrow q_2^* \end{cases} \quad (2.14)$$

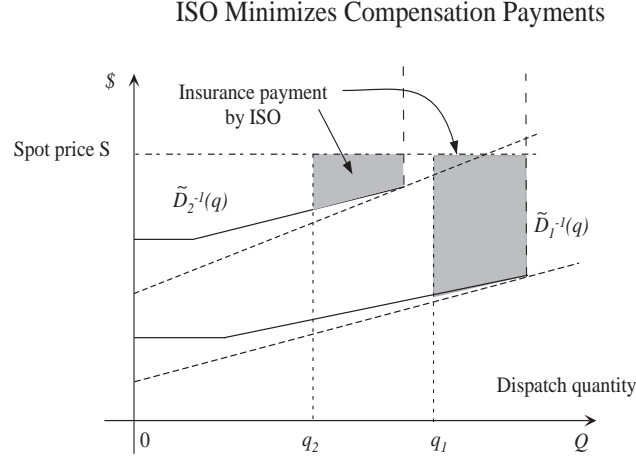


Figure 2.7: Objective of the ISO's minimization problem

Figure (2.7) gives a graphic representation of the ISO's objective of minimizing total insurance payments based on the revealed insured cost distribution curves.

Invoking the equilibrium condition c) in **Definition 2.2.1**, I solve for the free parameters of the rational expectation equilibrium and obtain $\{k_1 = 317.78, k_2 = 9, k_3 = \Leftrightarrow 39.72, k_4 = 2.25\}$. The resulting network access contingency sets corresponding to the rational expectation equilibrium are characterized by the boundary functions $\{S_i(c), i = 1, 2\}$, given by:

$$\begin{cases} S_1(c) = \begin{cases} \Leftrightarrow 9c + 317.78 & \text{for } c \in [29.53, 31.75] \\ 0 & \text{o.w.} \end{cases} \\ S_2(c) = \begin{cases} 2.25c \Leftrightarrow 39.72 & \text{for } c \in [31.88, 40.77] \\ \infty & \text{o.w.} \end{cases} \end{cases} \quad (2.15)$$

The spot price contingency sets in which network access is granted to each insurance level at the two supply nodes are illustrated in Figure (2.8). I substitute the solution

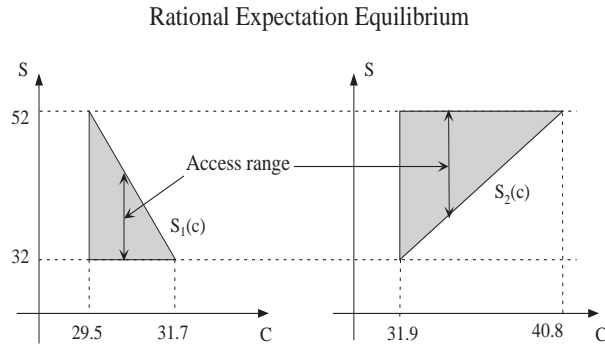


Figure 2.8: Rational expectation of network access price interval

$\{k_i, i = 1, 2, 3, 4\}$ into (2.14) and get the induced dispatch schedules $\{(q_1^*(s), q_2^*(s)), 32 \leq s \leq 52\}$ under the above priority insurance scheme. The expected social welfare of the induced schedules is $E[SW^*] = 10593$. This amounts to only 0.974% efficiency loss. For this simple example, my calculation shows that the efficiency losses associated with the minimum compensation dispatch solution under the priority insurance scheme is rather small when compared to the first-best solution. Figure 2.9 illustrates a comparison between the economic dispatch (first-best) solution and the minimum compensation (second best) for every realization of the spot price S . To check the robustness of the above result I perform a modest sensitivity analysis calculating the efficiency loss for slightly varied different sets of parameters. Basically, I vary the fixed costs of the true cost distribution curves so as to change the difference between true supply functions at the different supply nodes. The computation results reported in Table (2.1) indicate

First Best .vs. Second Best

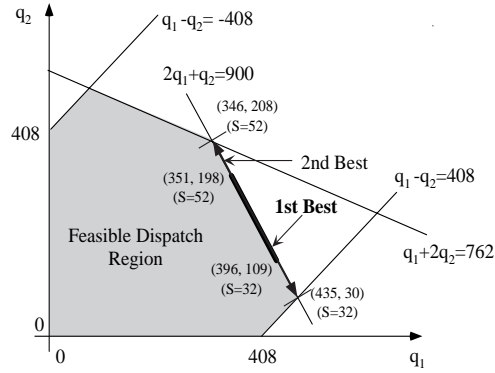


Figure 2.9: The comparison between 1st best and 2nd best solutions

that the efficiency losses are still of similar magnitudes.

Parameter set	$\begin{cases} v_1 = 9 + 0.05q_1 \\ v_2 = 22.5 + 0.1q_2 \end{cases}$	$\begin{cases} v_1 = 10 + 0.05q_1 \\ v_2 = 20 + 0.1q_2 \end{cases}$	$\begin{cases} v_1 = 10 + 0.05q_1 \\ v_2 = 23 + 0.1q_2 \end{cases}$
Efficiency loss	0.972 %	0.974 %	1.01 %

Table 2.1: Sensitivity of Efficiency Loss

2.3.2 Multiple spot markets: 4-node and 6-node networks

I next turn to the multiple zonal spot markets case. Consider a 4-node network with two spot markets and two supply nodes as shown in Figure (2.10). Node 1 and 4 belong to zone one while node 2 and 3 belong to zone two. The dashed line in Figure (2.10) represents the boundary of the two zones. The link 3-4 connecting the two zones is the only congested link with line-flow capacity of 80MW. All lines are of equal impedance of one. I assume the spot prices in zone 1 and zone 2 are jointly uniformly distributed over interval $[28, 32] \times [32, 40]$. The marginal distributions are $S_2 \sim U[28, 32]$ and $S_4 \sim$

Example: 4-node network

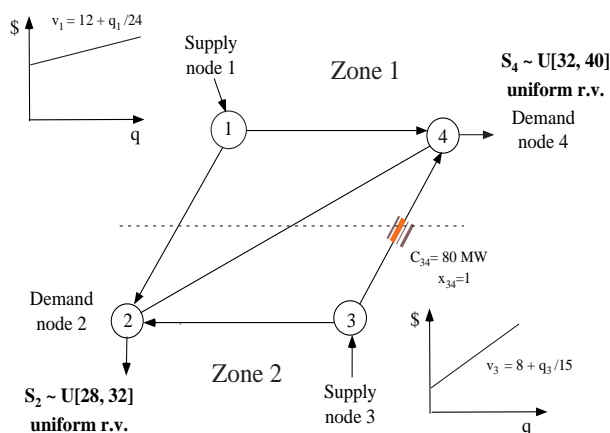


Figure 2.10: An example of four-node network

$U[32, 40]$, respectively. The true marginal cost functions at node 1 and node 3 are:

$$\begin{cases} v_1 = 12 + q_1/24 \\ v_3 = 8 + q_3/15 \end{cases} \quad (2.16)$$

The economic dispatch (first-best) solution for any given spot price vector (s_2, s_4) is given by

$$\begin{cases} \hat{q}_1 = \frac{12(s_2 + s_4 \Leftrightarrow 24)}{\Leftrightarrow 3056 + 399s_2 \Leftrightarrow 201s_4} \\ \hat{q}_2 = \frac{4}{15(5s_2 \Leftrightarrow 3s_4 \Leftrightarrow 16)} \\ \hat{q}_3 = \frac{1424 \Leftrightarrow 201s_2 + 159s_4}{4} \\ \hat{q}_4 = \frac{2}{4} \end{cases} \quad (2.17)$$

The expected social welfare of the first-best solutions is $E_S[SW] = 8652$.

I consider the simplest situation where the ISO offers a one-level insurance scheme in the two zones, i.e. network users selections are restricted to $\{c^1, x_i^1\}$ or $\{\infty, 0\}$ in zone i ($i = 1, 2$) where c^1 is the insurance level and x_i^1 is the corresponding insurance premium

in zone i ($i = 1, 2$). x_i^1 is given by $X_i(c^1)$ ($i = 1, 3$) where

$$\begin{aligned} X_1(c) &= E_{S_4}[\max(S_4 \Leftrightarrow c, 0)] \\ &= \begin{cases} 36 \Leftrightarrow c & , \quad c \leq 32 \\ \frac{1}{16}(40 \Leftrightarrow c)^2 & , \quad 32 < c \leq 40 \\ 0 & , \quad c > 40 \end{cases} \end{aligned} \quad (2.18)$$

and

$$\begin{aligned} X_3(c) &= E_{S_2}[\max(S_2 \Leftrightarrow c, 0)] \\ &= \begin{cases} 30 \Leftrightarrow c & , \quad c \leq 28 \\ \frac{1}{8}(32 \Leftrightarrow c)^2 & , \quad 28 < c \leq 32 \\ 0 & , \quad c > 32 \end{cases} \end{aligned} \quad (2.19)$$

A network user's self-selection problem amounts to the individual rationality condition, namely, the optimal insurance level $c_i^*(v)$ for a transaction unit with true cost v in zone i ($i = 1, 2$) equals c^1 if and only if the expected benefit of purchasing c^1 is no less than 0. The ISO minimizing insurance compensation problem is

$$\begin{aligned} \min_{\{q_i; q_i^\alpha\}} & \sum_{i=1,3} \sum_{\alpha=0}^1 p_i^\alpha (\bar{q}_i^\alpha(S) \Leftrightarrow q_i^\alpha) \Leftrightarrow (S_4 \Leftrightarrow S_2)(q_3 \Leftrightarrow q_2) \\ \text{s.t.} & \quad q_i = \sum_{\alpha=0}^1 q_i^\alpha \quad (i = 1, 3) \\ & \quad q_1 + q_3 \Leftrightarrow q_2 \Leftrightarrow q_4 = 0 \\ & \quad |q_{ij}(q_1, q_2, q_3)| \leq C_{ij} \\ & \quad q_i^\alpha \leq \bar{q}_i^\alpha(S) \quad (i = 1, 3; \alpha = 0, 1) \\ & \quad q_i \geq 0, q_i^\alpha \geq 0, \quad \forall i, \forall \alpha, \end{aligned} \quad (2.20)$$

where

S denotes a realization of random spot price vector (S_2, S_4)

q_i^1 is the number of access requests with insurance c^1 which are granted network access at node i ($i = 1, 3$)

q_i^0 is the number of uninsured access requests which are granted network access at node i ($i = 1, 3$)

$\bar{q}_i^1(S)$ is the total number of access requests with insurance c^1 at node i ($i = 1, 3$) for the realized spot price vector S

$\bar{q}_i^0(S)$ is the total number of uninsured access requests at node i ($i = 1, 3$) for the realized spot price vector S

$p_1^1 = \max(S_4 \Leftrightarrow c^1, 0)$, $p_3^1 = \max(S_2 \Leftrightarrow c^1, 0)$ are the insurance payments

$p_i^0 = 0$ ($i = 1, 3$)

By varying the insurance level c^1 , I calculate several equilibrium solutions and find that the social welfare efficiency losses is not very sensitive to the choice of insurance level c^1 . Taking $c^1 = 28.5$, the solution to the ISO problem for any realized $(S_2, S_4) \in [28, 32] \times [32, 40]$ is

$$\left\{ \begin{array}{ll} q_1 = 396MW, & q_2 = 0MW \\ q_3 = 48.8MW, & q_4 = 444.8MW; \quad \text{if } 5s_2 \Leftrightarrow 3s_4 \leq 57 \\ q_1 = 396MW, & q_2 = 646.75MW \\ q_3 = 307.5MW, & q_4 = 56.75MW; \quad \text{if } 5s_2 \Leftrightarrow 3s_4 > 57 \end{array} \right. \quad (2.21)$$

which yield an expected social welfare of 7254.0. The calculation accounts for random rationing among insured access requests when transmission constraints prohibit schedul-

ing of all such requests. The corresponding efficiency loss is equal to 16.15%, which is roughly the smallest efficiency loss achievable with one insurance level.

I now consider a two-level insurance scheme with one insurance level in each zone, i.e. network users selections are restricted to $\{c_i^1, x_i^1\}$ or $\{\infty, 0\}$ in zone i ($i = 1, 2$) and $c_1^1 \neq c_2^1$. The ISO compensation minimization problem becomes:

$$\begin{aligned}
& \min_{\{q_i; q_i^\alpha\}} \sum_{i=1,3} \sum_{\alpha=0}^1 p_i^\alpha (\bar{q}_i^\alpha(S) \Leftrightarrow q_i^\alpha) \Leftrightarrow (S_4 \Leftrightarrow S_2)(q_3 \Leftrightarrow q_2) \\
& \text{s.t.} \quad q_i = \sum_{\alpha=0}^1 q_i^\alpha \quad (i = 1, 3) \\
& \quad q_1 + q_3 \Leftrightarrow q_2 \Leftrightarrow q_4 = 0 \\
& \quad |q_{ij}(q_1, q_2, q_3)| \leq C_{ij} \\
& \quad q_i^\alpha \leq \bar{q}_i^\alpha(S) \quad (i = 1, 3; \alpha = 0, 1) \\
& \quad q_i \geq 0, q_i^\alpha \geq 0, \quad \forall i, \forall \alpha,
\end{aligned} \tag{2.22}$$

where

S denotes a realization of random spot price vector (S_2, S_4)

q_i^1 is the number of access requests with insurance c_i^1 which are granted network access at node i ($i = 1, 3$)

q_i^0 is the number of uninsured access requests which are granted network access at node i ($i = 1, 3$)

$\bar{q}_i^1(S)$ is the total number of access requests with insurance c_i^1 at node i ($i = 1, 3$) for the realized spot price vector S

$\bar{q}_i^0(S)$ is the total number of uninsured access requests at node i ($i = 1, 3$) for the realized spot price vector S

$p_1^1 = \max(S_4 \Leftrightarrow c_1^1, 0)$, $p_3^1 = \max(S_2 \Leftrightarrow c_3^1, 0)$

are the insurance payments

$p_i^0 = 0$ ($i = 1, 3$)

For the instance of $c_1^1 = 30$ and $c_2^1 = 21$, the total number of insured access requests under all possible realizations of $(S_2, S_4) \in [28, 32] \times [32, 40]$ at nodes 1 and 3, $\bar{q}_1^1(S)$ and $\bar{q}_3^1(S)$, are $432MW$ and $195MW$, respectively. Given $S = (s_2, s_4)$, the solutions to the ISO compensation minimization problem are:

$$\left\{ \begin{array}{ll} q_1 = 432MW, & q_2 = 0MW \\ q_3 = 41.6MW, & q_4 = 473.6MW; \text{ if } 5s_2 \Leftrightarrow 3s_4 \leq 42 \\ \\ q_1 = 432MW, & q_2 = 383.5MW \\ q_3 = 195MW, & q_4 = 243.5MW; \text{ if } 5s_2 \Leftrightarrow 3s_4 > 42 \end{array} \right.$$

The above dispatch schedules yield an expected social welfare of 8156.3, which amounts to an efficiency loss of 5.7% when compared to the expected social welfare of economic dispatch solutions. Note that given the rational expectation about the ISO minimum compensation dispatch over the corresponding spot price contingency region, the expected benefit for a transaction unit with true cost v purchasing c_1^1 and c_2^1 are $(c_1^1 \Leftrightarrow v)$ and $91(c_2^1 \Leftrightarrow v)/150$, respectively. Therefore the marginal insurance purchasing units at node 1 and node 2 have true costs of $v_1^* = c_1^1 = 30$ and $v_3^* = c_2^1 = 21$, respectively. By adding one more insurance level in each zone in the previous two-level insurance example, e.g. taking $c_1^1 = 30$ $c_1^2 = 31.5$ and $c_2^1 = 21$ $c_2^2 = 27$, I reduce the efficiency loss from 5.7% to 4.4%.

I further examine this scheme on a 6-node network which is similar to the example used in Chao and Peck [4]. A 6-node network divided into two interconnected zones is shown in Figure (2.11). Zone I consists of nodes 1, 2 and 3, and zone II consists of nodes 4, 5 and 6. Suppose congestion only occur to line 1-6 and line 4-6. The physical

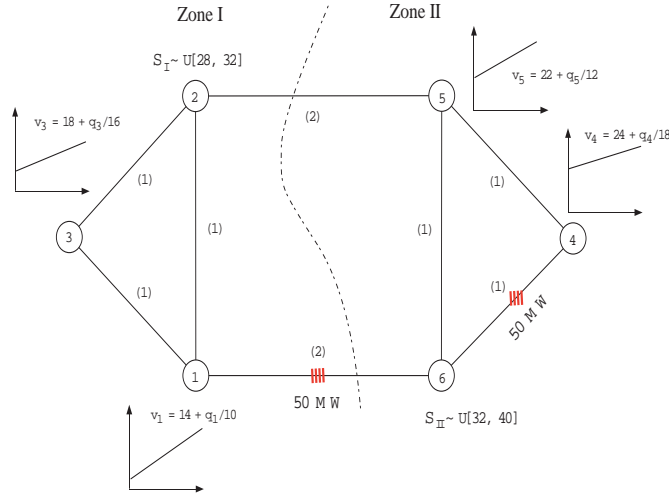


Figure 2.11: An example of six-node network

transmission capacities for the two lines are 50 MW each. The line resistances are given by the numbers in parentheses.

I assume that nodes 1, 3, 4 and 5 are the supply nodes, and nodes 2 and 6 are the demand nodes. The marginal cost functions at these nodes is summarized in Table (2.1). Again, the spot prices in zone 1 and zone 2 are assumed to be jointly uniformly

Node	Supply Function
1	$14 + q/10$
3	$18 + q/16$
4	$24 + q/18$
5	$22 + q/12$

Table 2.1: Supply functions

distributed over interval $[28, 32] \times [32, 40]$. The marginal distributions are $S_I \sim U[28, 32]$ and $S_{II} \sim U[32, 40]$, respectively. Let the ISO offer a two-level priority insurance scheme in each zone where the insurance levels are $c_1^1 = 26.8$ $c_1^2 = 30$ and $c_2^1 = 26.8$ $c_2^2 = 31$. The insurance premiums are given by (2.6). As I compute for the expected social welfare loss due to the ISO minimizing total insurance compensation, it is 4.58% of the expected social welfare of the first-best solutions. We shall note that these insurance levels are

not optimized to achieve the minimum efficiency loss. It is reasonable to expect that optimizing the insurance levels and adding more levels of insurance in each zone will further reduce the efficiency loss to an acceptable level.

2.4 Conclusion

At the intuitive level, this scheme can be viewed as a hybrid of priority insurance and a postage-stamp approach. The different levels of insurance characterized by the revealed opportunity costs may be interpreted as postage stamps with different priorities. These priorities allow for network users self-selection which in turn provides economic signals for the efficient rationing of scarce transmission resources. With a single zone in a transmission network, since the admissible insurance schemes is constrained to be uniform, a first-best solution cannot be expected. However, if we partition a network into more zones and allow more different insurance premium schedules to be offered, the efficiency gains can be improved. The limiting case, where the insurance scheme is node specific, is equivalent to a nodal pricing approach. In essence, this scheme takes out part of the time and locational “price variability” present in a nodal pricing scheme and allows “quantity variability” in the form of uncertain access at a given price. Stable prices with a measure of uncertainty in service quality is a prevalent practice in most service industries. What is important to realize is that the proposed pricing scheme and the corresponding congestion management protocols are quite simple. The mathematical complexity is in attempting to calculate the market equilibrium. In reality, that part is performed by the market itself.

Another important point to be made concerns the magnitude of the efficiency losses we have observed in my examples. My calculations for the discrete priority insurance levels resulted in efficiency losses ranging from 3 \leftrightarrow 5% which are quite significant if such losses were indeed persistent. Fortunately that is not the case. These losses were calculated under the assumption that congestion exists within the zone. In reality, zonal boundaries are defined so that intra-zonal congestion is rare. Typically, congestion may be present within a zone for at most 200 hours per year (about 2.5% of the time) which under worse case scenario may represent 10% of net annual social surplus. Hence, a 5% efficiency loss during periods of intra-zonal congestion would average to under 0.5% annual efficiency loss. This estimate is consistent with recent results by Green [16] who calculated efficiency losses due to zonal aggregation (with no intra-zonal priority pricing) in the UK system and estimated these losses at under 1% of social welfare.

Chapter 3

Stochastic Models for Electricity

Prices

Electricity markets emerge and grow rapidly as the restructuring of electricity supply industries is spreading in the United States and around the world. The global trend of electricity market reforms exposes the portfolios of generating assets and various supply contracts held by traditional electric power utility companies and the independent power producers to market price risks. Risk management and asset valuation needs require in-depth understanding and sophisticated modeling of electricity spot prices. Primarily motivated by the surging demands for risk management and asset valuation due to deregulation in the \$200 billion US electricity industry, I investigate the modeling of electricity prices in this chapter. The introduction part of Chapter 4 provides a detailed description of the various applications of the modeling methodology developed in this chapter.

3.1 Introduction

As noted in Chapter 1, modeling the price behaviors of electricity is a very challenging task for researchers and practitioners due to the distinguishing characteristics of electricity. First of all, electricity can not be stored or inventoried economically once generated. Moreover, electricity supply and demand has to be balanced continuously so as to prevent the electric power networks from collapsing. Electricity spot prices are extremely volatile because the supply and demand shocks cannot be smoothed by inventories. As for how volatile the electricity prices can be, the wholesale prices of electricity fluctuated between \$0/MWh and \$7000/MWh in the Midwest of US during the summer of 1998. It is not uncommon to see a 150% implied volatility in traded electricity options. Figure

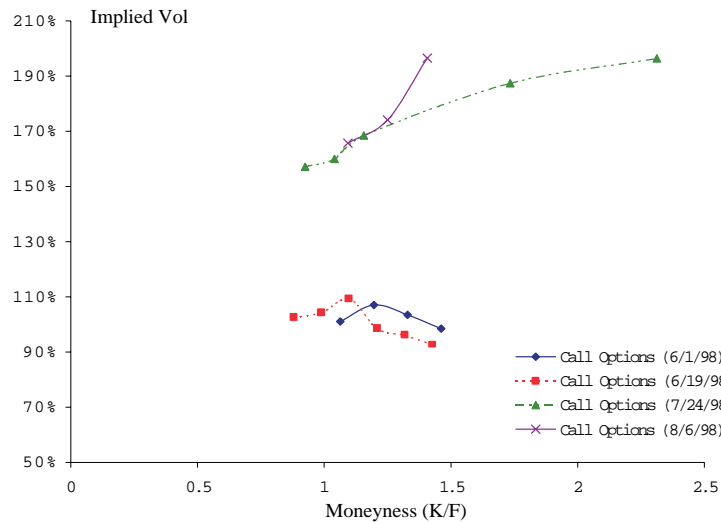


Figure 3.1: Implied Volatility of Call (Sept.) Options at Cinergy

(3.1) plots the implied volatility of electricity call options in the Midwestern US (Cinergy) across different strike prices at different points in time where the x-axis represents

the “moneyness”, i.e. the strike prices divided by the corresponding forward prices. On top of the tremendous levels of volatility, the highly seasonal patterns of electricity prices also complicate the modeling issues.

Recall from Chapter 1 that the most noticeable features of electricity prices are mean-reversion and the presence of price jumps and spikes. Figure (3.2) shows the historical on-peak electricity spot prices in Texas (ERCOT) and at the California and Oregon border (COB). I have explained the intuitions behind the mean-reversion and jumps in

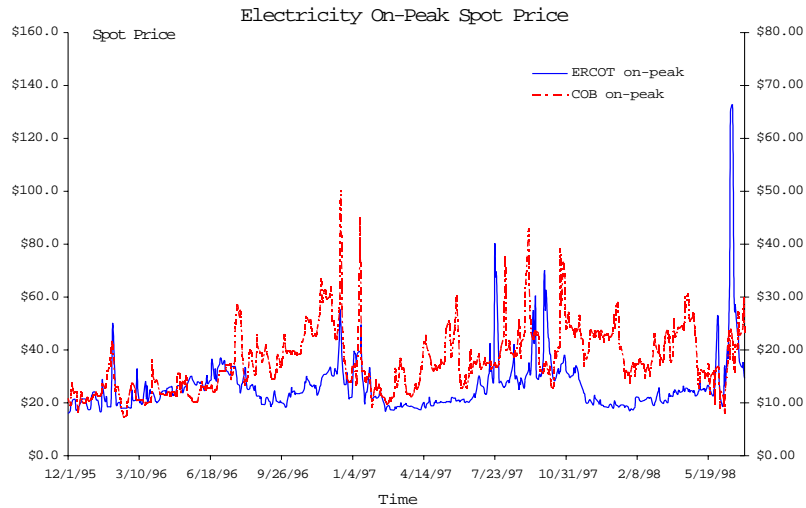


Figure 3.2: Electricity Historical Spot Prices

electricity prices in Chapter 1. When the contingency making the electricity price to jump high is short-term in nature, the high price will quickly fall back down to the normal range as the contingency disappears thus causing a spike in the electricity price process. In the summer of 1998, we observed the spot prices of electricity in the Eastern and the Midwestern US skyrocketing from \$50/MWh to \$7000/MWh because of the unexpected unavailability of some major power generation plants as well as the congestion on key

transmission lines. Within a couple of days the prices fell back to the \$50/MWh range as the lost generation and transmission capacities were restored. Electricity prices may also exhibit regime-switching, caused by weather patterns and varying precipitation, in markets where the majority of installed electricity supply capacity is hydro power such as in the Nord Pool and the Victoria Pool.

There have been few studies on modeling electricity prices since electricity markets only came into existence a few years ago in US. Schwartz (1997), and Miltersen and Schwartz (1998) are two of the most recent papers which concern the modeling of commodity spot prices. They investigate several stochastic models for commodity spot prices and performed an empirical analysis based on copper, gold and crude oil price data. They find that stochastic convenience yields could explain the term structure of forward prices and demonstrate the implications to hedging and real asset valuation by different models. Hilliard and Reis (1998) consider the effects of jumps and other factors in the spot price on the pricing of commodity futures, forwards, and futures options. One particular finding is that the jump in the spot price does not affect forward or futures prices. However, as I will illustrate later, this may not be true if the underlying commodity is almost non-storable such as electricity. Kaminski (1997) as well as Barz and Johnson (1998) are two papers on modeling electricity prices. Kaminski (1997) points out the needs of introducing jumps and stochastic volatility in modeling electricity prices. The Monte-Carlo simulation is used for pricing electricity derivatives under the jump-diffusion price models. Barz and Johnson (1998) suggest the inadequacy of the Geometric Brownian motion and mean-reverting process in modeling electricity spot prices. With the objective of reflecting the key characteristics of electricity prices, they

offer a price model which combines a mean-reverting process with a single jump process. However, they do not provide analytic results regarding derivative valuation under their proposed price model.

While some energy commodities, such as crude oil, may be properly modeled as traded securities, the nonstorability of electricity makes such an approach inappropriate. However, we can always view the spot price of electricity as a state variable. All the physical contracts/financial derivatives on electricity are therefore contingent claims on the state variable. In this chapter, I examine a broad class of stochastic models which can be used to model price characteristics such as jump, stochastic volatility, as well as stochastic convenience yield. I feel that models with jumps and stochastic volatility are particularly suitable for modeling the electricity price processes.

I specify the electricity price processes as affine jump-diffusion processes which were introduced in Duffie and Kan (1996). Affine jump-diffusion processes are flexible enough to allow me to capture the special characteristics of electricity prices such as mean-reversion, seasonality, and spikes¹. More importantly, I am able to compute the prices of various electricity derivatives under the assumed underlying affine jump-diffusion price processes by applying the transform analysis developed in Duffie, Pan and Singleton (1998). I consider not only the usual affine jump-diffusion models but also a regime-switching mean-reversion jump-diffusion model. The regime-switching model is used to model the random alternations between “abnormal” and “normal” equilibrium states of supply and demand for electricity.

The remainder of this chapter is organized as follows. In the next section, I propose

¹ “Spikes” refers to upward jumps followed shortly by downward jumps.

three alternative electricity price models and compute the transform functions needed for contingent-claim pricing. In Section 3.3, I present illustrative examples of the models specified in Section 3.2 and derive the pricing formulae of several electricity derivatives. The comparisons of the prices of electricity derivatives under different models are shown. I also provide a heuristic method for estimating the model parameters by matching moment conditions using historical spot price data and calibrating the parameters to prices of traded options. Section 3.4 concludes the chapter.

3.2 Mean-Reverting Jump-Diffusion Price Models

Keeping in mind the objective of capturing prominent physical characteristics of electricity prices such as mean-reversion, regime-switching, stochastic volatility, and jumps/spikes, I examine the following three types of mean-reverting jump-diffusion electricity price models.

1. Mean-reverting jump-diffusion price process with deterministic volatility.
2. Mean-reverting jump-diffusion price process with regime-switching.
3. Mean-reverting jump-diffusion price process with stochastic volatility.

I consider two types of jumps in all of the above models. While this analytical approach could handle multiple types of jumps, I feel that, with properly chosen jump intensities, two types of jumps suffice in mimicking the jumps and/or spikes in the electricity price processes. The case of one type of jumps is included as a special case when the intensity of type-2 jump is set to zero.

In addition to the electricity price process under consideration, I also jointly specify another factor process which can be correlated with the underlying electricity price. This additional factor could be the price of the generating fuel such as natural gas, or something else, such as the aggregate physical demand of electricity. A jointly specified price process of the generating fuel is essential for risk management involving cross commodity risks between electricity and the fuel. There is empirical evidence demonstrating a positive correlation between electricity prices and the generating fuel prices in certain geographic regions during certain time periods of a year. In all models the risk free interest rate, r , is assumed to be deterministic.

3.2.1 Model 1: A mean-reverting deterministic volatility process with two types of jumps

I start with specifying the spot price of electricity as a mean-reverting jump-diffusion process with two types of jumps. Let the factor process X_t in (3.1) denote $\ln S_t^e$, where S_t^e is the price of the underlying electricity. Y_t is the other factor process which can be used to specify the logarithm of the spot price of a generating fuel, *e.g.* $Y_t = \ln S_t^g$ where S_t^g is the spot price of natural gas. In this formulation, I have type-1 jump representing the upward jumps and type-2 jump representing the downward jumps. By setting the intensity functions of the jump processes in a proper way, we can mimic the spikes in the electricity price process. Suppose the state vector process $(X_t, Y_t)'$ given by (3.1) is

under the true measure² and the risk premia³ associated with all state variables are linear functions of state variables. Assuming there exists a risk-neutral probability measure⁴ Q over the state space represented by the state variables⁵, the state vector process has the same form as that of (3.1) under the risk-neutral measure, but with different coefficients. For the ease of pricing derivatives in Section 3.3, I choose to directly specify the state vector process under the risk-neutral measure from here on with the assumption that the risk premia associated with all state variables are linear functions of state variables.

Assume that, under regularity conditions, X_t and Y_t are strong solutions to the following stochastic differential equation (SDE) under the risk-neutral measure Q ,

$$d \begin{pmatrix} X_t \\ Y_t \end{pmatrix} = \begin{pmatrix} \kappa_1(t)(\theta_1(t) \Leftrightarrow X_t) \\ \kappa_2(t)(\theta_2(t) \Leftrightarrow Y_t) \end{pmatrix} dt + \begin{pmatrix} \sigma_1(t) & 0 \\ \rho(t)\sigma_2(t) & \sqrt{1 \Leftrightarrow \rho(t)^2}\sigma_2(t) \end{pmatrix} dW_t + \sum_{i=1}^2 \Delta Z_t^i \quad (3.1)$$

where $\kappa_1(t)$ and $\kappa_2(t)$ are the mean-reverting coefficients; $\theta_1(t)$ and $\theta_2(t)$ are the long term means; $\sigma_1(t)$ and $\sigma_2(t)$ are instantaneous volatility rates of X and Y ; W_t is a \mathcal{F}_t -adapted standard Brownian motion under Q in \mathbb{R}^2 ; Z^j is a compound Poisson process in \mathbb{R}^2 with the Poisson arrival intensity being $\lambda_j(t)$ ($j = 1, 2$). ΔZ^j denotes the random

²True measure refers to the probability measure defining the statistical properties of the underlying price process observed in the real world.

³Risk premium is a quantity established by the capital markets in equilibrium. It is the amount subtracted from the mean return of a financial asset or a project in order to compensate the owner of the asset or the project for bearing the associated risks.

⁴Risk-neutral measure refers to the normalized Arrow-Debreu state prices over the states of the world. Since the sum or the integral of these positive normalized state prices equals one, they can be interpreted as a probability measure over the states of the world. The risk-neutral measure is, in general, not unique due to incomplete markets.

⁵A risk-neutral measure exists as long as the no-arbitrage conditions hold. Given the existence of a risk-neutral measure, the price of a contingent claim is just the expected value of its discounted payoff under the risk-neutral measure. See Duffie (1996) for more details.

jump size in \mathfrak{R}^2 with cumulative distribution function $v^j(z)$ ($j = 1, 2$). Let $\phi_J^j(c_1, c_2, t) \equiv \int_{\mathbb{R}^2} \exp(c \cdot z) dv^j(z)$ be the transform function of the jump size distribution of type- j jumps ($j = 1, 2$).

The transform function Define the generalized transform function as

$$\varphi(u, X_t, Y_t, t, T) \equiv E^Q[e^{-r(T-t)} \exp(u_1 X_T + u_2 Y_T) | \mathcal{F}_t] \quad (3.2)$$

for any fixed time T where $E^Q[\cdot | \mathcal{F}_t]$ is the expected value operator under the risk-neutral measure Q conditioning on the information at time t and $u \equiv (u_1, u_2) \in C^2$ (a set of 2-tuples of complex numbers). The transform function φ is well-defined at a given u under technical regularity conditions on $\kappa_i(t)$, $\theta_i(t)$, $\sigma_i(t)$, $\rho_i(t)$, $\lambda_i(t)$, and $\phi_J^i(c_1, c_2, t)$ ($i = 1, 2$).

Under the regularity conditions (see Appendix B), $\varphi \cdot e^{-rt}$ is a martingale under the risk-neutral measure Q since it is a \mathcal{F}_t -conditional expectation of a single random variable $\exp(u_1 X_T + u_2 Y_T)$. Therefore the drift term of $\varphi \cdot e^{-rt}$ is zero. Applying Ito's lemma for complex functions, we observe that φ needs to satisfy the following fundamental partial differential equation (PDE)

$$\mathcal{D}f \Leftrightarrow r f = 0 \quad (3.3)$$

where

$$\mathcal{D}f \equiv \partial_t f + \mu_X \cdot \partial_X f + \frac{1}{2} \text{tr}(\partial_X^2 f \Sigma \Sigma^T) + \sum_{j=1}^2 \lambda_j(t) \int_{\mathbb{R}^2} [f(X_t + \Delta Z_t^j, t) \Leftrightarrow f(X_t, t)] dv_j(z)$$

It is conjectured that, under regularity conditions, φ takes the form:

$$\varphi(u, X_t, Y_t, t, T) = \exp[\alpha(t, u) + \beta_1(t, u)X_t + \beta_2(t, u)Y_t] \quad (3.4)$$

where α and $\beta \equiv [\beta_1 \ \beta_2]'$ satisfy the complex-valued ordinary differential equations

$$\begin{aligned} \frac{d}{dt}\beta(t, u) + B(\beta(t, u), t) &= 0, & \beta(0, u) &= u \\ \frac{d}{dt}\alpha(t, u) + A(\beta(t, u), t) &= 0, & \alpha(0, u) &= 0 \end{aligned} \quad (3.5)$$

with $A(\cdot, \cdot) : C^2 \times R \rightarrow C^1$ and $B(\cdot, \cdot) : C^2 \times R \rightarrow C^2$ being

$$\begin{aligned} A(\beta, t) &= \sum_{i=1}^2 [\kappa_i \theta_i \beta_i + \frac{1}{2} \sigma_i^2 \beta_i^2] + \rho \sigma_1 \sigma_2 \beta_1 \beta_2 \Leftrightarrow r + \sum_{j=1}^2 \lambda_j(t) (\phi_J^j(\beta_1, \beta_2, t) \Leftrightarrow 1) \\ B(\beta, t) &= \begin{pmatrix} \kappa_1 \beta_1 \\ \kappa_2 \beta_2 \end{pmatrix} \end{aligned} \quad (3.6)$$

Now, we integrate α and β out with the corresponding initial conditions to get solutions (3.7).

$$\varphi(u, X_t, Y_t, t, T) = \exp(\alpha(t, u) + \beta_1(t, u)X_t + \beta_2(t, u)Y_t)$$

where

$$\begin{aligned} \beta_1(t, [u_1, u_2]') &= u_1 \exp(\Leftrightarrow \int_t^T \kappa_1(s) ds) \\ \beta_2(t, [u_1, u_2]') &= u_2 \exp(\Leftrightarrow \int_t^T \kappa_2(s) ds) \\ \alpha(t, u) &= \int_t^T \left(\sum_{i=1}^2 [\kappa_i(s) \theta_i(s) \beta_i(s, u) + \frac{1}{2} \sigma_i^2(s) \beta_i^2(s, u)] \right. \\ &\quad \left. + \rho(s) \sigma_1(s) \sigma_2(s) \beta_1(s, u) \beta_2(s, u) \right. \\ &\quad \left. \Leftrightarrow r + \sum_{j=1}^2 \lambda_j(s) (\phi_J^j(\beta_1(s, u), \beta_2(s, u), s) \Leftrightarrow 1) \right) ds \end{aligned} \quad (3.7)$$

3.2.2 Model 2: A regime-switching mean-reverting process with two types of jumps

To motivate this model, I consider the electricity prices in regions where the majority of power generation capacity is hydro-power. The level of precipitation causes the electricity price levels to alternate between “high” and “low” regimes. Other plausible scenarios for electricity prices to exhibit regime-switching are that the forced outages of power generation plants or unexpected contingencies in transmission networks often result in abnormally high electricity spot prices for a short time period and then a quick price fall-back. In order to capture the phenomena of spot prices switching between “high” and “normal” states, I extend model 1 to a Markov regime-switching model which I describe in detail below.

Let U_t be a continuous-time two-state Markov chain

$$dU_t = 1_{U_t=0} \cdot \delta(U_t)dN_t^{(0)} + 1_{U_t=1} \cdot \delta(U_t)dN_t^{(1)} \quad (3.8)$$

where 1_A is an indicator function for event A , $N_t^{(i)}$ is a Poisson process with arrival intensity $\lambda^{(i)}$ ($i = 0, 1$) and $\delta(0) = \Leftrightarrow\delta(1) = 1$. I next define the corresponding compensated continuous-time Markov chain $M(t)$ as

$$dM_t = \Leftrightarrow\lambda(U_t)\delta(U_t)dt + dU_t \quad (3.9)$$

The joint specification of electricity and the generating fuel price processes under the

risk-neutral measure Q is given by:

$$d \begin{pmatrix} X_t \\ Y_t \end{pmatrix} = \begin{pmatrix} \kappa_1(t)(\theta_1(t) \Leftrightarrow X_t) \\ \kappa_2(t)(\theta_2(t) \Leftrightarrow Y_t) \end{pmatrix} dt + \begin{pmatrix} \sigma_1(t) & 0 \\ \rho(t)\sigma_2(t) & \sqrt{1 \Leftrightarrow \rho(t)^2\sigma_2(t)} \end{pmatrix} dW_t \\ + \sum_{j=1}^2 \Delta Z_t^j + \iota(U_{t-})dM_t \quad (3.10)$$

where W_t is a \mathcal{F}_t -adapted standard Brownian motion under Q in \mathfrak{R}^2 ; $\{\iota(i) \equiv (\iota_1(i), \iota_2(i))'; i = 0, 1\}$ denotes the sizes of the random jumps in state variables when regime-switching occurs. Let $\phi_{\iota(i)}(c_1, c_2, t) \equiv \int_{\mathbb{R}^2} \exp(c \cdot z) dv_{\iota(i)}(z)$ be the transform function of the regime-jump size distribution $v_{\iota(i)}$ ($i = 1, 2$). Z^j , ΔZ^j and $\phi_J^j(c_1, c_2, t)$ are similarly defined as those in Model 1. Strong solutions to (3.10) exist under regularity conditions.

The transform function $F^i(\bar{x}, t)$ ($i = 0, 1$) denotes

$$E[e^{-r(T-t)} \exp(u_1 X_T + u_2 Y_T) | X_t = x, Y_t = y, U_t = i] \quad (3.11)$$

where U_t is the Markov regime state variable. The infinitesimal generator \mathcal{D} of F^i is given by

$$\begin{aligned} \mathcal{D}F^0(\bar{x}, t) &= dF^0(\bar{x}, t) + \lambda^{(0)} \int_{\mathbb{R}^2} [F^1(\bar{x} + \iota(0), t) \Leftrightarrow F^0(\bar{x}, t)] dv_t(\iota(0)) \\ \mathcal{D}F^1(\bar{x}, t) &= dF^1(\bar{x}, t) + \lambda^{(1)} \int_{\mathbb{R}^2} [F^0(\bar{x} + \iota(1), t) \Leftrightarrow F^1(\bar{x}, t)] dv_t(\iota(1)) \end{aligned} \quad (3.12)$$

where

$$\begin{aligned} dF^i(\bar{x}, t) &= F_t^i + F_{\bar{x}}^i \cdot \mu^i(\bar{x}, t) + \frac{1}{2} tr[F_{\bar{x}\bar{x}}^i \sigma^i(\bar{x}, t) \sigma^i(\bar{x}, t)^T] \\ &\quad + \sum_{j=1}^2 \lambda_j^i(\bar{x}, t) \int_{\mathbb{R}^2} [F^i(\bar{x} + z, t) \Leftrightarrow F^i(\bar{x}, t)] dv_{j,t}(z) \end{aligned}$$

($i = 0, 1$ is the regime state variable)

The fundamental PDEs satisfied by the transform functions $F^i(\bar{x}, t)$ ($i = 0, 1$) are

$$\mathcal{D}F^i(x, y, t) \Leftrightarrow rF^i(x, y, t) = 0 \quad (i = 0, 1) \quad (3.13)$$

The solutions to (3.13) assume the following forms

$$F^0(x, y, t) = \exp(\alpha_0(t) + \beta_1(t)x + \beta_2(t)y) \quad (3.14)$$

$$F^1(x, y, t) = \exp(\alpha_1(t) + \beta_1(t)x + \beta_2(t)y)$$

Substituting (3.14) into (3.13) with $\alpha(t) \equiv \alpha(t, u) \equiv (\alpha_0(t, u), \alpha_1(t, u))'$ and $\beta(t) \equiv \beta(t, u) \equiv (\beta_1(t, u), \beta_2(t, u))'$, we get the following ordinary differential equations (ODEs)

$$\begin{aligned} \frac{d}{dt}\beta(t, u) + B(\beta(t, u), t) &= 0, & \beta(0, u) &= u \\ \frac{d}{dt}\alpha(t, u) + A(\alpha(t, u), \beta(t, u), t) &= 0, & \alpha(0, u) &= 0 \end{aligned} \quad (3.15)$$

where

$$\begin{aligned} A(\alpha(t), \beta(t), t) &= \begin{pmatrix} A_1(\beta(t), t) + \lambda^{(0)}[\exp(\alpha_1(t) \Leftrightarrow \alpha_0(t))\phi_{i(0)}(\beta(t), t) \Leftrightarrow 1] \\ A_1(\beta(t), t) + \lambda^{(1)}[\exp(\alpha_0(t) \Leftrightarrow \alpha_1(t))\phi_{i(1)}(\beta(t), t) \Leftrightarrow 1] \end{pmatrix} \\ B(\beta(t), t) &= \begin{pmatrix} \kappa_1(t)\beta_1(t) \\ \kappa_2(t)\beta_2(t) \end{pmatrix} \end{aligned} \quad (3.16)$$

and

$$A_1(\beta(t), t) = \sum_{i=1}^2 [\kappa_i \theta_i \beta_i + \frac{1}{2} \sigma_i^2 \beta_i^2] \Leftrightarrow \rho \sigma_1 \sigma_2 \beta_1 \beta_2 \Leftrightarrow r + \sum_{j=1}^2 \lambda_j (\phi_j^j(\beta, t) \Leftrightarrow 1)$$

$\phi_J^j(\beta, t)$ and $\phi_{i(\cdot)}(\beta(t), t)$ are transform functions of the random variables representing jump sizes in state variables within a regime and associated with the regime-switching, respectively. When ODEs (3.15) do not have closed-form solutions, we need to numerically solve (3.15) in order to obtain the transform function values.

3.2.3 Model 3: A mean-reverting stochastic volatility process with two types of jumps

I consider a three-factor affine jump-diffusion process with two types of jumps in this model (3.17). Let X_t and Y_t denote the logarithm of the spot prices of electricity and a generating fuel, e.g. natural gas, respectively. V_t represents the stochastic volatility factor. There is empirical evidence alluding to the fact that the volatility of electricity price is high when the aggregate load (or, demand) is high and vice versa. Therefore, V_t can be thought as a factor which is proportional to the regional aggregate demand process for electricity. Jumps may appear in both X_t and V_t since weather conditions such as unusual heat waves may cause simultaneous jumps in both the electricity price and the aggregate load. The state vector process $(X_t, V_t, Y_t)'$ is specified by (3.17). Under proper regularity conditions, there exists a Markov process which is the strong solution to the following SDEs under the risk-neutral measure Q .

$$d \begin{pmatrix} X_t \\ V_t \\ Y_t \end{pmatrix} = \begin{pmatrix} \kappa_1(t)(\theta_1(t) \Leftrightarrow X_t) \\ \kappa_V(t)(\theta_V(t) \Leftrightarrow V_t) \\ \kappa_2(t)(\theta_2(t) \Leftrightarrow Y_t) \end{pmatrix} dt + \Sigma dW_t + \sum_{i=1}^2 \Delta Z_t^i \quad (3.17)$$

where Σ is given by

$$\Sigma \equiv \begin{pmatrix} \sqrt{V_t} & 0 & 0 \\ \rho_1(t)\sigma_2(t)\sqrt{V_t} & \sqrt{1 \Leftrightarrow \rho_1^2(t)\sigma_2(t)\sqrt{V_t}} & 0 \\ \rho_2(t)\sigma_3(t)\sqrt{V_t} & 0 & \sigma_3(t) \end{pmatrix};$$

W is a \mathcal{F}_t -adapted standard Brownian motion under Q in \mathfrak{R}^3 ; Z^j is a compound Poisson process in \mathfrak{R}^3 with the Poisson arrival intensity being $\lambda^j(X_t, V_t, Y_t, t)$ ($j = 1, 2$). I model the spiky behavior by assuming that the intensity function of type-1 jumps is only a function of time t , denoted by $\lambda^{(1)}(t)$, and the intensity of type-2 jumps is a function of V_t , i.e. $\lambda^{(2)}(V_t, t) = \lambda_2(t)V_t$. Let $\phi_j^j(c_1, c_2, c_3, t) \equiv \int_{\mathfrak{R}^2} \exp(c \cdot z) dv^j(z)$ denote the transform function of the jump-size distribution of type- j jumps, $v^j(z)$, ($j = 1, 2$).

The transform function Following similar arguments to those used in Model 1, we know that the transform function

$$\varphi(u, X_t, V_t, Y_t, t, T) \equiv E^Q[e^{-r(T-t)} \exp(u_1 X_T + u_2 V_T + u_3 Y_T) \mid \mathcal{F}_t]$$

is of form

$$\varphi(u, X_t, V_t, Y_t, t, T) = \exp(\alpha(t, u) + \beta_1(t, u)X_T + \beta_2(t, u)V_T + \beta_3(t, u)Y_T) \quad (3.18)$$

where $\alpha(u, t)$ and $\beta(u, t) \equiv (\beta_1(u, t), \beta_2(u, t), \beta_3(u, t))'$ are solutions to the following ordinary differential equations

$$\begin{aligned} \frac{d}{dt}\beta(t, u) + B(\beta(t, u), t) &= 0, & \beta(0, u) &= u \\ \frac{d}{dt}\alpha(t, u) + A(\beta(t, u), t) &= 0, & \alpha(0, u) &= 0 \end{aligned} \quad (3.19)$$

with $A(\cdot, \cdot) : C^3 \times R \rightarrow C^1$ and $B(\cdot, \cdot) : C^3 \times R \rightarrow C^3$ being

$$\begin{aligned} A(\beta, t) &= \Leftrightarrow r + \sum_{i=1}^3 \kappa_i \theta_i \beta_i + \frac{1}{2} \beta_3^2 \sigma_3^2(t) + \lambda_1(t) (\phi_J^{(1)}(\beta, t) \Leftrightarrow 1) \\ B(\beta, t) &= \begin{pmatrix} \kappa_1(t) \beta_1(t, u) \\ \kappa_2(t) \beta_2(t, u) + \lambda_2(t) (\phi_J^{(2)}(\beta, t) \Leftrightarrow 1) + \frac{1}{2} B_1(\beta, t) \\ \kappa_3(t) \beta_3(t, u) \end{pmatrix} \end{aligned} \quad (3.20)$$

and

$$\begin{aligned} B_1(\beta, t) &= \beta_1(t, u) (\beta_1(t, u) + \beta_2(t, u) \rho_1(t) \sigma_2(t) + \beta_3(t, u) \rho_2(t) \sigma_3(t)) \\ &\quad + \beta_2(t, u) (\beta_1(t, u) \rho_1(t) \sigma_2(t) + \beta_2(t, u) \sigma_2^2(t) + \beta_3(t, u) \rho_1(t) \rho_2(t) \sigma_2(t) \sigma_3(t)) \\ &\quad + \beta_3(t, u) (\beta_1(t, u) \rho_2(t) \sigma_3(t) + \beta_2(t, u) \rho_1(t) \rho_2(t) \sigma_2(t) \sigma_3(t) \\ &\quad + \beta_3(t, u) \rho_2^2(t) \sigma_3^2(t)) \end{aligned} \quad (3.21)$$

3.3 Electricity Derivative Pricing

Having specified the mean-reverting jump-diffusion price models and demonstrated how to compute the generalized transform functions of the state vector at any given time T , the prices of European-type contingent claims on the underlying electricity under the proposed models can then be obtained through the inversion of the transform functions.

Suppose \bar{X}_t is a state vector in R^n and $u \in C^n$ (a set of n -tuples of complex numbers) and the generalized transform function is given by

$$\begin{aligned}\varphi(u, \bar{X}_t, t, T) &\equiv E^Q[e^{-r(T-t)} \exp(u \cdot \bar{X}_T) | \mathcal{F}_t] \\ &= \exp[\alpha(t, u) + \beta(t, u) \cdot \bar{X}_t]\end{aligned}\tag{3.22}$$

Let $G(v, X_t, Y_t, t, T; \bar{a}, \bar{b})$ denote the time- t price of a contingent claim which pays out

$$\exp(\bar{a} \cdot \bar{X}_T), \text{ if } \bar{b} \cdot \bar{X}_T \leq v \text{ is true at time } T$$

where \bar{a}, \bar{b} are vectors in R^n and $v \in R^1$, then we have (see Duffie, Pan and Singleton [13] for a formal proof):

$$\begin{aligned}G(v, \bar{X}_t, t, T; \bar{a}, \bar{b}) &= E^Q[e^{-r(T-t)} \exp(\bar{a} \cdot \bar{X}_T) \mathbf{1}_{\bar{b} \cdot \bar{X}_T \leq v} | \mathcal{F}_t] \\ &= \frac{\varphi(\bar{a}, \bar{X}_t, t, T)}{2} \Leftrightarrow \frac{1}{\pi} \int_0^\infty \frac{\text{Im}[\varphi(\bar{a} + iw\bar{b}, \bar{X}_t, t, T)e^{-i w v}]}{w} dw\end{aligned}\tag{3.23}$$

For properly chosen constants v , \bar{a} , and \bar{b} , $G(v, X_t, Y_t, t, T; \bar{a}, \bar{b})$ serves as a building block in pricing contingent claims such as forwards/futures, call/put options, and cross-commodity spread options. To illustrate this point, I take some concrete examples of the models proposed in Section 3.2 and compute the prices of several commonly traded electricity derivatives. Specifically, model *Ia* is a special case of model *I* ($I = 1, 2, 3$). Closed-form solutions of the derivative securities (up to the Fourier inversion) are provided whenever available.

3.3.1 Illustrative Models

The illustrative models presented here are obtained by setting the model parameters to be constants in the proposed three general models. The jumps appear in the electricity price process and the volatility process (model 3a) only. The jump sizes are distributed as independent exponential random variables in R^n thus having the following transform function:

$$\phi_J^j(\bar{c}, t) \equiv \prod_{k=1}^n \frac{1}{1 \Leftrightarrow \mu_j^k c_k} \quad (3.24)$$

The simulated price paths under the three illustrative models are shown in Figure (3.3)

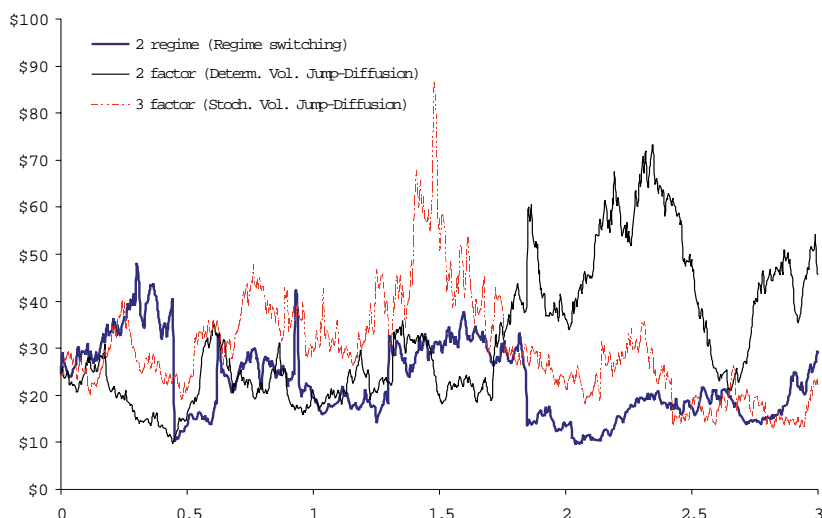


Figure 3.3: Simulated Spot Prices under the Three Models

for parameters given in Table (3.1). The x-axis represents the simulation time horizon in the number of years while the y-axis represents the electricity price level in dollars.

Model 1a

Model 1a (3.25) is a special case of (3.1) with all parameters being constants. The jumps are in the logarithm of the electricity spot price, X_t . The size of a type- j jump ($j = 1,$

2) is exponentially distributed with mean μ_j^j ($j = 1, 2$). The transform function of the jump-size distribution is $\phi_J^j(c_1, c_2, t) \equiv \frac{1}{1 \Leftrightarrow \mu_j^j c_1}$ ($j = 1, 2$).

$$d \begin{pmatrix} X_t \\ Y_t \end{pmatrix} = \begin{pmatrix} \kappa_1(\theta_1 \Leftrightarrow X_t) \\ \kappa_2(\theta_2 \Leftrightarrow Y_t) \end{pmatrix} dt + \begin{pmatrix} \sigma_1 & 0 \\ \rho_1 \sigma_2 & \sqrt{1 \Leftrightarrow \rho_1^2 \sigma_2^2} \end{pmatrix} dW_t \quad (3.25)$$

$$+ \sum_{i=1}^2 \Delta Z_t^i$$

where W is a \mathcal{F}_t -adapted standard Brownian motion in \mathfrak{R}^2 .

The transform function φ_{1a} The closed-form solution of the transform function can be written out explicitly for this model.

$$\varphi_{1a}(u, X_t, Y_t, t, T) = \exp[\alpha(\tau) + \beta_1(\tau)X_t + \beta_2(\tau)Y_t] \quad (3.26)$$

where $\tau = T \Leftrightarrow t$. By solving the ordinary differential equations in (3.6) with all parameters being constants, I obtain the following solutions.

$$\begin{aligned} \beta_1(\tau, u_1) &= u_1 \exp(\Leftrightarrow \kappa_1 \tau) \\ \beta_2(\tau, u_2) &= u_2 \exp(\Leftrightarrow \kappa_2 \tau) \\ \alpha(\tau, u) &= \Leftrightarrow r \tau \Leftrightarrow \sum_{j=1}^2 \frac{\lambda_j^j}{\kappa_1} \ln \frac{u_1 \mu_j^j \Leftrightarrow 1}{u_1 \mu_j^j \exp(\Leftrightarrow \kappa_1 \tau) \Leftrightarrow 1} + \frac{a_1 \sigma_1^2 u_1^2}{4 \kappa_1} + \frac{a_2 \sigma_2^2 u_2^2}{4 \kappa_2} \\ &\quad + u_1 \theta_1 (1 \Leftrightarrow \exp(\Leftrightarrow \kappa_1 \tau)) + u_2 \theta_2 (1 \Leftrightarrow \exp(\Leftrightarrow \kappa_2 \tau)) \\ &\quad + \frac{u_1 u_2 \rho_1 \sigma_1 \sigma_2 (1 \Leftrightarrow \exp(\Leftrightarrow (\kappa_1 + \kappa_2) \tau))}{\kappa_1 + \kappa_2} \end{aligned} \quad (3.27)$$

with $a_1 = 1 \Leftrightarrow \exp(\Leftrightarrow 2 \kappa_1 \tau)$ and $a_2 = 1 \Leftrightarrow \exp(\Leftrightarrow 2 \kappa_2 \tau)$.

Model 2a

Model 2a (3.28) is a regime-switching model with the regime-jumps appearing only in the electricity price process. For instance, this model is suitable for modeling the occasional price spikes in the electricity spot prices caused by forced outages of the major power generation plants or line contingency in transmission networks. I assume for simplicity that there are no jumps within each regime.

$$d \begin{pmatrix} X_t \\ Y_t \end{pmatrix} = \begin{pmatrix} \kappa_1(\theta_1 \Leftrightarrow X_t) \\ \kappa_2(\theta_2 \Leftrightarrow Y_t) \end{pmatrix} dt + \begin{pmatrix} \sigma_1 & 0 \\ \rho_1 \sigma_2 & \sqrt{1 \Leftrightarrow \rho_1^2 \sigma_2^2} \end{pmatrix} dW_t + \iota(U_{t-}) dM_t \quad (3.28)$$

where W is a \mathcal{F}_t -adapted standard Brownian motion in \mathfrak{R}^2 . U_t is the regime state process as defined in (3.8). The sizes of regime-jumps are assumed to be distributed as independent exponential random variables and the transform functions of the regime-jump sizes are $\phi_\iota(c_1, c_2, t) \equiv \frac{1}{1 \Leftrightarrow \mu_\iota c_1}$ ($\iota = 0, 1$) where $\mu_0 \geq 0$ (i.e. upward jumps) and $\mu_1 \leq 0$ (i.e. downward jumps).

The transform function φ_{2a} For model 2a, the transform function φ_{2a} cannot be solved in closed-form completely. We have

$$\begin{aligned} \varphi_{2a}^0(x, y, t) &= \exp(\alpha_0(t) + \beta_1(t)x + \beta_2(t)y) \\ \varphi_{2a}^1(x, y, t) &= \exp(\alpha_1(t) + \beta_1(t)x + \beta_2(t)y) \end{aligned} \quad (3.29)$$

where $\beta(t) \equiv \beta(t, u) \equiv (\beta_1(t, u), \beta_2(t, u))'$ has the closed-form solution of

$$\begin{aligned}\beta_1(\tau, u_1) &= u_1 \exp(\Leftrightarrow \kappa_1 \tau) \\ \beta_2(\tau, u_2) &= u_2 \exp(\Leftrightarrow \kappa_2 \tau)\end{aligned}\tag{3.30}$$

but $\alpha(t) \equiv \alpha(t, u) \equiv (\alpha_0(t, u), \alpha_1(t, u))'$ needs to be numerically computed from

$$\begin{aligned}\frac{d}{dt} \begin{pmatrix} \alpha_0(t) \\ \alpha_1(t) \end{pmatrix} &= \Leftrightarrow \begin{pmatrix} A_1(\beta(t), t) + \lambda^{(0)} \left[\frac{\exp(\alpha_1(t) \Leftrightarrow \alpha_0(t))}{1 \Leftrightarrow \mu_0 \beta_1(t, u_1)} \Leftrightarrow 1 \right] \\ A_1(\beta(t), t) + \lambda^{(1)} \left[\frac{\exp(\alpha_0(t) \Leftrightarrow \alpha_1(t))}{1 \Leftrightarrow \mu_1 \beta_1(t, u_1)} \Leftrightarrow 1 \right] \end{pmatrix} \\ \begin{pmatrix} \alpha_0(0, u) \\ \alpha_1(0, u) \end{pmatrix} &= \begin{pmatrix} 0 \\ 0 \end{pmatrix}\end{aligned}\tag{3.31}$$

with

$$A_1(\beta(t), t) = \Leftrightarrow r + \sum_{i=1}^2 [\kappa_i \theta_i \beta_i + \frac{1}{2} \sigma_i^2 \beta_i^2] \Leftrightarrow \rho_1 \sigma_1 \sigma_2 \beta_1 \beta_2$$

Model 3a

Model 3a (3.32) is a stochastic volatility model in which the type-1 jumps are simultaneous jumps in the electricity spot price and the volatility, and the type-2 jumps are in the electricity spot price only. All parameters are constants.

$$\begin{aligned}d \begin{pmatrix} X_t \\ V_t \\ Y_t \end{pmatrix} &= \begin{pmatrix} \kappa_1 (\theta_1 \Leftrightarrow X_t) \\ \kappa_V (\theta_V \Leftrightarrow V_t) \\ \kappa_2 (\theta_2 \Leftrightarrow Y_t) \end{pmatrix} dt + \begin{pmatrix} \sqrt{V_t} & 0 & 0 \\ \rho_1 \sigma_2 \sqrt{V_t} & \sqrt{1 \Leftrightarrow \rho_1^2} \sigma_2 \sqrt{V_t} & 0 \\ \rho_2 \sigma_3 \sqrt{V_t} & 0 & \sigma_3 \end{pmatrix} dW_t \\ &\quad + \sum_{i=1}^2 \Delta Z_t^i\end{aligned}\tag{3.32}$$

where W is a \mathcal{F}_t -adapted standard Brownian motion in \mathfrak{R}^3 ; Z^i ($i = 1, 2$) is a compound Poisson process in \mathfrak{R}^3 . The Poisson arrival intensity functions are $\lambda^1(X_t, V_t, Y_t, t) = \lambda_1$ and $\lambda^2(X_t, V_t, Y_t, t) = \lambda_2 V_t$. The transform functions of the jump-size distributions are

$$\begin{aligned}\phi_J^1(c_1, c_2, c_3, t) &\equiv \frac{1}{(1 \Leftrightarrow \mu_1^1 c_1)(1 \Leftrightarrow \mu_1^2 c_2)} \\ \phi_J^2(c_1, c_2, c_3, t) &\equiv \frac{1}{1 \Leftrightarrow \mu_2^1 c_1}\end{aligned}$$

where μ_J^k is the mean size of the type- J ($J = 1, 2$) jump in factor k ($k = 1, 2$).

The transform function φ_{3a} From Section 3.2, we know that φ_{3a} is of form

$$\varphi_{3a}(u, X_t, V_t, Y_t, t, T) = \exp(\alpha(t, u) + \beta_1(t, u)X_T + \beta_2(t, u)V_T + \beta_3(t, u)Y_T) \quad (3.33)$$

Similar to model 2a, the transform function φ_{3a} does not have a closed-form solution.

I numerically solve for both $\alpha(t, u)$ and $\beta(t, u) \equiv [\beta_1(t, u), \beta_2(t, u), \beta_3(t, u)]'$ from the following ordinary differential equations (ODEs)

$$\begin{aligned}\frac{d}{dt}\beta(t, u) + B(\beta(t, u), t) &= 0, & \beta(0, u) &= u \\ \frac{d}{dt}\alpha(t, u) + A(\beta(t, u), t) &= 0, & \alpha(0, u) &= 0\end{aligned} \quad (3.34)$$

with

$$\begin{aligned}A(\beta, t) &= \Leftrightarrow r + \sum_{i=1}^3 \kappa_i \theta_i \beta_i(t, u) + \frac{1}{2} \beta_3^2(t) \sigma_3^2 \\ &\quad + \lambda_1 \left[\frac{1}{(1 \Leftrightarrow \mu_1^1 \beta_1(t, u))(1 \Leftrightarrow \mu_1^2 \beta_2(t, u))} \Leftrightarrow 1 \right] \\ B(\beta, t) &= \begin{pmatrix} \kappa_1 \beta_1(t, u) + \lambda_{21} \left(\frac{1}{1 \Leftrightarrow \mu_2^1 \beta_1(t, u)} \Leftrightarrow 1 \right) \\ \kappa_2 \beta_2(t, u) + \lambda_{22} \left(\frac{1}{1 \Leftrightarrow \mu_2^1 \beta_1(t, u)} \Leftrightarrow 1 \right) + \frac{1}{2} B_1(\beta, t) \\ \kappa_3 \beta_3(t, u) \end{pmatrix}\end{aligned} \quad (3.35)$$

and

$$\begin{aligned}
B_1(\beta, t) = & \beta_1(t, u)(\beta_1(t, u) + \beta_2(t, u)\rho_1\sigma_2 + \beta_3(t, u)\rho_2\sigma_3) \\
& + \beta_2(t, u)(\beta_1(t, u)\rho_1\sigma_2 + \beta_2(t, u)\sigma_2^2 + \beta_3(t, u)\rho_1\rho_2\sigma_2\sigma_3) \\
& + \beta_3(t, u)(\beta_1(t, u)\rho_2\sigma_3 + \beta_2(t, u)\rho_1\rho_2\sigma_2\sigma_3 + \beta_3(t, u)\rho_2^2\sigma_3^2) \quad (3.36)
\end{aligned}$$

3.3.2 Electricity Derivatives

In this subsection, I derive the pricing formulae for the futures/forwards, call options, spark spread options, and locational spread options. The derivative prices are calculated using the parameters given in Table (3.1). I compare the derivative prices under different models as well.

Futures/Forward Price

A futures (forward) contract promising to deliver one unit of electricity S^i at a future time T for a price of F has the following payoff at time T

$$\text{Payoff} = S_T^i \Leftrightarrow F \quad .$$

Since no initial payment is required to enter into a futures contract, the futures price F at time t is given by

$$F(S_t^i, t, T) = E^Q[S_T^i \mid \mathcal{F}_t] \quad (3.37)$$

where $E^Q[\cdot | \mathcal{F}_t]$ is the conditional expectation under the risk-neutral measure Q .

Rewrite the above expression as

$$\begin{aligned} F(S_t^i, t, T) &= E^Q[S_T^i | \mathcal{F}_t] \\ &= e^{r\tau} E^Q[e^{-r\tau} \cdot \exp(X_T^i) | \mathcal{F}_t] \end{aligned} \quad (3.38)$$

We thus have

$$F(S_t^i, t, T) = e^{r\tau} \cdot \varphi(\bar{e}_i^T, \bar{X}_t, \tau) \quad (3.39)$$

where $\varphi(u, \bar{X}_t, \tau)$ is the transform function given by (3.22); $\tau = T \Leftrightarrow t$; \bar{e}_i is the vector with i^{th} component being 1 and all other components being 0.

Futures price (model 1a) Recall the transform function φ_{1a} is obtained in (3.26) and (3.27). By setting $u = [1, 0]'$ in φ_{1a} , we get

$$\varphi_{1a}([1, 0]', X_t, Y_t, \tau) = \exp[X_t \exp(\Leftrightarrow \kappa_1 \tau) \Leftrightarrow r\tau + \frac{a_1 \sigma_1^2}{4\kappa_1} + \theta_1 (1 \Leftrightarrow \exp(\Leftrightarrow \kappa_1 \tau)) \Leftrightarrow j(\tau)]$$

where $\tau = T \Leftrightarrow t$, $X_t = \ln(S_t)$, $a_1 = 1 \Leftrightarrow \exp(\Leftrightarrow 2\kappa_1 \tau)$ and $j(\tau) = \sum_{j=1}^2 \frac{\lambda_j^j}{\kappa_1} \ln \frac{\mu_j^j \Leftrightarrow 1}{\mu_j^j \exp(\Leftrightarrow \kappa_1 \tau) \Leftrightarrow 1}$.

Therefore by (3.39), we have the following proposition.

Proposition 3.3.1 *In Model 1a, the futures price of electricity S_t at time t with delivery time T is*

$$\begin{aligned} F(S_t, t, T) &= e^{r\tau} \cdot \varphi_{1a}([1, 0]', X_t, Y_t, \tau) \\ &= \exp[X_t \exp(\Leftrightarrow \kappa_1 \tau) + \frac{a_1 \sigma_1^2}{4\kappa_1} + \theta_1 (1 \Leftrightarrow \exp(\Leftrightarrow \kappa_1 \tau)) \Leftrightarrow j(\tau)] \end{aligned} \quad (3.40)$$

where $\tau = T - t$, $X_t = \ln(S_t)$, $a_1 = 1 - \exp(-2\kappa_1\tau)$ and $j(\tau) = \sum_{j=1}^2 \frac{\lambda_j^j}{\kappa_1} \ln \frac{\mu_j^j - 1}{\mu_j^j \exp(-\kappa_1\tau) - 1}$.

Note that the futures price in this model is simply the scaled-up futures price in the Ornstein-Uhlenbeck mean-reversion model with the scaling factor being $\exp(j(\tau))$. If we interpret the spikes in the electricity price process as upward jumps followed shortly by downward jumps of similar sizes, then over a long time horizon both the frequencies and the average sizes of the upwards jumps and the downwards jumps are roughly the same, i.e. $\lambda_j^1 = \lambda_j^2$ and $\mu_j^1 \approx \mu_j^2$. One might intuitively think that the up-jumps and down-jumps would offset each other's effect in the futures price. What (3.40) tells us is that this intuition is not quite right and indeed, in the case where $\lambda_j^1 = \lambda_j^2$ and $\mu_j^1 = \mu_j^2$, the futures price is definitely higher than that corresponding to the no-jump case.

Futures price (model 2a) The futures price at time t in model 2a is

$$F(S_t, t, T) = e^{r\tau} \cdot \varphi_{2a}^i([1, 0]', X_t, Y_t, \tau) \quad (i = 0, 1) \quad (3.41)$$

where the transform functions φ_{2a}^i are computed in (3.29); i is the Markov regime state variable; and $\tau = T - t$.

Futures price (model 3a) The futures price at time t in model 3a is

$$F(S_t, t, T) = e^{r\tau} \cdot \varphi_{3a}([1, 0, 0]', X_t, V_t, Y_t, \tau) \quad (3.42)$$

where the transform function φ_{3a} is given in (3.33) and $\tau = T - t$.

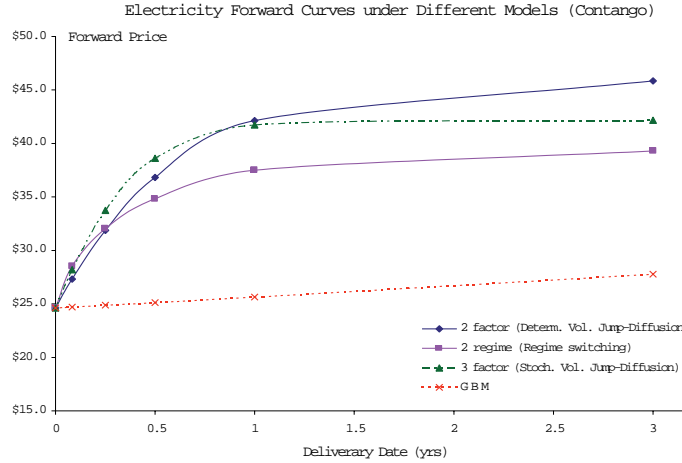


Figure 3.4: Forward Curves under Different Models (Contango)

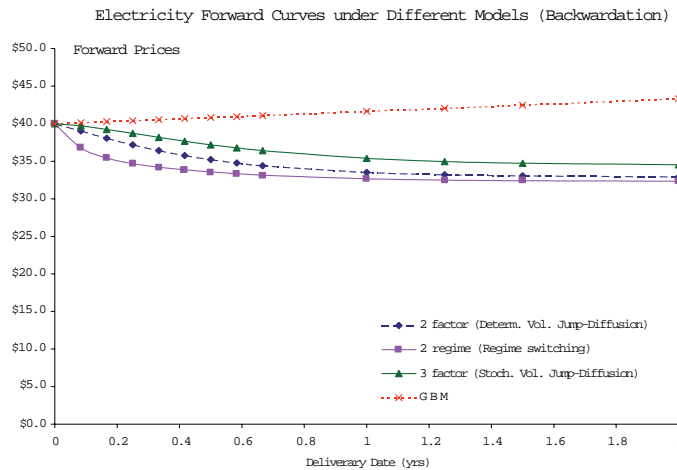


Figure 3.5: Forward Curves under Different Models (Backwardation)

Forward curves Using the parameters in Table (3.1) for modeling the electricity spot price in the Midwestern US (Cinergy to be specific), I obtain forward curves at Cinergy under each of the three illustrative models. The jointly specified factor process is the spot price of natural gas at Henry Hub. For the initial values of $S_e = \$24.63$, $S_g = \$2.105$, $V = 0.5$, $U = 0$ and $r = 4\%$, Figure (3.4) illustrates three forward curves of electricity, which are all in contango form since the initial value S_e is lower than the

long-term mean value given by θ_e . Figure (3.5) plots three electricity forward curves in backwardation when the initial electricity price S_e is set to be \$40 which is higher than the corresponding long-term mean value. The forward curves under the Geometric Brownian motion (GBM) price model are also shown in the two figures. Under the GBM price model, the forward prices always exhibit a fixed rate of growth.

Call Option

A “plain vanilla” European call option on electricity S^i with strike price K has the payoff of

$$C(S_T^i, K, T, T) = \max(S_T^i \Leftrightarrow K, 0)$$

at maturity time T . The price of the call option at time t is given by

$$\begin{aligned} C(S_t^i, K, t, T) &= E^Q[e^{-r(T-t)} \max(S_T^i \Leftrightarrow K, 0) \mid \mathcal{F}_t] \\ &= E^Q[e^{-r\tau} \exp(X_T^i) 1_{X_T^i \geq \ln K} \mid \mathcal{F}_t] \Leftrightarrow K \cdot E^Q[e^{-r\tau} 1_{X_T^i \geq \ln K} \mid \mathcal{F}_t] \\ &= G_1 \Leftrightarrow K \cdot G_2 \end{aligned} \quad (3.43)$$

where $\tau = T \Leftrightarrow t$ and G_1, G_2 are obtained by setting $\{a = \bar{\epsilon}_i, b = \Leftrightarrow \bar{\epsilon}_i, v = \Leftrightarrow \ln K\}$ and $\{a = \bar{0}, b = \Leftrightarrow \bar{\epsilon}_i, v = \Leftrightarrow \ln K\}$ in (3.23), respectively.

$$\begin{aligned} G_1 &= E^Q[e^{-r\tau} \exp(X_T) 1_{X_T \geq \ln K} \mid \mathcal{F}_t] \\ &= \frac{F_t^i e^{-r\tau}}{2} \Leftrightarrow \frac{1}{\pi} \int_0^\infty \frac{\text{Im}[\varphi([1 \Leftrightarrow w \cdot i, 0], \bar{X}_t, \tau) \exp(i \cdot w \ln K)]}{w} dw \\ &= F_t^i e^{-r\tau} \left(\frac{1}{2} \Leftrightarrow \frac{1}{\pi} \int_0^\infty \frac{\text{Im}[\varphi([1 \Leftrightarrow w \cdot i, 0], \bar{X}_t, \tau) \cdot e^{(r\tau + i \cdot w \ln K)}]}{w F_t^i} dw \right) \end{aligned} \quad (3.44)$$

where $F_t^i = e^{r\tau} \cdot \varphi(\bar{e}_i^T, \bar{X}_t, \tau)$ is the time- t forward price of commodity S^i with delivery time T .

$$\begin{aligned}
 G_2 &= E^Q[e^{-r\tau} 1_{X_t^i \geq \ln K} | \mathcal{F}_t] \\
 &= \frac{\varphi(\bar{0}, \bar{X}_t, t, T)}{2} \Leftrightarrow \frac{1}{\pi} \int_0^\infty \frac{\text{Im}[\varphi(i \cdot w \bar{e}_i, \bar{X}_t, t, T) e^{i \cdot w \ln K}]}{w} dw \\
 &= e^{-r\tau} \left(\frac{1}{2} \Leftrightarrow \frac{1}{\pi} \int_0^\infty \frac{\text{Im}[\varphi(i \cdot w \bar{e}_i, \bar{X}_t, t, T) e^{r \cdot \tau + i \cdot w \ln K}]}{w} dw \right) \quad (3.45)
 \end{aligned}$$

Call option price Substituting φ_{1a} , φ_{2a} , and φ_{3a} into (3.44) and (3.45) we have the call option price given by (3.43) under **Model 1a**, **2a** and **3a**, respectively.

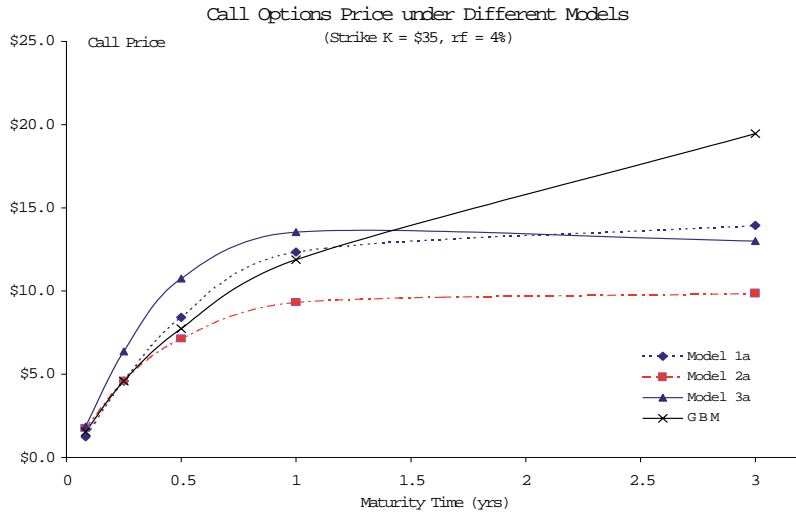


Figure 3.6: Call Options Price under Different Models

Volatility smile With the model parameters given in Table (3.1), Figure (3.6) plots the call option values with different maturity time under different models. The call option prices under a Geometric Brownian motion (GBM) model are also plotted for comparison purpose. Note that, as maturity time increases, the value of a call option converges to the underlying electricity spot price under the GBM price model (with

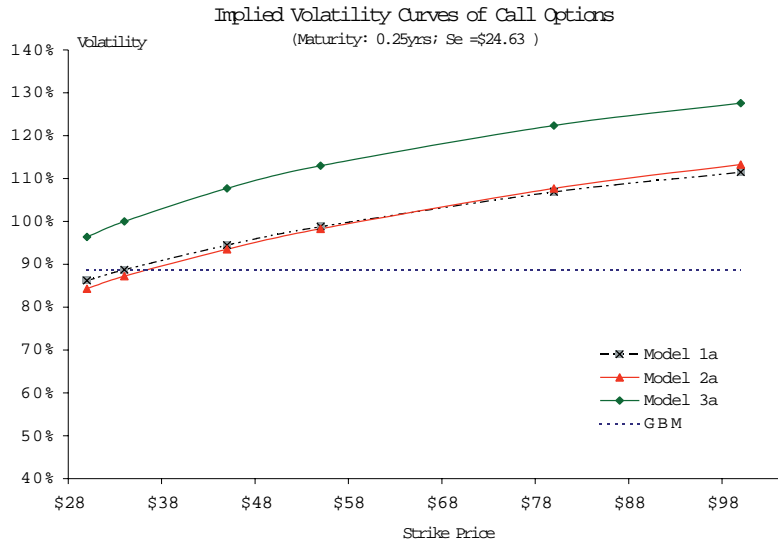


Figure 3.7: Volatility-Smile under Different Models

no convenience yields). However, under the three proposed price models, the mean-reversion effects cause the value of a call option to converge to a long-term value, which is most likely to be depending on fundamental characteristics of electricity supply and demand, rather than the underlying spot price. Figure (3.7) illustrates the implied volatility⁶ curves under the three illustrative models, which all exhibit the similar kinds of volatility “smile” or “smirk” to the market implied volatility curves as shown in Figure (3.1).

Cross Commodity Spread Option

In energy commodity markets, cross commodity derivatives play crucial roles in risk management. Crack spread options in crude oil markets as well as the spark spread

⁶Implied volatility refers to the volatility parameter corresponding to a given call option value through the Black-Scholes call option pricing formula. It is obtained by inverting the Black-Scholes pricing formula using the given call option value and other known parameters as inputs.

and locational spread options in electricity markets are good examples. The spark spread options, which are derivatives on electricity and the fossil fuels used to generate electricity, can have various applications in risk management for utility companies and power marketers. Moreover, such options are essential in asset valuation for fossil fuel electricity generating plants. A European *spark spread call (SSC)* option pays out the positive part of the difference between the electricity spot price and the generating fuel cost at the time of maturity. Its payoff function at maturity time T is:

$$SSC(S_T^e, S_T^g, H, T) = \max(S_T^e - H \cdot S_T^g, 0) \quad (3.46)$$

where S_T^e and S_T^g are the prices of electricity and the generating fuel, respectively; the constant H , termed *strike heat rate*, represents the number of units of generating fuel contracted to generate one unit of electricity.

Another type of cross commodity option, which I term it locational spread option, involves electricity at two different locations. A locational spread option pays out the positive part of the price difference between the electricity prices at two different delivery points. Electricity locational spread options serve the purposes of hedging the transmission risks and they can also be used to value transmission expansion projects as shown in Chapter 4. The time T payoff of a European *locational spread call* option is

$$LSC(S_T^a, S_T^b, L, T) = \max(S_T^b - L \cdot S_T^a, 0) \quad (3.47)$$

where S_T^a and S_T^b are the time- T electricity prices at location a and b , respectively. The constant L is a loss factor reflecting the transportation/transmission losses or costs

associated with transmitting one unit of electricity from location a to b .

Observing the similar payoff structures of the above two spread options, I define a general *cross-commodity spread call* option as an option with the following payoff at maturity time T ,

$$CSC(S_T^1, S_T^2, K, T) = \max(S_T^1 \Leftrightarrow K \cdot S_T^2, 0) \quad (3.48)$$

where S_T^i is the spot price of commodity i ($i = 1, 2$) and K is a scaling constant associated with the spot price of commodity two. The interpretation of K is different in different examples. For instance, K represents the strike heat rate H in a spark spread option, and it represents the loss factor L in a locational spread option.

The time- t value of a European cross-commodity spread call option on two commodities is given by

$$\begin{aligned} CSC(S_t^1, S_t^2, K, t) &= E^Q[e^{-r(T-t)} \max(S_T^1 \Leftrightarrow K \cdot S_T^2, 0) \mid \mathcal{F}_t] \\ &= E_t^Q[e^{-r\tau} \exp(X_T^1) 1_{S_T^1 - K \cdot S_T^2 \geq 0}] \Leftrightarrow E_t^Q[e^{-r\tau} K \exp(X_T^2) 1_{S_T^1 - K \cdot S_T^2 \geq 0}] \\ &= G_1 \Leftrightarrow G_2 \end{aligned} \quad (3.49)$$

where

$$\begin{aligned} G_1 &= G(0, \ln S_t^1, \ln(K \cdot S_t^2), t, T; [1, 0, \dots, 0]', [\Leftrightarrow 1, 1, 0, \dots, 0]') \\ G_2 &= G(0, \ln S_t^1, \ln(K \cdot S_t^2), t, T; [0, 1, 0, \dots, 0]', [\Leftrightarrow 1, 1, 0, \dots, 0]') \end{aligned} \quad (3.50)$$

and recall that

$$G(v, \bar{X}_t, t, T; \bar{a}, \bar{b}) = \frac{\varphi(\bar{a}, \bar{X}_t, t, T)}{2} \Leftrightarrow \frac{1}{\pi} \int_0^\infty \frac{Im[\varphi(\bar{a} + iw\bar{b}, \bar{X}_t, t, T)e^{-i w v}]}{w} dw$$

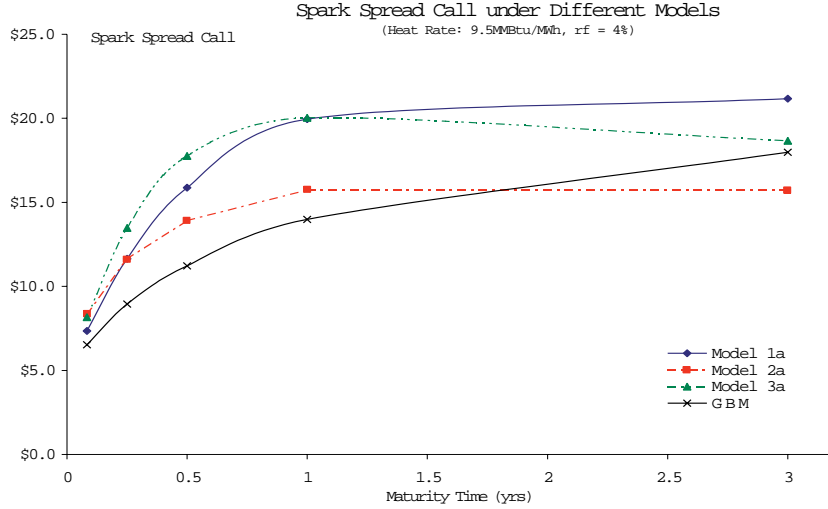


Figure 3.8: Spark Spread Call Price under Different Models

Cross commodity spread call option price under each of the three models are obtained by substituting φ_{1a} , φ_{2a} , and φ_{3a} into (3.49) and (3.50).

The spark spread call option values with strike heat rate $H = 9.5$ for different maturity time are shown in Figure (3.8). Again, the spark spread call option value converges to the underlying spot price under the GBM price model (with no convenience yields). However, under the mean-reversion jump-diffusion price models, it converges to a long-term value which is most likely to be depending on fundamental characteristics of supply and demand.

3.3.3 Parameter Estimation

In this subsection, I provide a heuristic method for estimating the model parameters using the electricity price data. As an illustration, I pick **Model 1a** and derive the moment conditions from the transform function of the unconditional distribution of the underlying price return. I assume that the risk premium associated with each factor

	Model 1a	Model 2a	Model 3a
κ_1	1.70	1.37	2.17
κ_2	1.80	1.80	3.50
κ_3	N/A	N/A	1.80
θ_1	3.40	3.30	3.20
θ_2	0.87	0.87	0.85
θ_3	N/A	N/A	0.87
σ_1	0.74	0.80	N/A
σ_2	0.34	0.34	0.80
σ_3	N/A	N/A	0.54
ρ_1	0.20	0.20	0.25
ρ_2	N/A	N/A	0.20
λ_1	6.08	6.42	6.43
μ_{11}	0.19	0.26	0.23
μ_{12}	N/A	N/A	0.22
λ_2	7.00	8.20	5.00
μ_{21}	-0.11	-0.20	-0.14

Table 3.1: Parameters for the Illustrative Models

X is proportional to X , i.e. the risk premium is of form $\xi_X \cdot X$ where ξ_X is a scalar parameter. For simplicity, I further assume the risk premia associated with the jumps are zero. As noted earlier, the price processes under the true measure are of the same forms as (3.25). In particular, the model parameters under the true measure are:

$$\begin{aligned}
\kappa_i &= \kappa_i^* + \xi_i \\
\theta_i &= \frac{\kappa_i^* \cdot \theta_i^*}{\kappa_i^* + \xi_i} \\
\lambda_j &= \lambda_j^* \\
\mu_j &= \mu_j^*
\end{aligned} \tag{3.51}$$

where the parameters with a superscript “*” are risk-neutral parameters. I then use the electricity and natural gas spot and futures price series to get the estimates for the model parameters under the true measure and the risk premia by matching moment conditions as well as the futures prices. The following proposition provides the unconditional mean, variance and skewness of the logarithm of the electricity price in **Model 1a**.

Proposition 3.3.2 *In Model 1a, let $X_\infty \equiv \lim_{t \rightarrow \infty} X_t$ denote the unconditional distribution of X_t where $X_t = \ln S_t^e$. If $E[|X_\infty|^n] < \infty$, then the mean, variance and skewness of X_∞ are*

$$\begin{aligned} \text{mean} &= \theta_1 + \frac{\lambda_1 \mu_1 + \lambda_2 \mu_2}{\kappa_1} \\ \text{variance} &= \frac{\sigma_1^2}{2\kappa_1} + \frac{\lambda_1 \mu_1^2 + \lambda_2 \mu_2^2}{\kappa_1} \\ \text{skewness} &= \frac{4\sqrt{2\kappa_1}(\lambda_1 \mu_1^3 + \lambda_2 \mu_2^3)}{(\sigma_1^2 + 2\lambda_1 \mu_1^2 + 2\lambda_2 \mu_2^2)^{\frac{3}{2}}} \end{aligned}$$

Proof. In the transform function φ_{1a} as defined by (3.26) and (3.27), let $u = i \cdot w$ and $t \rightarrow \infty$, I obtain the characteristic function of X_∞ to be

$$\Phi_{X_\infty}(w) = \exp[i \cdot w \theta_1 \Leftrightarrow \frac{w^2 \sigma_1^2}{4\kappa_1} \Leftrightarrow \sum_{j=1}^2 \frac{\lambda_j^j}{\kappa_1} \ln(1 \Leftrightarrow i \cdot w \mu_j^j)]$$

If $E[|X_\infty|^n] < \infty$, then the n^{th} moment of X_∞ is given by

$$E[X_\infty^n] = (\Leftrightarrow i)^n \left. \frac{d^n}{dw^n} \Phi_{X_\infty}(w) \right|_{w=0}$$

In particular,

$$\begin{aligned} E[X_\infty] &= (\Leftrightarrow i) \left. \frac{d}{dw} \Phi_{X_\infty}(w) \right|_{w=0} \\ &= \theta_1 + \frac{\lambda_1 \mu_1 + \lambda_2 \mu_2}{\kappa_1} \end{aligned}$$

The formulae for variance and skewness are obtained in the same fashion. ■

As shown in the proof of the Proposition 3.3.2, we can derive as many moment conditions as we desire for X_∞ from the characteristic function of X_∞ for estimating the model parameters of **Model 1a**. The parameters in **Model 2a** and **Model 3a** are obtained

by minimizing the mean squared errors of the traded options prices.

3.4 Conclusion

In this chapter, I propose three types of mean-reversion jump-diffusion models for modeling electricity spot prices with jumps and spikes. I demonstrate how the prices of the electricity derivatives can be obtained by means of transform analysis. The market anticipation of jumps and spikes in the electricity spot price processes explains the enormous implied volatility observed from market prices of traded electricity options. Contrary to the commonly used Geometric Brownian motion model, the proposed mean-reversion jump-diffusion spot price models yield call option values that approximate the market values of short-maturity out-of-the-money options very well. I mention briefly how I can fit the models using electricity price data. With the ability of pricing electricity derivatives and extracting model parameters from electricity market data, I am ready to proceed to construct a real-options approach for valuing the electricity generation and transmission assets in the next chapter.

Chapter 4

Risk Management and Asset Valuation

Under the traditional regulatory regime, electricity prices were set by the regulators based on cost of service. Investments in generation capacity by the utility firms needed to be approved by the regulators in order to earn an appropriate return. However, this paradigm is being changed by the restructuring of the electricity supply industries. Competitive and volatile electricity markets have been created worldwide. In a competitive market environment, market participants need to consciously manage their risks associated with daily operations in the short-run. At the same time, they need to adopt new market-based methodologies to plan their generation and transmission capacity, to evaluate investment opportunities and to earn a competitive market-based return in the long-run.

In this chapter, I first demonstrate a couple of risk management applications of the electricity derivatives introduced in Chapter 3. I then construct a real-options approach

for valuing generation and transmission assets in the competitive electricity markets. Under the proposed mean-reverting jump-diffusion electricity price models, I calculate the theoretical value of a natural gas fired electric power plant ignoring the plant's physical operating characteristics such as start-up cost, ramp-up time, etc., and examine the implications of modeling assumptions on capacity valuation. Finally, for the purpose of incorporating the operational constraints into capacity valuation, I develop a discrete-time stochastic dynamic programming approach for valuing generation assets in which the mean-reverting price processes of electricity and the generating fuel are represented by a trinomial lattice. The impacts of operational characteristics of a real asset on its valuation are investigated through numerical examples.

4.1 Risk Management with Electricity Derivatives

Derivative securities are the most valuable tools in the design, development, and implementation of financial risk management strategies. In what follows, I illustrate the roles of two cross-commodity spread options, the spark spread option and the locational spread option, in hedging daily operations and trading activities through two examples.

One example is the hedging of daily productions of a fossil fuel electric power plant using spark spread options. Recall from **Section 3.3.2** that the payoff of a spark spread call option at its maturity time T is $\max(S_T^e - K_H S_T^g, 0)$ where S_T^e and S_T^g are the electricity price and the generating fuel price at time T , respectively. K_H is the strike heat rate. Figure (4.1) shows the payoff of a spark spread call option maturing at different times t where the x-axis is the time axis. The solid curve plots the historical

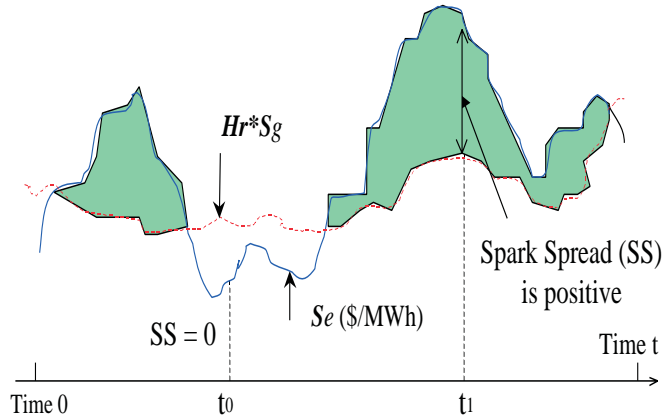


Figure 4.1: Payoff of a Spark Spread Call Option

electricity price path and the dashed curve represents the heat rate adjusted historical fuel costs. Had we held a series of spark spread call options with exact one option maturing in each hour between time 0 and time t_1 , then we would have received a total payoff that equals the shaded areas between 0 and t_1 .

We note that the total payoffs represented by the shaded areas between time 0 and time t_1 in Figure (4.1) could also be yielded by one megawatt (MW) of electricity generating capacity which converts every K_H units of natural gas into one unit of electricity ignoring the operational characteristics of the generating capacity such as start-up cost, unit ramp-up time, etc. In fact, for an electric power generating asset which is used to transform some fuel into electricity, its economic value is determined by the spread between the price of electricity and the cost of the fuel that is used to generate electricity. The amount of fuel that a particular power generating asset requires to generate a given amount of electricity depends on the asset's operating efficiency. This efficiency is summarized by the asset's **operating heat rate**, which is defined as the number of British thermal units (Btus) of the input fuel (measured in millions, i.e. MBtus)

required to generate one megawatt hour (MWh) of electricity. The lower the operating heat rate, the more efficient the facility. Given the right to operate a generation asset at a time epoch t , a value-maximizing operator would, abstracting the aforementioned operational characteristics, turn on the generating units whenever the market price of electricity is greater than the operating cost at time t but shut down the units otherwise. Such operating policy at time t produces a cash payout which equals that of a properly defined European-style spark spread call option maturing at time t . In particular, the value of the right to operate a generation asset with operating heat rate K_H that uses generating fuel g at time t is clearly given by the value of a spark spread call option with “strike” heat rate K_H written on generating fuel g maturing at the same time t because they two yield the same payoff¹.

Based on this observation, a merchant electric power plant² owner can effectively hedge his daily productions over certain time periods by selling a series of spark spread call options, with maturing times covering the corresponding time periods, against the total capacity or a fraction of it. For instance, to hedge an 100MW natural gas fired electric power merchant plant with an operating heat rate of 8000 MBtu/MWh for the next calendar year, its owner could sell 360 spark spread call options each maturing on a different day of the 360 days for each megawatt of the 100MW capacity. For the purpose of hedging, the strike heat rates of these spark spread options should be no less than the operating heat rate of the power plant which is 8000 MBtu/MWh. Due to the

¹The physical operating characteristics of an electric power plant such as start-up cost, ramp-up time and variable heat rate are not considered here, but they will be addressed explicitly later.

²A merchant electric power plant is a power plant which is free of any long-term power supply commitments and whose operations are purely based on the market price of electricity and the operating costs.

fact that a merchant power plant owner has the operational flexibility of turning on and off the power plant depending upon market conditions, selling spark spread call options is a better approach for hedging a merchant plant than any other approaches such as locking into forward contracts of electricity and the generating fuel.

The other example of operational hedging is to use the locational spread options in hedging transmission risks. As described in **Section 3.3.2**, a locational spread call option pays the positive part of the price difference between the electricity prices at two locations at its maturity time T , i.e. $\max(S_T^1 - K_{loss} \cdot S_T^2, 0)$ where K_{loss} is the strike loss factor³ and S_T^i is the electricity price at location i ($i = 1, 2$). Suppose an electric power marketer enters into a bilateral contract to supply electricity from California Oregon Border (COB) to Palo Verde (PV) in Arizona (see Figure (4.2)). Having no firm transmission capacity rights on the transmission links between COB and PV, the power marketer is subject to the risks of not being able to transmit electricity from COB to PV to fulfill the contract at the time of delivery due to possible transmission line congestion. When the line congestion occurs, he would have to dispose of the electricity he has at COB at the COB local spot price and buy electricity to deliver at PV at the PV local spot price therefore incurring a possibly large *ex post* cost. In order to avoid this potential huge *ex post* cost, the power marketer can perfectly hedge the transmission risks associated with the bilateral contract by purchasing the locational spread call options on electricity at COB and PV with strike loss factor K_{loss} being 1 and with the maturity times matching the delivery times of the bilateral contract.

³When transmitting one unit of electricity from one location to another, it always takes more than one unit of electricity at the injection location due to transmission losses, i.e. K_{loss} should be a constant greater than one for the purpose of hedging physical transmission rights.

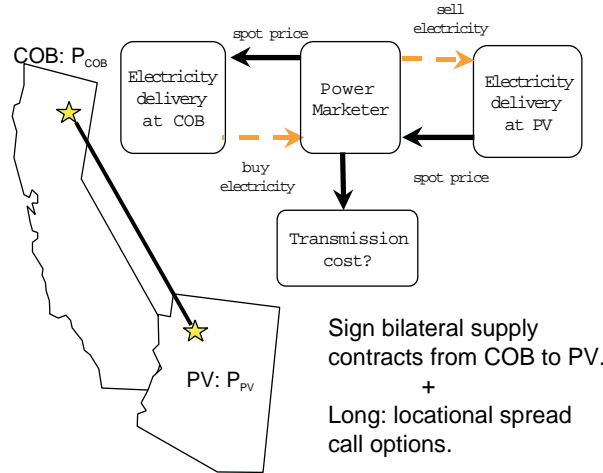


Figure 4.2: Hedging Transmission Risks

By applying the pricing formulas developed for the spark spread options and the locational spread options in **Section 3.3.2**, we can readily evaluate the costs of implementing the above hedging strategies. In the next section, I will show that these hedging strategies actually serve as the basis for the market-based valuation of electricity generation and transmission assets.

4.2 Real-Options Valuation of Capacity without Physical Constraints

In this section, I construct a real options approach for the valuation of installed capacity or real assets in the deregulated electric power industry. In particular, I illustrate how to use derivative securities to value generation and transmission facilities without considering the physical operating characteristics of the facilities. The implications of modeling assumptions on capacity valuation will be examined.

According to the no-arbitrage pricing principles, if the financial payoffs of a real asset over its life span can be perfectly replicated or hedged by a portfolio of financial instruments (called replicating or hedging portfolio), then the market value of the real asset should be equal to the value of this replicating portfolio absent the transaction costs. Take a natural gas fired electric power plant as an example. Assuming that the operational characteristics of the gas-fired power plant such as start-up cost, ramp-up time and variable heat rate are negligible, the payoff of the right to operate the power plant in any given hour during its life span can be matched exactly by that of a spark spread call option on electricity and natural gas maturing in the same hour with strike heat rate being the operating heat rate of the power plant. Therefore, the value of this power plant should be given by the sum of the value of all these spark spread call options with maturity time covering the whole life span of the plant.

Similarly, the value of a transmission asset that connects location 1 and location 2 equals the sum of the value of the locational spread options to buy electricity at location 1 and sell it at location 2 as well as the value of the options to buy electricity at location 2 and sell it a location 1 with the strike loss factor K_{loss} being equal to the corresponding transmission line loss factor⁴ (in both cases, less the appropriate transmission costs if any).

This equivalence between the value of appropriately defined spark and locational spread options and the right to operate a generation or a transmission asset motivates the real options approach for valuing such assets. I demonstrate this approach by developing

⁴A transmission link connecting locations A and B has a line loss factor of K_{loss} meaning that it requires K_{loss} units of electricity injected at location A for each unit of electricity delivered at location B via the transmission link.

a simple spark spread based model for the valuation of a fossil fuel generation asset. Once established, I fit the model and use it to estimate the value of several gas-fired plants that have recently been sold. The accuracy of the model is validated by comparing the theoretical estimates to the prices at which the assets were actually sold.

In the analysis I make the following simplifying assumptions about the operating characteristics of the generation asset under consideration:

Assumption 4.2.1 Ramp-ups and ramp-downs of the generation facility can be done with no advance notice.

Assumption 4.2.2 The facility's variable operation and maintenance costs are constants.

Assumption 4.2.3 The start-up and shutdown costs are negligible.

Assumption 4.2.4 The operating heat rate of the generating unit is a constant.

Assumptions 4.2.1 & 4.2.2 are reasonable since for a typical combined cycle gas turbine cogeneration plant the response time (ramp-up/ramp-down) is several hours and the variable costs (e.g. operating and maintenance) are generally stable over time. Assumptions 4.2.3 & 4.2.4 are made purely for the purpose of simplifying the valuation model. I will investigate the impacts on capacity valuation due to Assumptions 4.2.1, 4.2.3, & 4.2.4 in the later section.

To construct a spark spread based estimate of the value of a generation asset, I estimate the value of the right to operate the asset over its remaining useful life. This value can be found by integrating the value of the spark spread call options over the remaining life of the asset. Specifically,

Definition 4.2.1 *Let one unit of the time- t capacity right of a fossil fuel fired electric power plant represent the right to convert K_H units of generating fuel into one unit of electricity by using the plant at time t , where K_H is the plant's operating heat rate.*

The payoff of one unit of time- t capacity right is $\max(S_t^e - K_H S_t^g, 0)$, where S_t^e and S_t^g are the spot prices of electricity and the generating fuel at time t , respectively. Denote the value of one unit of the time- t capacity right by $u(t)$.

For a natural gas fired power plant, the value of $u(t)$ is given by the corresponding spark spread call option on electricity and natural gas with a strike heat rate of K_H . However, for a coal-fired power plant, it often has long-term coal supply contracts which guarantee the supply of coal at a predetermined price c . Therefore, the payoff of one unit of time- t capacity right for a coal plant degenerates to that of a call option with strike price $K_H \cdot c$. In this case, $u(t)$ is equal to the value of a simple call option on electricity.

Definition 4.2.2 *Denote the virtual value of one unit of capacity of a fossil fuel power plant by V . Then V is obtained through integrating the value of one unit of the plant's time- t capacity right over the remaining life $[0, T]$ of the power plant, i.e. $V = \int_0^T u(t)dt$.*

Proposition 4.2.1 *Under Assumption 4.2.1 - 4.2.4, the value of a fossil fuel power plant with W megawatt of generating capacity is given by $W \cdot V$ less the present value of the future O&M costs where V is defined in Definition 4.2.2.*

Proof. Under Assumption 4.2.1 - 4.2.4, the optimal operating policy for the power plant is to turn on the plant and operate at its maximum capacity level W whenever

the electricity price is greater than the generating fuel cost, and to turn off the plant otherwise. Such an optimal operating policy yields the capacity value of $W \cdot V$. ■

Since the O&M costs are assumed to be constants and they do not vary with model parameters, I set them to be zero from now on.

In what follows, I shall investigate the sensitivity of capacity value with respect to model parameters under the setting of **Model 1a**. I calculate the virtual capacity value for a hypothetical gas-fired power plant using spark spread valuation with parameters given in Table (4.1). The operating life-time of the hypothetical power plant is assumed to be 15 years. The risk-free rate is assumed to be 4.5%.

κ_1	4	κ_2	3
θ_1	3.15	θ_2	0.87
σ_1	0.75	σ_2	0.87
ρ	0.3		
λ_1	2	λ_2	2
μ_1	0.1934	μ_2	-0.1934
S_1^0	21.7	S_2^0	3.16

Table 4.1: Parameters (Model 1a) for Capacity Valuation

I first examine how the presence of jumps in commodity prices affects the capacity value. Figure (4.3) plots the capacity value of a fictitious natural gas fired power plant, for the operating heat rate varying from 7,000 MBtu/MWh to 15,000 MBtu/MWh, both with and without jumps ($\lambda_1 = \lambda_2 = 0$) in the electricity price process. The axis on the left is for the capacity value and the axis on the right is for the difference in capacity value of the two cases. The solid curve with diamonds represents the capacity value with jumps in the electricity price using parameters in Table (4.1) which is the base for the comparison. Dashed curve with squares represents the capacity value without jumps in the electricity price. Figure (4.3) illustrates the change in capacity value in

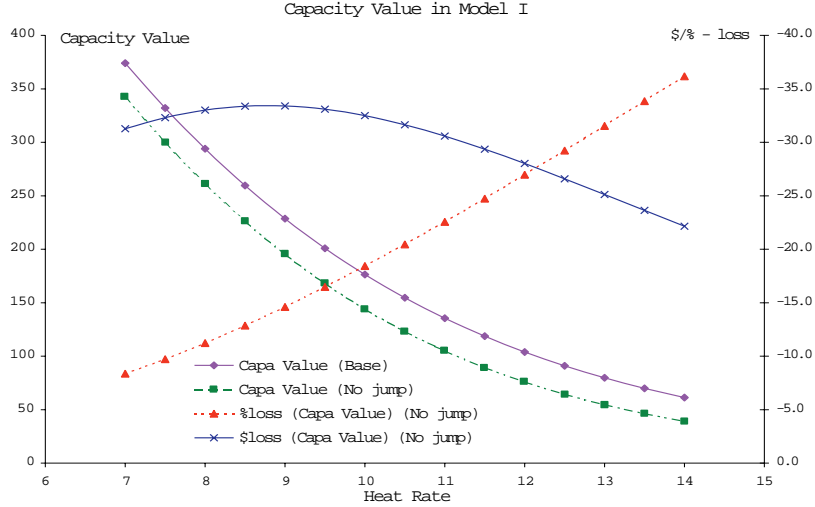


Figure 4.3: Capacity Value with/without Jumps (Model 1a)

absolute dollar term (plotted as the solid curve with crosses) and in percentage term (plotted as the dashed curve with triangles) on the right axis as a result of setting the jump intensities to zero in **Model 1a**. We can see that the less efficient a power plant the larger is the portion of its capacity value attributed to the jumps in the spot price process. The presence of jumps makes up as much as 35% of the capacity value of the very inefficient power plants. I note that the capacity values with jumps (plotted as the solid curve with diamonds) computed here will also serve as the basis for the subsequent comparative static analysis on capacity valuation regarding the changes in other model parameters.

In Figure (4.4), I plot the changes in capacity value due to a 10% increase or a 10% decrease in the electricity price volatility parameter σ_1 , respectively. The solid curves represent the dollar value change with respect to the base case in Figure (4.3) on the left-side axis and the dotted curves show the percentage change with respect to the base case on the right-side axis. It is clear that the change in volatility causes greater dollar

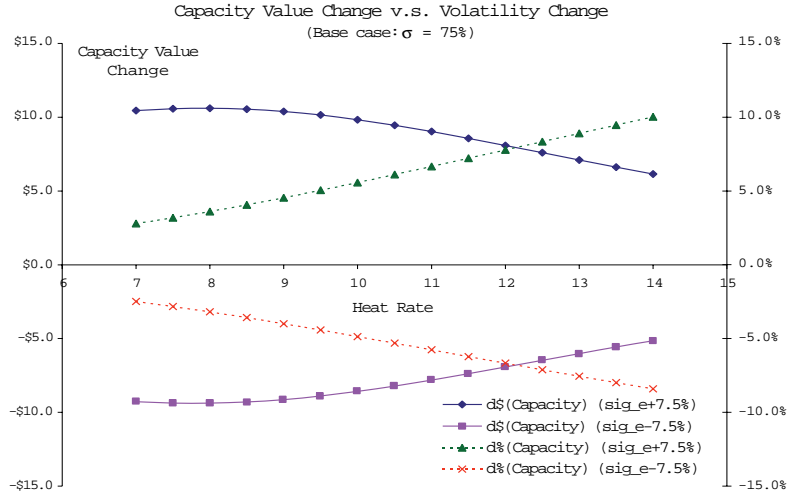


Figure 4.4: Sensitivity of Capacity Value to Electricity Spot Volatility (Model 1a)

value changes for efficient plants than for inefficient plants.

The sensitivity of capacity value with respect to the correlation coefficient between the generating fuel price and the electricity price is illustrated in Figure (4.5). While it is

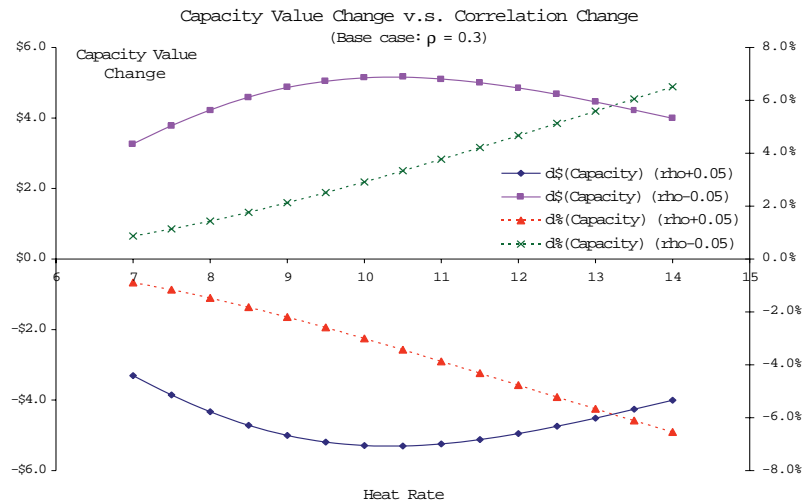


Figure 4.5: Sensitivity of Capacity Value to the Correlation Coefficient (Model 1a)

still true that the percentage change of capacity value varies monotonically with respect to the efficiency measure (operating heat rate) of a power plant, the largest dollar value change does not occur to the most efficient plant but to the plant with heat rate close

to the market implied heat rate⁵.

To compare the theoretical valuation of generation capacity with the market valuation, I plot a capacity value curve in Figure (4.6) using the NYMEX electricity futures prices at Palo Verde on 10/15/97 and the parameters obtained by fitting **Model 1a** to the NYMEX electricity futures prices at Palo Verde and the natural gas futures prices at Henry Hub. Figure (4.6) also plots the capacity value curve obtained by using the

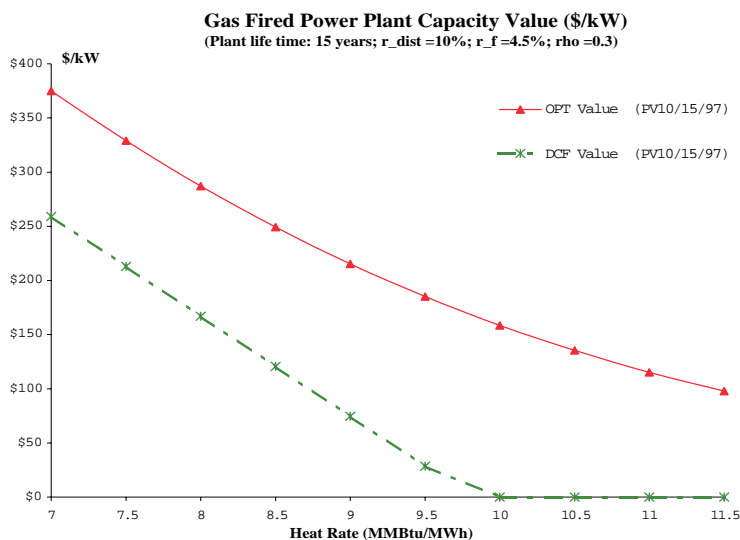


Figure 4.6: Value of Capacity: Spark Spread approach vs. DCF approach

discounted cash flow (DCF) method for comparison purpose⁶. At the heat rate level of 9500, the capacity value of a natural gas power plant is around \$200/kW under **Model 1a**. The discounted cash flow method predicts a value of \$29/kW. To put things in perspective, I take a look at the four gas-fired power plants which Southern California Edison recently sold to Houston Industries. Unfortunately, not all of the individual plant

⁵Market implied heat rate is defined to be the ratio of spot price of electricity to the spot price of the generating fuel.

⁶The capacity value curve is based on spark spread options on monthly on-peak (23x16) electricity and natural gas. The correlation coefficient of gas-to-electricity is assumed to be 0.3. The discount rate for the DCF approach is 10%. I assume that a power plant will be operated for 15 years and there is no O&M costs.

dollar investments have been made public yet. As a proxy I use the total investment made by Houston Industries (\$237 million to purchase four plants - Coolwater, Ellwood, Etiwanda and Mandalay), divided by the total number of megawatts (MW) of capacity (2172MW) to get approximately \$110,000 per MW (or \$110/kW) of capacity. However, the Coolwater Plant⁷, in Daggett, California, is the most efficient (with an average heat rate of 9,500) of the four plants in the package and thus should have a higher value per MW. I therefore assume that the implied market value for Coolwater could range from \$110,000 to \$220,000 per MW, or equivalently, \$110/kW to \$220/kW. The real-options based estimate of the capacity value, \$200/kW, explains the market valuation much better than does the discounted cash flow estimate, \$29/kW.

4.3 Capacity Valuation with Operational Characteristics

When applying the real-options approach to value a real asset, we must be aware of the physical operating characteristics of the asset. In the previous section, by valuing a fossil fuel electric power plant as a series of spark spread call options, I assumed the absence of all the operational characteristics including the start-up cost, the ramp-up time and the variable operating heat rate. Intuitively, operational constraints and transaction costs decrease the value of the underlying real asset because they either reduce the operating flexibility of the asset or impose “exercising” costs on the embedded options

⁷The Coolwater Plant is made up of four units. Two 256MW Combined Cycle Gas Turbines plus a steam turbine; and two conventional turbines with capacity 65MW and 81MW each. Some re-power work has been done on the larger units.

of the asset. However, it is not clear that to what extent the operational characteristics affect the value of a real asset. The purpose of this section is to examine the impacts of physical operating characteristics on asset valuation through examples in which I evaluate an electricity generation asset taking into consideration the aforementioned physical characteristics.

For the market-based valuation of an electricity generation asset, we first need to make assumptions regarding the price dynamics of electricity and the generating fuel. Instead of assuming some continuous-time price models, I employ two discrete-time processes in the form of an end-recombining trinomial tree (i.e. trinomial lattice) for modeling the prices of electricity and the generating fuel. With the presence of several operational constraints, even if we could formulate a power plant valuation model under the continuous-time price models, it would be very difficult to solve the valuation model. Under a trinomial lattice price model, the valuation of a power plant can be formulated and solved as a stochastic dynamic program with the operational characteristics easily incorporated. The recombining feature of the price tree keeps the state space grow polynomially with time horizon which enables us to handle relatively long time horizon. As the trinomial lattice converges weakly (or, in distribution) in the limit to some continuous-time price processes of electricity and the generating fuel, the value of a power plant under the trinomial lattice price model also converges to that under the corresponding continuous-time price models.

The rest of this section is organized as follows. I first construct a trinomial lattice describing the price evolution of electricity and the generating fuel. With properly imposed risk-neutral probabilities, the trinomial lattice converges weakly to either two correlated

geometric Brownian motion (GBM) processes or two correlated mean-reverting processes in the limit. I then formulate a stochastic dynamic program (SDP) over the trinomial lattice with the value function being the value of a fossil fuel power plant. The SDP formulation incorporates several operational characteristics of the power plant such as the start-up cost, ramp-up time and the variable operating heat rate. Finally, I solve the SDP for specific numerical examples and illustrate the implications of the operational characteristics on the valuation of a real asset.

4.3.1 Construction of the Discrete Price Processes

Suppose we are concerned with the value of a natural gas fired electricity power plant over time horizon T . The time interval $[0, T]$ is divided into N small time intervals of length Δt where $\Delta t = \frac{T}{N}$. S_t^e and S_t^g are the prices of electricity and natural gas at time point $t \in \{t_0 = 0, t_1, \dots, t_N = T\}$ where $t_n = t_{n-1} + \Delta t$ ($n = 1, 2, \dots, N$). The time points t_0, t_1, \dots, t_N are referred to as periods $0, 1, 2, \dots, N$, respectively. Let the price state vector (X_t, Y_t) denote $(\ln S_t^e, \ln S_t^g)$. I assume that the local price movements are trinomial movements, namely, in each time interval the price state vector moves from its initial value (X_n, Y_n) to one of three new values as illustrated in Figure (4.7). Different constructions of the end-recombining trinomial price trees correspond to different continuous-time price models. I shall focus on constructing trinomial lattices corresponding to the geometric Brownian motion and the mean-reversion price models.

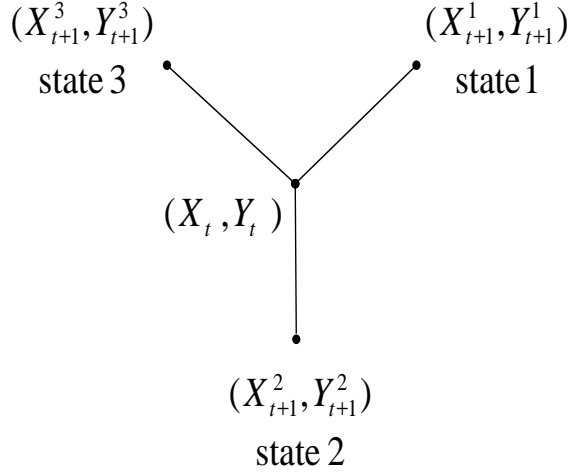


Figure 4.7: Construction of a Trinomial Lattice

Geometric Brownian motion price models

Suppose the prices of electricity and natural gas, S_t^e and S_t^g , follow two correlated geometric Brownian motion (GBM) processes in continuous-time. The logarithm of the price processes are given by

$$\begin{aligned}
 dX_t &= \mu_e dt + \sigma_e dB_t^1 \\
 dY_t &= \mu_g dt + \rho\sigma_g dB_t^1 + \sqrt{1-\rho^2}\sigma_g dB_t^2
 \end{aligned}
 \tag{4.1}$$

where $X_t = \ln S_t^e$ and $Y_t = \ln S_t^g$; μ_e and μ_g are annualized growth rates of the electricity price and the natural gas price, respectively; σ_e and σ_g are the instantaneous price volatilities of electricity and natural gas, respectively; ρ is the instantaneous correlation coefficient between the electricity and the natural gas price returns; B_t^1 and B_t^2 are two independent standard Brownian motions.

One particular way to set the price state movements is:

$$\begin{aligned}
X_{n+1} &= \begin{cases} X_n + \mu_e \cdot \Delta t + \sigma_e \sqrt{\frac{3}{2}} \sqrt{\Delta t} & \text{(state 1)} \\ X_n + \mu_e \cdot \Delta t & \text{(state 2)} \\ X_n + \mu_e \cdot \Delta t \Leftrightarrow \sigma_e \sqrt{\frac{3}{2}} \sqrt{\Delta t} & \text{(state 3)} \end{cases} \\
Y_{n+1} &= \begin{cases} Y_n + \mu_g \cdot \Delta t + \rho \sigma_g \sqrt{\frac{3}{2}} \sqrt{\Delta t} + \sigma_g \sqrt{1 \Leftrightarrow \rho^2} \sqrt{\frac{1}{2}} \sqrt{\Delta t} & \text{(state 1)} \\ Y_n + \mu_g \cdot \Delta t \Leftrightarrow \sigma_g \sqrt{1 \Leftrightarrow \rho^2} \frac{2}{\sqrt{2}} \sqrt{\Delta t} & \text{(state 2)} \\ Y_n + \mu_g \cdot \Delta t \Leftrightarrow \rho \sigma_g \sqrt{\frac{3}{2}} \sqrt{\Delta t} + \sigma_g \sqrt{1 \Leftrightarrow \rho^2} \sqrt{\frac{1}{2}} \sqrt{\Delta t} & \text{(state 3)} \end{cases} \quad (4.2)
\end{aligned}$$

where $\Delta t = \frac{T}{N}$; σ_e and σ_g are the instantaneous price volatilities of electricity and natural gas, respectively, which can be estimated from the market-traded options on electricity and natural gas; and ρ is the instantaneous correlation coefficient between the electricity and the natural gas price returns which can be estimated from the historical price series of electricity and natural gas. Let p_i denote the transition probability of moving from the current state into state i ($i = 1, 2, 3$) in the next period. It has been shown that the trinomial lattice defined by (4.2) weakly converges⁸ to (4.1) if the risk-neutral transition probabilities $P \equiv (p_1, p_2, p_3)'$ are set to be $(\frac{1}{3}, \frac{1}{3}, \frac{1}{3})'$ in any state (X_n, Y_n) , i.e.

$$P = \begin{cases} p_1 : \frac{1}{3} \\ p_2 : \frac{1}{3} \\ p_3 : \frac{1}{3} \end{cases}$$

⁸Let X^N and X be the stochastic processes defined on the probability spaces $(\Omega_N, \mathcal{F}_N, \mu_N)$ and $(\Omega, \mathcal{F}, \mu)$ with values in $D^M[0, T]$, the space of functions from $[0, T]$ to \mathcal{R}^M which are right-continuous with left limits. The sequence of processes X^N is said to converge weakly to X if, for any bounded continuous mapping, h , from $D^M[0, T]$ to \mathcal{R} , we have $E_N[h(X^N)] \rightarrow E[h(X)]$. See Billingsley (1968, chapter 1) for details.

Mean-reverting price models

The following continuous-time mean-reversion models are used by Deng, Johnson and Sogomonian (1998) for modeling the price returns of electricity and natural gas:

$$\begin{aligned} dX_t &= \kappa_e(\theta_e \Leftrightarrow X_t)dt + \sigma_e dB_t^1 \\ dY_t &= \kappa_g(\theta_g \Leftrightarrow Y_t)dt + \rho\sigma_g dB_t^1 + \sqrt{1 \Leftrightarrow \rho^2}\sigma_g dB_t^2 \end{aligned} \quad (4.3)$$

where $X_t = \ln S_t^e$ and $Y_t = \ln S_t^g$; θ_e and θ_g are the long-term means of X_t and Y_t , respectively; κ_e and κ_g are two positive mean-reverting coefficients indicating the rates at which the electricity price and the natural gas price revert to their respective long-term means; σ_e and σ_g are the instantaneous price volatilities of electricity and natural gas, respectively; ρ is the instantaneous correlation coefficient between the electricity and the natural gas price returns; B_t^1 and B_t^2 are two independent standard Brownian motion processes.

Employing the notations in (4.3), I construct a trinomial lattice representing some discrete-time mean-reverting price models for electricity and natural gas as follows. Let the price state movements on the trinomial lattice be

$$\begin{aligned} X_{n+1} &= \begin{cases} X_n + \sigma_e \sqrt{\frac{3}{2}} \sqrt{\Delta t} & \text{(state 1)} \\ X_n & \text{(state 2)} \\ X_n \Leftrightarrow \sigma_e \sqrt{\frac{3}{2}} \sqrt{\Delta t} & \text{(state 3)} \end{cases} \\ Y_{n+1} &= \begin{cases} Y_n + \rho\sigma_g \sqrt{\frac{3}{2}} \sqrt{\Delta t} + \sigma_g \sqrt{1 \Leftrightarrow \rho^2} \sqrt{\frac{1}{2}} \sqrt{\Delta t} & \text{(state 1)} \\ Y_n \Leftrightarrow \sigma_g \sqrt{1 \Leftrightarrow \rho^2} \frac{2}{\sqrt{2}} \sqrt{\Delta t} & \text{(state 2)} \\ Y_n \Leftrightarrow \rho\sigma_g \sqrt{\frac{3}{2}} \sqrt{\Delta t} + \sigma_g \sqrt{1 \Leftrightarrow \rho^2} \sqrt{\frac{1}{2}} \sqrt{\Delta t} & \text{(state 3)} \end{cases} \end{aligned} \quad (4.4)$$

where $\Delta t = \frac{T}{N}$. I then define a set of risk-neutral transition probabilities on the trinomial

lattice so that the resulting discrete-time price models for electricity and natural gas are mean-reverting. Let p_i denote the transition probability moving from a given state (X_n, Y_n) to state X_{n+1}^i ($i = 1, 2, 3$) and let $P \equiv (p_1, p_2, p_3)'$. If the following conditions hold

$$\begin{cases} \Leftrightarrow \frac{1}{3} < \left[\frac{\kappa_e(\theta_e - X_n)}{\sqrt{6\sigma_e}} + \frac{\kappa_g(\theta_g - Y_n)}{2\sqrt{6\sigma_g}} \right] \sqrt{\Delta t} < \frac{2}{3} \\ \Leftrightarrow \frac{2}{3} < \frac{\kappa_g(\theta_g - Y_n)}{\sqrt{6\sigma_g}} \sqrt{\Delta t} < \frac{1}{3} \\ \Leftrightarrow \frac{2}{3} < \left[\frac{\kappa_e(\theta_e - X_n)}{\sqrt{6\sigma_e}} \Leftrightarrow \frac{\kappa_g(\theta_g - Y_n)}{2\sqrt{6\sigma_g}} \right] \sqrt{\Delta t} < \frac{1}{3} \end{cases} \quad (4.5)$$

then P is given by

$$P = \begin{cases} p_1 : \frac{1}{3} + \left[\frac{\kappa_e(\theta_e - X_n)}{\sqrt{6\sigma_e}} + \frac{\kappa_g(\theta_g - Y_n)}{2\sqrt{6\sigma_g}} \right] \sqrt{\Delta t} \\ p_2 : \frac{1}{3} \Leftrightarrow \frac{\kappa_g(\theta_g - Y_n)}{\sqrt{6\sigma_g}} \sqrt{\Delta t} \\ p_3 : \frac{1}{3} \Leftrightarrow \left[\frac{\kappa_e(\theta_e - X_n)}{\sqrt{6\sigma_e}} \Leftrightarrow \frac{\kappa_g(\theta_g - Y_n)}{2\sqrt{6\sigma_g}} \right] \sqrt{\Delta t} \end{cases} \quad (4.6)$$

The conditions in (4.5) are for the purpose of making sure that the probabilities p_i ($i = 1, 2, 3$) are numbers between 0 and 1. If any of the conditions in (4.5) is not satisfied, then P is defined below:

$$\begin{aligned} \text{If } \frac{\kappa_g(\theta_g \Leftrightarrow Y_t)}{\sqrt{6\sigma_g}} \sqrt{\Delta t} \geq \frac{1}{3}, \quad P &= \begin{cases} p_1 : \frac{1}{2} \\ p_2 : 0 \\ p_3 : \frac{1}{2} \end{cases} \\ \text{If } \frac{\kappa_g(\theta_g \Leftrightarrow Y_t)}{\sqrt{6\sigma_g}} \sqrt{\Delta t} \leq \Leftrightarrow \frac{2}{3}, \quad P &= \begin{cases} p_1 : 0 \\ p_2 : 1 \\ p_3 : 0 \end{cases} \end{aligned} \quad (4.7)$$

$$\begin{aligned}
\text{If } \left\{ \begin{array}{l} \Leftrightarrow \frac{2}{3} < \frac{\kappa_g(\theta_g - Y_t)}{\sqrt{6\sigma_g}} \sqrt{\Delta t} < \frac{1}{3} \\ \left[\frac{\kappa_e(\theta_e - X_t)}{\sqrt{6\sigma_e}} + \frac{\kappa_g(\theta_g - Y_t)}{2\sqrt{6\sigma_g}} \right] \sqrt{\Delta t} \leq \Leftrightarrow \frac{1}{3} \end{array} \right. , \quad P = \begin{cases} p_1 : 0 \\ p_2 : \frac{1}{3} \Leftrightarrow \frac{\kappa_g(\theta_g - Y_t)}{\sqrt{6\sigma_g}} \sqrt{\Delta t} \\ p_3 : \frac{2}{3} + \frac{\kappa_g(\theta_g - Y_t)}{\sqrt{6\sigma_g}} \sqrt{\Delta t} \end{cases} \\
\text{If } \left\{ \begin{array}{l} \Leftrightarrow \frac{2}{3} < \frac{\kappa_g(\theta_g - Y_t)}{\sqrt{6\sigma_g}} \sqrt{\Delta t} < \frac{1}{3} \\ \left[\frac{\kappa_e(\theta_e - X_t)}{\sqrt{6\sigma_e}} + \frac{\kappa_g(\theta_g - Y_t)}{2\sqrt{6\sigma_g}} \right] \sqrt{\Delta t} \geq \frac{2}{3} \end{array} \right. \quad P = \begin{cases} p_1 : \frac{2}{3} + \frac{\kappa_g(\theta_g - Y_t)}{\sqrt{6\sigma_g}} \sqrt{\Delta t} \\ p_2 : \frac{1}{3} \Leftrightarrow \frac{\kappa_g(\theta_g - Y_t)}{\sqrt{6\sigma_g}} \sqrt{\Delta t} \\ p_3 : 0 \end{cases} \tag{4.8}
\end{aligned}$$

$$\begin{aligned}
\text{If } \left\{ \begin{array}{l} \Leftrightarrow \frac{1}{3} < \left[\frac{\kappa_e(\theta_e - X_n)}{\sqrt{6\sigma_e}} + \frac{\kappa_g(\theta_g - Y_n)}{2\sqrt{6\sigma_g}} \right] \sqrt{\Delta t} < \frac{2}{3} \\ \Leftrightarrow \frac{2}{3} < \frac{\kappa_g(\theta_g - Y_t)}{\sqrt{6\sigma_g}} \sqrt{\Delta t} < \frac{1}{3} \\ \left[\frac{\kappa_e(\theta_e - X_n)}{\sqrt{6\sigma_e}} \Leftrightarrow \frac{\kappa_g(\theta_g - Y_n)}{2\sqrt{6\sigma_g}} \right] \sqrt{\Delta t} \leq \Leftrightarrow \frac{2}{3} \end{array} \right. , \quad P = \begin{cases} p_1 : 0 \\ p_2 : \frac{1}{3} \Leftrightarrow \frac{\kappa_g(\theta_g - Y_t)}{\sqrt{6\sigma_g}} \sqrt{\Delta t} \\ p_3 : \frac{2}{3} + \frac{\kappa_g(\theta_g - Y_t)}{\sqrt{6\sigma_g}} \sqrt{\Delta t} \end{cases} \\
\tag{4.9}
\end{aligned}$$

$$\begin{aligned}
\text{If } \left\{ \begin{array}{l} \Leftrightarrow \frac{1}{3} < \left[\frac{\kappa_e(\theta_e - X_n)}{\sqrt{6\sigma_e}} + \frac{\kappa_g(\theta_g - Y_n)}{2\sqrt{6\sigma_g}} \right] \sqrt{\Delta t} < \frac{2}{3} \\ \Leftrightarrow \frac{2}{3} < \frac{\kappa_g(\theta_g - Y_t)}{\sqrt{6\sigma_g}} \sqrt{\Delta t} < \frac{1}{3} \\ \left[\frac{\kappa_e(\theta_e - X_n)}{\sqrt{6\sigma_e}} \Leftrightarrow \frac{\kappa_g(\theta_g - Y_n)}{2\sqrt{6\sigma_g}} \right] \sqrt{\Delta t} \geq \frac{1}{3} \end{array} \right. \quad P = \begin{cases} p_1 : \frac{2}{3} + \frac{\kappa_g(\theta_g - Y_t)}{\sqrt{6\sigma_g}} \sqrt{\Delta t} \\ p_2 : \frac{1}{3} \Leftrightarrow \frac{\kappa_g(\theta_g - Y_t)}{\sqrt{6\sigma_g}} \sqrt{\Delta t} \\ p_3 : 0 \end{cases}
\end{aligned}$$

It is clear that the risk-neutral probabilities defined in (4.6), (4.7), (4.8) and (4.9) yield two mean-reverting price processes for electricity and natural gas. For instance, suppose the conditions in (4.5) are satisfied in the current state (X_n, Y_n) thus (p_1, p_2, p_3) is given by (4.6). In (4.6), if the current Y_n is greater than θ_g meaning that the current natural gas price is above its long-term mean, then the term $\frac{\kappa_g(\theta_g - Y_n)}{\sqrt{6\sigma_g}}$ is a negative number, therefore from (4.6) we see that p_2 , which is the probability of moving towards a decreasing level of Y_n , is increased. On the other hand, if the current Y_n is a number less than θ_g meaning that the current natural gas price is below its long-term mean, then the term $\frac{\kappa_g(\theta_g - Y_n)}{\sqrt{6\sigma_g}}$ becomes a positive number, therefore from (4.6) we see that p_1 and p_3 , which are the probabilities of moving towards increasing levels of Y_n , is increased. Similarly, when the

current X_n is greater/less than its long-term mean θ_e , the probability of moving towards a decreasing/increasing level of X_n is increased. The risk-neutral probabilities defined in (4.7) (4.8) and (4.9) also have such mean-reverting properties with respect to the price state vector (X_n, Y_n) ⁹.

4.3.2 Valuation of Electricity Generation Assets with Operational Characteristics

Having constructed a trinomial lattice representing the price dynamics of electricity and natural gas, I proceed to the valuation of a natural gas fired power plant taking into consideration its operational characteristics.

Incorporating Physical Operating Characteristics

One approach would be to take all the physical characteristics of a power plant and transaction costs into consideration and formulate the asset valuation problem as a stochastic dynamic program. However, such approach will undoubtedly result in a state space of huge dimensions thus the “curse of dimensionality” makes it impossible to implement this approach. In general, the more details about the operational characteristics one would like to incorporate into the asset valuation, the larger state space it requires to formulate the asset valuation problem. We need to trade off between the granularity of the description of the operational characteristics when formulating an asset valuation problem and the computational complexity required to solve the asset valuation

⁹This discrete-time model may not converge weakly to the previously mentioned continuous-time mean-reversion model. The parameters need to be estimated directly from the discrete model structure.

problem.

While all operational characteristics affect the valuation of a real asset, some characteristics have more significant impacts on asset valuation than others do. In the context of valuing a natural gas fired power plant, the start-up cost, the ramp-up time and the variable heat rates are considered the most significantly influencing operational characteristics. I shall briefly describe what these characteristics are and how I incorporate them into the valuation through simplifying assumptions.

Operational Characteristics 1 Each time a fossil fuel electric power generating unit is turned on, a **start-up cost** is incurred because the water in the boiler of the generator must be heated before the generator can generate power. Moreover, the cost to start up the generating unit depends on how long the unit has been turned off. The longer the unit is off, the more heat is dissipated from its boiler thus a higher cost is incurred when reheating the water. I simplify this effect assuming that a constant start-up cost, c_{start} , is incurred whenever the power plant is turned on.

Operational Characteristics 2 Once a power plant is turned on, it always takes a short period of time (i.e. **ramp-up time**) for its generating unit¹⁰ to reach certain operating output levels. Similar to the case of start-up cost, the length of the ramp-up time also depends on how long the power plant has been off. To reflect this aspect to first order, I assume that there is a constant time lag between the time point at which a generating unit is turned on and the time point at which the

¹⁰For the ease of exposition, I assume that a power plant only has one generating unit. In general, a power plant often has several generating units.

generating unit reaches its full output capacity.

Operational Characteristics 3 While a power plant is in operation, its operating efficiency measured by its **operating heat rate** varies with the output level, i.e. the operating heat rate is output dependent rather than a constant over time. When operated at its rated maximum capacity level, the power plant is very efficient (i.e. operating heat rate is at the low end of the heat rate range); when operated at its rated minimum capacity level, the power plant is very inefficient (i.e. operating heat rate is at the high end of the heat rate range). The operating heat rate of a generating unit is often modeled as a quadratic function of the electricity output quantity (see Wood and Wollenberg (1984)). However, I simplify this dependency assuming that a generating unit operates (when turned on) at two output levels, either at the maximum capacity level Q_{\max} or at the minimum capacity level Q_{\min} . The operating heat rates of the generating unit at the two output levels are HR_{\max} and HR_{\min} , respectively.

A Stochastic Dynamic Programming Formulation

For valuing a natural gas fired electric power plant, I make the following assumptions.

Assumption 4.3.1 The power plant of interest is only subject to the three operational constraints described in **Section 4.3.2**.

Assumption 4.3.2 When running the power plant, the operator takes one of the three possible actions at discrete time points. The three possible actions are: to shut down the plant, to run the power plant at its minimum capacity level (turn on

the plant first if it is currently off), and to run the plant at its maximum capacity level (turn on the plant first if it is currently off). I denote these three actions by “**off**”, “**on_min**”, and “**on_max**”, respectively.

The operator of the power plant seeks to maximize the expected total profit of the power plant with respect to the random price vector (S_t^e, S_t^g) over the operating time horizon by making optimal decisions regarding whether to turn on or shut down the generating unit as well as how to operate the unit. Under the risk-neutral probabilities, the expected total profit of a power plant over its operating time horizon yields the value of the power plant during that time period.

Before getting into the formulation of the valuation problem, I shall introduce the following notations. The operating time horizon T is divided into N periods. The power plant operator makes the operational decisions at the beginning of every m periods, i.e. the operator takes actions only in periods $0, m, 2m, 3m, \dots, km, \dots$. Additional variables will be introduced when necessary.

- n : index for periods $(1, 2, \dots, N)$
- X_n : state variable indicating the logarithm of the electricity price in period n
- Y_n : state variable indicating the logarithm of the natural gas price in period n
- w : state variable indicating whether the power plant is currently on or off; “ $w = 0$ ” means that the power plant is currently “off”; “ $w = 1$ ” means that the plant is currently “on”
- β : discount factor over one time period
- a_n : action taken by the power plant operator in period n
- Φ : the action space, and $\Phi \equiv \{\text{off, on_min, on_max}\}$

$c_{start}, Q_{\min}, HR_{\min}, Q_{\max}, HR_{\max}$ are defined in the previous section. The ramp-up time is assumed to be one-period's delay for simplicity¹¹. Let the value function $V_n(X_n, Y_n, w)$ be the expected total profit of the power plant over time periods $n, n+1, n+2, \dots, N$ given the current price state vector (X_n, Y_n) and the current operating state w of the power plant. Then $V_n(X_n, Y_n, w)$ is defined by the following three recursive formulas.

If $n \neq k \cdot m$ where $k = 0, 1, 2, \dots$, then the operator takes no action in period n . The value of a power plant is equal to the discounted expected future values of the power plant.

$$V_n(X_n, Y_n, w) = \beta \cdot E_n[V_{n+1}(X_{n+1}, Y_{n+1}, w)] \quad (4.10)$$

where $E_n[\cdot]$ is the conditional expectation function conditioned on information available in period n .

If $n = k \cdot m$ where $k = 0, 1, 2, \dots$, and $w = 0$, then

$$V_n(X_n, Y_n, 0) = \max_{a_n \in \Phi} \begin{cases} on_max : & \Leftrightarrow c_{start} + \beta \cdot E_n[V_{n+1}(X_{n+1}, Y_{n+1}, 1)] \\ on_min : & \Leftrightarrow c_{start} + \beta \cdot E_n[V_{n+1}(X_{n+1}, Y_{n+1}, 1)] \\ off : & \beta \cdot E_n[V_{n+1}(X_{n+1}, Y_{n+1}, 0)] \end{cases} \quad (4.11)$$

¹¹I assume that the time lag required for switching the output levels between Q_{\max} and Q_{\min} is shorter than one period. Therefore, it is not considered in this formulation.

If $n = k \cdot m$ where $k = 0, 1, 2, \dots$, and $w = 1$, then

$$V_n(X_n, Y_n, 1) = \max_{a_n \in \Phi} \begin{cases} \text{on_max} : & Q_{\max} \cdot [\exp(X_n) \Leftrightarrow HR_{\max} \cdot \exp(Y_n)] + \\ & \beta \cdot E_n[V_{n+1}(X_{n+1}, Y_{n+1}, 1)] \\ \text{on_min} : & Q_{\min} \cdot [\exp(X_n) \Leftrightarrow HR_{\min} \cdot \exp(Y_n)] + \\ & \beta \cdot E_n[V_{n+1}(X_{n+1}, Y_{n+1}, 1)] \\ \text{off} : & \beta \cdot E_t[V_{t+1}(X_{t+1}, Y_{t+1}, 0)] \end{cases} \quad (4.12)$$

The Solution of the Stochastic Dynamic Program (SDP)

Under both trinomial price models constructed in **Section 4.3.1**, the optimal policies to the SDP have a barrier control form. There exists a “no-action” band on the plane of the natural gas price and the electricity price. If the price vector (S_t^g, S_t^e) consisting of the market prices of natural gas and electricity is inside this band, then it is optimal for the plant operator to maintain the status quo. If the price vector is above the upper boundary of the band, then, depending on the state of the power plant, the operator should increase the output level of the plant from “off” to “on” or from half capacity to full capacity. If the price vector is below the lower boundary of the band, then it is optimal for the operator to reduce the output level of the power plant to “off” or half capacity depending on the state of the plant.

4.3.3 Numerical Examples and Comparative Statics

I have implemented this proposed methodology for valuing a natural gas fired power plant accounting for operational characteristics in C programs. This section reports some numerical results on valuing a hypothetical 100 MW gas fired power plant over

a 720-day period. I assume that the gas power plant incurs a start-up cost whenever turned on and it takes one day to ramp up the power plant from the “off” state to a desired output state but there is no delay in increasing/decreasing output level once the power plant is on. For start-up cost, I examine two possible values, \$6000/start and \$12000/start. The maximum and the minimum capacity levels are assumed to be 100 MW and 50 MW, respectively. Moreover, the ratio between the operating heat rates at the minimum and the maximum capacity levels of the power plant is assumed to be 1.38 : 1. Under both the GBM and the mean-reversion price assumptions for electricity and natural gas, the trinomial lattices are built with Δt being 1 day. The operator of the power plant makes operating decisions at all nodes of the lattice, i.e. $m = 1$. The initial prices of electricity and natural gas are assumed to be \$21.7 and \$3.16, respectively, which are sampled from the historical market prices.

Geometric Brownian motion price assumption

Assuming that the prices of electricity and natural gas follow two correlated GBM processes in continuous-time, I construct a trinomial lattice according to (4.2) with the parameters given in Table (4.2). I then compute the value of the gas fired power plants

μ_e	2%	μ_g	2%
σ_e	0.75	σ_g	0.6
ρ	0.3		

Table 4.2: Parameters for GBM Price Models

subject to the three operating constraints for different operating heat rates using this trinomial lattice. The start-up costs of \$6000 and \$12000 are chosen as numbers close to the one-day on-peak operating profits of the underlying 100 MW natural gas power

plant. I also compute the value of the power plant in the case where none of the three operational characteristics is considered as well as in the case where only the start-up cost is ignored. The numerical results are reported in Table (4.3). For instance, suppose the power plant under consideration has a start-up cost of \$6000 and a operating heat rate of 9500 MBtu/MWh when operated at its maximum capacity level, its value (or, operating profit) per year is \$4.776 million. If we ignore all three physical operating characteristics, then the value of the power plant becomes \$4.803 million per year which would be 0.56% higher than the value with three physical characteristics. The solid

Heat Rate (HR_{\max} MMBtu/MWh)	8000	9500	12000	14000
Cap. Value (nophy. constr.)	5.990 mill.	4.803 mill.	3.489 mill.	2.790 mill.
Cap. Value (3 phy. constr./stup=\$6k)	5.958 mill.	4.776 mill.	3.469 mill.	2.774 mill.
Pctg. Val. Overstate. (ignoring 3 phy./stup=\$6k)	0.54%	0.56%	0.58%	0.60%
Cap. Value (2 phy. constr./stup=\$0)	5.988 mill.	4.801 mill.	3.488 mill.	2.789 mill.
Pctg. Val. Overstate. (ignoring stup only/stup=\$6k)	0.50%	0.51%	0.53%	0.54%
Cap. Value (3 phy. constr./stup=\$12k)	5.941 mill.	4.763 mill.	3.459 mill.	2.765 mill.
Pctg. Val. Overstate. (ignoring 3 phy./stup=\$12k)	0.83%	0.85%	0.89%	0.91%
Cap. Value (2 phy. constr./stup=\$0)	5.988 mill.	4.801 mill.	3.488 mill.	2.789 mill.
Pctg. Val. Overstate. (ignoring stup only/stup=\$12k)	0.79%	0.81%	0.83%	0.85%

Table 4.3: Value of a NG fired Power Plant under GBM Price Models

curves in Figure (4.8) plot the value of the underlying power plant across different heat rates with start-up cost being \$6000 and \$12000, respectively, against the capacity value axis on the left. The dashed curves in Figure (4.8) plot the percentages of capacity value overstated by ignoring the three physical characteristics across different heat rates against the percentage axis on the right. We can see that the higher level of operating

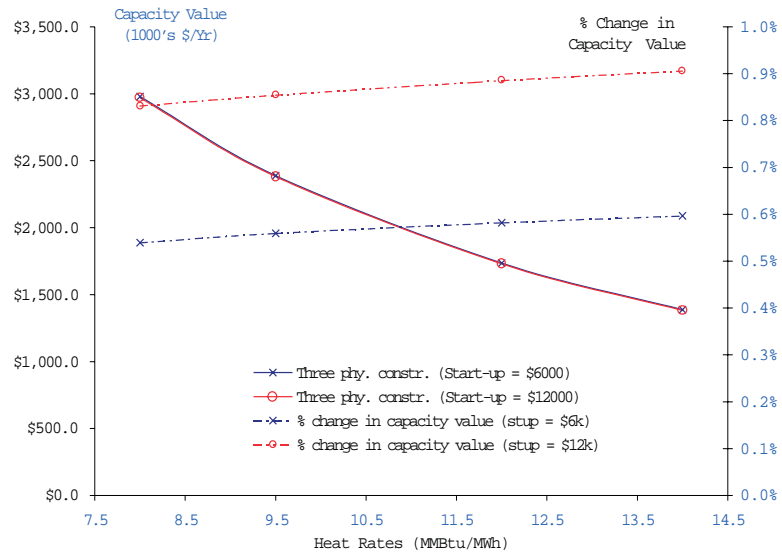


Figure 4.8: Valuation of A Power Plant with/without Physical Characteristics Under GBM Price Models

heat rate or the higher start-up cost corresponds to the higher percentage of overstatement in capacity valuation in general. But the percentage of capacity value which is overstated is under 1% for operating heat rate up to the level of 14000 MMBtu/MWh under the GBM price models.

Table (4.3) also shows the value of the underlying power plant as well as the corresponding percentage of overstatement in valuation when only the start-up costs are ignored. These results are plotted in Figure (4.9) with the x-axis representing different operating heat rates. The plain solid curve plots the value of the underlying power plant without taking into accounts the start-up costs when the start-up cost is \$6000 or \$12000 for different operating heat rates. The solid curves with crosses and circles represent the percentages of valuation which are overstated by ignoring the start-up costs of \$6000/start-up and \$12000/start-up, respectively. The percentages of valuation over-

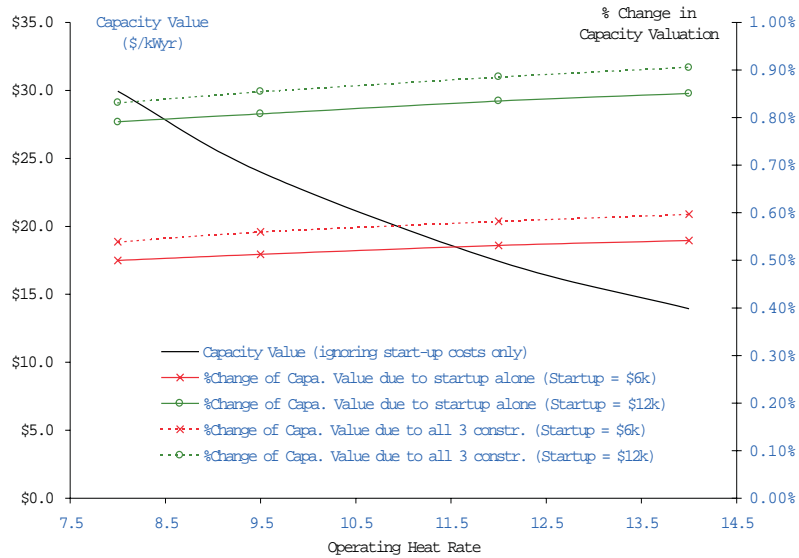


Figure 4.9: Valuation of A Power Plant with/without the Start-up Cost under GBM Price Models

stated by ignoring all three operating characteristics are plotted by dashed curves with crosses and circles for comparison purposes. Ignoring the start-up costs alone accounts for more than 60% of the overstated value of a power plant due to ignoring the three operating characteristics in valuation for various operating heat rates.

Mean-reverting price assumption

I next examine the impacts of operational characteristics on the valuation of a power plant under the assumption that both the electricity price and the natural gas price are mean-reverting which is a more reasonable assumption than the GBM assumption. The parameters used to construct the mean-reverting trinomial lattice are given in Table (4.4). The value of the underlying power plant is calculated for each of the three cases: considering all three physical operating characteristics, ignoring the three operating characteristics, and ignoring the start-up cost only. The numerical results are presented

κ_1	3	κ_2	2.25
θ_1	3.15	θ_2	0.87
σ_1	0.75	σ_2	0.6
ρ	21.7		

Table 4.4: Parameters for Mean-Reversion Price Models

in Table (4.5). Similar to the previous section, I plot the value of the power plant

Heat Rate (HR_{\max} MMBtu/MWh)	8000	9500	12000	14000
Cap. Value (nophy. constr.)	5.211 mill.	3.236 mill.	1.381 mill.	0.679 mill.
Cap. Value (3phy. constr./stup=\$6k)	5.153 mill.	3.176 mill.	1.335 mill.	0.648 mill.
Pctg. Val. Overstate. (ignoring 3 phy./stup=\$6k)	1.13%	1.88%	3.43%	4.83%
Cap. Value (2 phy. constr./stup=\$0)	5.207 mill.	3.230 mill.	1.378 mill.	0.677 mill.
Pctg. Val. Overstate. (ignoring stup only/stup=\$6k)	1.06%	1.70%	3.21%	4.51%
Cap. Value (3 phy. constr./stup=\$12k)	5.121 mill.	3.144 mill.	1.312 mill.	0.632 mill.
Pctg. Val. Overstate. (ignoring 3 phy./stup=\$12k)	1.75%	2.93%	5.28%	7.45%
Cap. Value (2 phy. constr./stup=\$0)	5.207 mill.	3.230 mill.	1.378 mill.	0.677 mill.
Pctg. Val. Overstate. (ignoring stuponly/stup=\$12k)	1.68%	2.74%	5.05%	7.12%

Table 4.5: Value of a NG fired Power Plant under Mean-Reversion Price Models

accounting for all three operating characteristics for different heat rates in Figure (4.10). The x-axis represents different heat rates. The solid curves with crosses and circles plot the capacity value per year with start-up cost being \$6000/start-up and \$12000/start-up, respectively. The capacity value ignoring the three operating characteristics for different heat rates is plotted by the plain solid curve. All three curves are plotted against the capacity value axis on the left. The dashed curves with circles and crosses plot the percentages by which the capacity value is overstated due to ignoring the physical operating characteristics with the start-up cost being \$6000 and \$12000, respectively. The percentage for which the capacity value is overstated due to ignoring the operating

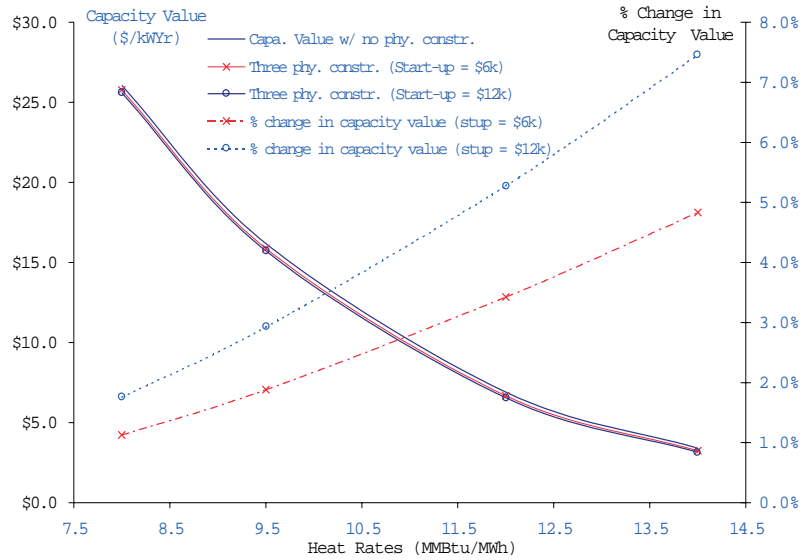


Figure 4.10: Valuation of A Power Plant with/without Physical Characteristics Under Mean-Reversion Price Models

characteristics ranges from 1.13% for the most efficient plant with a low start-up cost to 7.45% for the least efficient plant with a high start-up cost.

Figure (4.11) plots the values of the power plant with and without the start-up cost only. We can see that the impact of the start-up cost on capacity valuation is very significant. Ignoring the start-up cost while considering the other aspects accounts for more than 90% of the overstated capacity value of the underlying power plant.

4.3.4 Conclusion

To summarize the above numerical results, I conclude that the operational characteristics affect the valuation of a power plant to different extents depending on the operating efficiency of the power plant and the assumptions about the electricity and the generating fuel prices. In general, the impacts of physical operating characteristics on the power

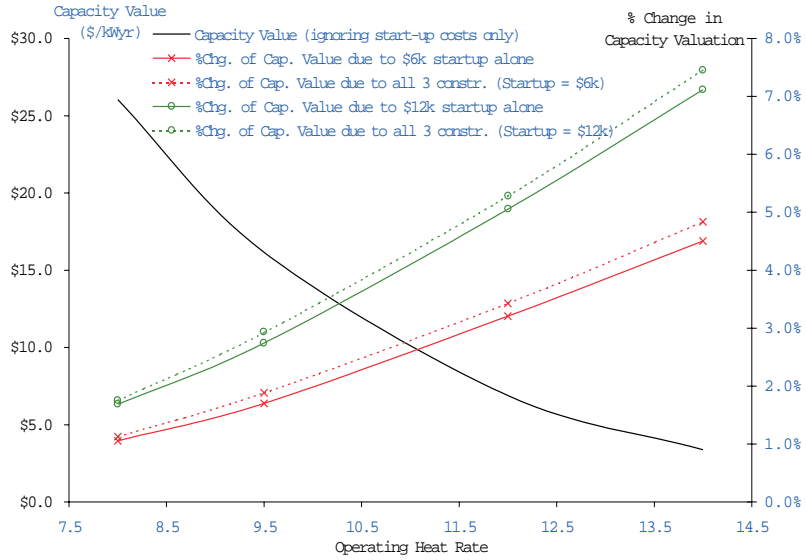


Figure 4.11: Valuation of A Power Plant with/without the Start-up Cost Under Mean-Reversion Price Models

plant valuation are far more significant under the mean-reversion price models than they are under the geometric Brownian motion price models. Under each price model, the more efficient a power plant is, the less its valuation is affected by the operational constraints and vice versa. In the examples with mean-reverting commodity price processes, the impacts on capacity valuation range from 1.13% for the most efficient plant with a low start-up cost to 7.45% for the least efficient plant with a high start-up cost. Among the three operational characteristics of a power plant which I consider here, start-up cost affects the capacity valuation the most. The reason is two-fold. The first-order effect of the start-up cost on capacity valuation is that it directly imposes a transaction cost on exercising the embedded spark spread options in a fossil fuel power plant when the electricity price is greater than the fuel cost. The second-order effect of the start-up cost is that it forces the power plant to keep operating at a loss or to forego a profit when the

start-up cost cannot be justified by the expected cost-saving or the expected profit that would result from turning the power plant off or on. In other words, the start-up cost reduce the “option value” of a power plant. My sensitivity analysis reveals that, under the mean-reversion models, ignoring the start-up cost alone can explain more than 90% of the overstated capacity value of a power plant (as compared to the overstated value when all three operational characteristics are ignored).

Chapter 5

Summary and Future Research

In this dissertation, I have addressed the issues of transmission pricing design, modeling electricity spot prices and pricing electricity financial instruments as well as market-based valuation of real assets. I shall summarize the findings of this thesis and point out some directions for future research.

5.1 Transmission Pricing

Regarding the transmission pricing design, it is still an on-going debate as to which approach works the best. For instance, the nodal pricing approach emphasizes the short-run efficiency of an electrical system. However, the promising aspect of short-run efficiency relies on generators and loads revealing their true marginal costs or willingness-to-pay. Therefore, the day-to-day efficient operation of a power system under a nodal spot pricing scheme depends on the incentive effects which are not addressed by the nodal pricing approach. From the implementation point of view, one other difficulty of

the nodal spot pricing approach is that it impedes trading and price discovery due to low liquidity at the nodal markets, lack of transparency in how prices are determined, and the fact that exact prices are only known *ex post*.

The priority insurance based transmission pricing scheme proposed in Chapter 2 attempts to strike a proper balance between the economic efficiency and the simplicity of implementation. Through customer self-selection, thus incentive-compatible, the ISO manages to achieve a second best solution in the efficient allocation of the scarce transmission capacity when network congestion occurs. This scheme provides approximate signals indicating the locational advantages for investment in generation and load. Last but not the least, it is simple and easy to be implemented.

The long-run efficiency issues of signaling the need for investment in a transmission system and compensating the owners of existing transmission assets were not addressed in the current analysis. Under the proposed transmission pricing scheme, one interesting problem is to investigate whether the ISO could signal the need for transmission investment by imposing a proper set of insurance premium functions in all zones. Another interesting problem is to design a scheme for the allocation of the ISO's profits resulting from the collection of the insurance premia and the congesting management such that the owners of the existing transmission assets are sufficiently compensated.

5.2 Electricity Spot Price Modeling

The needs of trading electricity, performing risk management and asset valuation, as well as financing new investments require sophisticated modeling of electricity spot prices. To

accurately model electricity prices, I take into consideration the physical characteristics of electricity. Resorting to jump-diffusion processes, I have examined three stochastic price models which capture the mean-reversion, regime-switching, jumps and spikes and many other prominent price behaviors of electricity. I provide the specification for these models and demonstrate how to compute prices of various electricity derivatives under each model using the Fourier transform methods in Chapter 3.

I find that the market anticipation of jumps and spikes in the electricity spot prices explains the enormous implied volatility observed from market prices of traded electricity options. Contrary to the commonly used geometric Brownian motion (GBM) model, the proposed mean-reversion jump-diffusion spot price models approximate the market values of short-maturity out-of-the-money options very well. The mean-reversion jump-diffusion models capture the effect of spikes that cause the unusually high market implied volatility in the short-maturity out-of-the-money call options on electricity. I mentioned briefly how I can fit the models using electricity price data but a formal parameter estimation was out of the scope of Chapter 3. As for future research, I feel that it is important to develop an efficient econometric model, e.g. taking a Generalized Method of Moments approach, to perform a rigorous parameter estimation as more electricity market data becomes available.

5.3 Risk Management and Asset Valuation

As the competitive and volatile electricity markets become more prevalent, market participants feel the urgent needs for establishing their risk management programs. Through

two examples, I demonstrate how to structure and evaluate hedge strategies for the operational risks and the transmission risks using the spark spread options and the locational spread options.

On the asset valuation side, a market-based methodology for valuing an investment project such as a power plant construction or acquisition is required in place of the traditional discounted cash flow approach. I first construct a real options approach for valuing the electricity generation and transmission assets abstracting the operating characteristics of the real assets such as start-up cost, ramp-up time and variable heat rate. In the context of valuing a power plant, I find that the option-value based valuation yields a much better approximate to observed market values than does the DCF valuation. The implication of jumps and spikes in electricity prices on capacity valuation is that, in the near-term when the effects of jumps and spikes are significant, even a very inefficient power plant can be quite valuable. This could explain why recently sold power plants fetched hefty premia over book value.

To investigate the impacts of operational characteristics on the valuation of a real asset, I employ discrete-time price models for the underlying commodity prices and formulate the valuation of a real asset with operating characteristics as a stochastic dynamic program. Through several numerical examples of valuing a natural gas fired power plant, I illustrate that the significance of physical characteristics in asset valuation depends on the assumptions about the electricity and the generating fuel prices. Moreover, the more (less) efficient a power plant is, the less (more) significant the operating characteristics are to its valuation. These conclusions are made under the discrete-time price models which are counterparts of the continuous-time GBM and mean-reverting price models.

In future work, I expect to incorporate jumps into the discrete-time mean-reversion price models and examine the implications of jumps on the above conclusions.

Appendix A

Proofs in Chapter 2

A.1 Proof of Proposition 1

Proof. Notice that the (ED) problem and the $(ISO2)$ have the same set of constraints. It is therefore sufficient to show that the objectives of the two problems are equivalent provided $\widetilde{D}_i(c^*(v)) = D_i(v)$. Let $v_i(q)$ denote $D_i^{-1}(q)$.

$$\begin{aligned}
 & \max \sum_{i \in N_D} q_i \cdot S_{m(i)} \Leftrightarrow \sum_{i \in N_S} \int_0^{q_i} v_i(q) dq \quad (ED \text{ objective}) \\
 \Leftrightarrow & \max \sum_{i \in N_D} q_i \cdot S_{m(i)} \Leftrightarrow \sum_{i \in N_S} \int_0^{D_i(S_{m(i)})} v_i(q) dq + \sum_{i \in N_S} \int_{q_i}^{D_i(S_{m(i)})} v_i(q) dq \\
 \Leftrightarrow & \max \sum_{i \in N_D} q_i \cdot S_{m(i)} + \sum_{i \in N_S} (D_i(S_{m(i)}) \Leftrightarrow q_i) S_{m(i)} \Leftrightarrow \sum_{i \in N_S} (D_i(S_{m(i)}) \Leftrightarrow q_i) S_{m(i)} \\
 & \quad + \sum_{i \in N_S} \int_{q_i}^{D_i(S_{m(i)})} v_i(q) dq
 \end{aligned} \tag{A.1}$$

$$\begin{aligned}
&\Leftrightarrow \max \sum_{i \in N_D} q_i \cdot S_{m(i)} + \sum_{i \in N_S} (D_i(S_{m(i)}) \Leftrightarrow q_i) S_{m(i)} \Leftrightarrow \sum_{i \in N_S} \int_{q_i}^{D_i(S_{m(i)})} [S_{m(i)} \Leftrightarrow v_i(q)] dq \\
&\Leftrightarrow \max \sum_{i \in N_D} q_i \cdot S_{m(i)} + \sum_{i' \in N_S} q_{i'} \cdot S_{m(i')} \Leftrightarrow IP \\
&\Leftrightarrow \max \sum_{j=1}^k Q_j \cdot S_j \Leftrightarrow IP \\
&\Leftrightarrow \min IP \Leftrightarrow \sum_{j=1}^k Q_j \cdot S_j \\
&\Leftrightarrow \min IP \Leftrightarrow \frac{1}{k} \sum_{1 \leq l < j \leq k} (Q_l \Leftrightarrow Q_j)(S_l \Leftrightarrow S_j) \text{ (ISO2 objective)}
\end{aligned}$$

where

$$\begin{aligned}
Q_k &\equiv \sum_{i \in Z_k} q_i \text{ with } Z_k \text{ denoting the node set of zone } k. \\
IP &\equiv \sum_{i \in N_S} \int_{q_i}^{D_i(S_{m(i)})} [S_{m(i)} \Leftrightarrow v_i(q)] dq
\end{aligned}$$

The last equivalent relationship utilizes the fact that $\sum_{i=1}^k Q_i = 0$. ■

Appendix B

Technical Conditions in Chapter 3

B.1 Conditions for $\varphi \cdot e^{\leftrightarrow r t}$ to be a martingale in

Section 3.2

A particular set of technical conditions are¹:

1. The coefficients in (3.1), $\kappa_i(t)$, $\theta_i(t)$, $\sigma_i(t)$, $\rho(t)$ and $\lambda_i(t)$ ($i = 1, 2$), are bounded continuous functions on $[0, \infty)$. When the jump intensity λ_i ($i = 1, 2$) is a function of the state vector \overline{X}_t , we further assume that $\int_0^t \lambda_i(\overline{X}_s, s) ds < \infty P \Leftrightarrow a.s., \forall t \geq 0$.
2. $\phi_J^i(c_1, c_2, t)$ ($i = 1, 2$) is well defined on C^2 and it is measurable.
3. For an initial condition $((x_0, y_0), 0)$, the system of ODEs (3.5) has a unique solution α and β .
4. $E[\int_0^T |\gamma_t^i| dt] < \infty$, where $\gamma_t^i = \Psi_t \cdot (\phi_J^i(\beta_1, \beta_2, t) \Leftrightarrow 1) \cdot \lambda_i(t)$ ($i = 1, 2$).

¹See Duffie, Pan and Singleton (1998) for a more general setup.

5. $E[(\int_0^T \eta_t \cdot \eta_t dt)^{1/2}] < \infty$, where

$$\eta_t = \Psi_t \cdot \beta^T \begin{pmatrix} \sigma_1(t) & 0 \\ \rho(t)\sigma_2(t) & \sqrt{1 - \rho(t)^2}\sigma_2(t) \end{pmatrix}.$$

6. $E[|\Psi_T|] < \infty$, where

$$\Psi_t = e^{-rt} \exp[\alpha(t, u) + \beta_1(t, u)X_t + \beta_2(t, u)Y_t]$$

for each $t \leq T$.

Bibliography

- [1] Barz, G. and B. Johnson (1998), "Modeling the Prices of Commodities that are Costly to Store: the Case of Electricity," *Proceedings of the Chicago Risk Management Conference* (May 1998), Chicago, IL.
- [2] Bates, D. (1996), "Jump and Stochastic Volatility: Exchange Rate Processes Implicit in Deutsche Mark Options," *The Review of Financial Studies*, 9, 69-107.
- [3] Black, F. and M. Scholes (1973), "The Pricing of Options and corporate Liabilities," *Journal of Political Economy*, 81 (May-June), 637-59.
- [4] Chao, Hung-po and Stephen Peck (1998), "Reliability Management in Competitive Electricity Market," *Journal of Regulatory Economics* 14: 189-200.
- [5] Chao, Hung-po and Stephen Peck (1997), "An Institutional Design for an Electricity Contract Market with Central Dispatch," *The Energy Journal* 18(1): 85-110.
- [6] Chao, Hung-po and Stephen Peck (1996), "A Market Mechanism for Electric Power Transmission," *Journal of Regulatory Economics* 10(1) July: 25-60.

- [7] Chao, Hung-po and Robert Wilson (1987), "Priority Service: Pricing, Investment, and Market Organization," *American Economic Review* 77(5): 899-916.
- [8] Cox, J.C., J.E. Ingersoll, and S.A. Ross (1985), "A Theory of the Term Structure of Interest Rates," *Econometrica*, 53(2), 385-407.
- [9] Deng, Shijie, B. Johnson, and A. Sogomonian (1998), "Exotic Electricity Options and the Valuation of Electricity Generation and Transmission Assets," *Proceedings of the Chicago Risk Management Conference* (May 1998), Chicago, IL.
- [10] Dixit, A.K. and R.S. Pindyck (1994), *Investment under Uncertainty*, Princeton University Press, NJ.
- [11] Duffie, D. (1996), *Dynamic Asset Pricing Theory*, 2nd ed. Princeton University Press, NJ.
- [12] Duffie, D. and R. Kan (1996), "A Yield-Factor Model of Interest Rate," *Mathematical Finance*, 6(4), 379-406.
- [13] Duffie, D., J. Pan, and K. Singleton (1998), "Transform Analysis and Option Pricing for Affine Jump-Diffusion," Working Paper, Graduate School of Business, Stanford University.
- [14] Gilbert, R. and J. Henly (1991), "The Value of Rate Reform in a Competitive Electric Power Market," In *Regulatory Choices: A Perspective on Developments in Energy Policy*, edited by R. Gilbert. Berkeley: University of California Press.

- [15] Green, Richard (1997), "Electricity Transmission Pricing: an International Comparison," *Utilities Policy*, Vol. 6, No. 3, 177-184.
- [16] Green, Richard (1998), "Electricity Transmission Pricing: How much does it cost to get it wrong," *Power Report PWP-058 (May 1998)*, University of California Energy Institute, CA.
- [17] Harrison, M. and D. Kreps (1979), "Martingales and Arbitrage in Multi-period Securities Markets," *Journal of Economic Theory*, 20, 381-408.
- [18] He, H. (1990), "Convergence from Discrete- to Continuous-Time Contingent Claims Prices," *The Review of Financial Studies*, 3, 523-546.
- [19] Heston, S. (1993), "A Closed-Form Solution of Options with Stochastic Volatility with Applications to Bond and Currency Options," *The Review of Financial Studies*, 6, 327-343.
- [20] Hilliard, J. and J. Reis (1998), "Valuation of Commodity Futures and Options under Stochastic Convenience Yields, Interest Rates, and Jump Diffusions in the Spot," *Journal of Financial & Quantitative Analysis*, v33, n1 (Mar 1998), 61-86.
- [21] Hogan, William (1992), "Contract Networks for Electric Power Transmission," *Journal of Regulatory Economics*, v.4, no.3: 211-242.
- [22] *International Comparisons of Electricity Regulation*, edited by R. Gilbert and E. Kahn. Cambridge University Press, 1996.

- [23] Joskow, Paul (1997), "Restructuring, Competition and Regulatory Reform in the U.S. Electricity Sector, " *Journal of Economic Perspectives*, 11(3): 119-138.
- [24] Kaminski, Vincent (1997), "The Challenge of Pricing and Risk Managing Electricity Derivatives," *The US Power Market*, 149-171. Risk Publications.
- [25] Merton, R.C. (1973), "Theory of Rational Option Pricing," *Journal of Economics and Management Science*, 4 (Spring 1973), 141-83.
- [26] Miltersen, K. and E. Schwartz (1998), "Pricing of Options on Commodity Futures with Stochastic Term Structures of Convenience Yields and Interest Rates," *Journal of Financial & Quantitative Analysis*, v33, n1 (Mar 1998): 33-59.
- [27] Oren, Shmuel S. (1997). "Economic Inefficiency of Passive Transmission Rights in Congested Electricity Systems with Competitive Generation." *The Energy Journal*, 18(1): 63-84.
- [28] Oren, Shmuel, P. Spiller, P. Varaiya, and F. Wu (1995), "Nodal Prices and Transmission Rights: A Critical Appraisal," *Electricity Journal*, v8, n3 (Apr 1995): 24-35.
- [29] Protter, P. (1990), *Stochastic Integration and Differential Equations*, Springer-Verlag, New York.

- [30] Schwartz, Eduardo S. (1997), “The Stochastic Behavior of Commodity Prices: Implications for Valuation and Hedging”, *Journal of Finance*, (July 1997), 923-973.
- [31] Schweppe, F., M. Caramanis, R. Tabors and R. Bohn (1988), *Spot Pricing of Electricity*, Kluwer Academic Publishers.
- [32] Stein, E. and J. Stein (1991), “Stock Price Distributions with Stochastic Volatility: An Analytic Approach,” *The Review of Financial Studies*, 4, 725-752.
- [33] Vasicek, O. (1977), “An Equilibrium Characterization of the term structure,” *Journal of Finance*, 5, 177-188.
- [34] Wilson, Robert (1989), “Efficient and Competitive Rationing,” *Econometrica*, 57: 1-40.
- [35] Wilson, Robert (1997), “Implementation of Priority Insurance in Power Exchange Markets,” *The Energy Journal*, 18(1): 111-125.
- [36] Wolak, Frank (1997), “Market Design and Price Behavior in Restructured Electricity Markets: An International Comparison,” mimeo, Stanford University.
- [37] Wood, A. and B. Wollenberg (1984), *Power Generation, Operation and Control*, John Wiley & Sons, New York.

- [38] Wu, Felix, P. Varaiya, P. Spiller, and S. S. Oren (1996), “Folk Theorems on Transmission Access: Proofs and Counterexamples”, *Journal of Regulatory Economics*, 10(1) July: 5-23.